Immune Mechanisms in Parkinson's Disease and Epilepsy. Preclinical Findings and Clinical Perspectives.

Fredlund, Filip

2024

Document Version:
Publisher's PDF, also known as Version of record

Immune Mechanisms in Parkinson's Disease and Epilepsy

Preclinical Findings and Clinical Perspectives

FILIP FREDLUND
EXPERIMENTAL MEDICAL SCIENCE | FACULTY OF MEDICINE | LUND UNIVERSITY

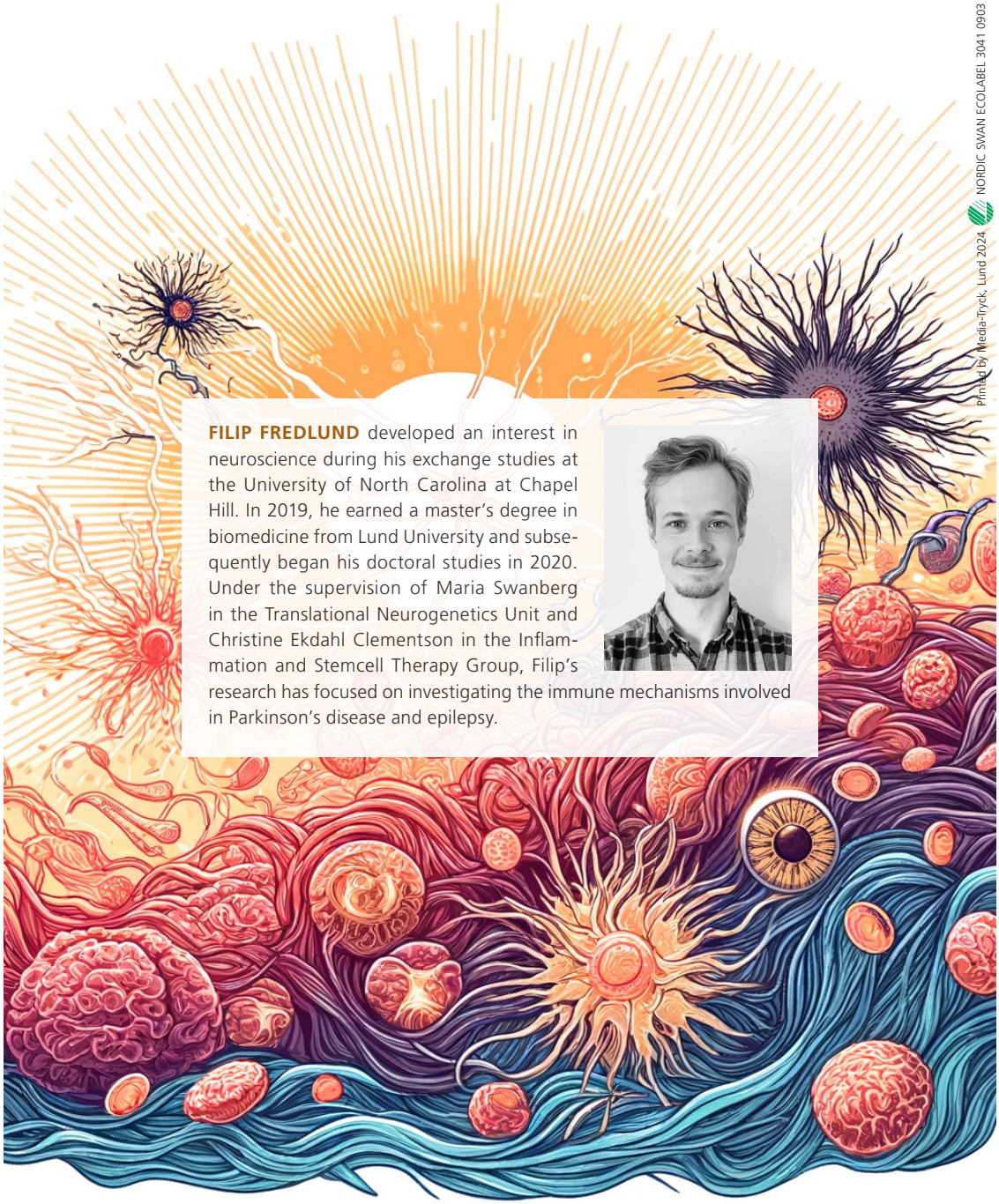

FILIP FREDLUND developed an interest in neuroscience during his exchange studies at the University of North Carolina at Chapel Hill. In 2019, he earned a master's degree in biomedicine from Lund University and subsequently began his doctoral studies in 2020. Under the supervision of Maria Swanberg in the Translational Neurogenetics Unit and Christine Ekdahl Clementson in the Inflammation and Stemcell Therapy Group, Filip's research has focused on investigating the immune mechanisms involved in Parkinson's disease and epilepsy.

Printed by Media-Tryck, Lund 2024 NORDIC SWAN ECOLABEL 3041 0903

LUND UNIVERSITY

FACULTY OF MEDICINE

Department of Experimental Medical Science

Lund University, Faculty of Medicine
Doctoral Dissertation Series 2024:104
ISBN 978-91-8021-600-5
ISSN 1652-8220

Immune Mechanisms in Parkinson's Disease and Epilepsy

Preclinical Findings and Clinical Perspectives

Immune Mechanisms in Parkinson's Disease and Epilepsy

Preclinical Findings and Clinical Perspectives

Filip Fredlund

LUND
UNIVERSITY

DOCTORAL DISSERTATION

Doctoral dissertation for the degree of Doctor of Philosophy (PhD) at the Faculty of Medicine at Lund University to be publicly defended on 19th of September at 09.00 in Belfrage Hall, BMC D15, Klinikgatan 32, Lund, Sweden

Faculty opponent

Associate Professor Ashley Harms, PhD
University of Alabama at Birmingham, Alabama, USA

Organization: LUND UNIVERSITY

Document name: Doctoral thesis **Date of issue:** 2024-09-19

Author: Filip Fredlund **Sponsoring organization:**

Title and subtitle: Immune Mechanisms in Parkinson's Disease and Epilepsy – Preclinical Findings and Clinical Perspectives

Abstract:

Parkinson's disease (PD) and epilepsy are neurological disorders in which immune reactions are believed to contribute to disease susceptibility and progression. Despite differing manifestations, both conditions share neuroinflammatory features such as glia cell activation, proinflammatory cytokine production, and leukocyte infiltration. However, the precise role of immune reactions in disease susceptibility and progression remains unclear. Currently, only symptomatic treatments exist for both disorders, highlighting the need for new therapeutic targets that address the underlying causes. This thesis investigates immune mechanisms in PD and epilepsy using preclinical *in vivo* models with the aim to enhance the understanding of disease susceptibility and progression.

We used a combination of recombinant adeno-associated virus mediated α-Synuclein (α-Syn) overexpression in the substantia nigra and striatal seeding of α-Syn preformed fibrils to model α-Syn-induced pathology, neuroinflammation, and neurodegeneration of PD. We demonstrate that allelic variants of the class II transactivator (*Ciita*), the master regulator of major histocompatibility complex class II expression, affect susceptibility and progression of α-Syn-induced neurodegeneration, motor impairment, and α-Syn pathological spread. Immunohistochemical and flow cytometry analyses revealed that reduced *Ciita* levels were associated with more inflammatory-prone microglia both in naïve rats and in a region-dependent manner in rats exposed to exogenous α-Syn. Additionally, reduced *Ciita* levels were associated with elevated soluble tumor necrosis factor (sTNF) levels in serum. However, inhibiting sTNF did not protect against α-Syn-induced neurodegeneration, neuroinflammation, or α-Syn pathology, suggesting that chronic microglial activity, rather than sTNF, drives PD pathology.

To investigate the role of immune reactions in epilepsy development we explored systemic interleukin-6 receptor antibody (IL-6R ab) treatment to block IL-6 signaling in synapsin 2 knockout mice, which develop epileptic seizures from around two months of age. Initiating IL-6R ab treatment before seizure onset significantly reduced the frequency of handling-induced seizures and delayed seizure development without affecting synaptic protein levels or neuroinflammation. These results suggest that systemic immunomodulation can mitigate epilepsy development, although the exact mechanisms remain unclear.

Overall, this thesis underscores the importance of genetic and immunological factors in the pathogenesis of PD and epilepsy and suggests potential immunomodulatory strategies for their treatment. Future studies should continue to explore the therapeutic potential of targeting specific immune pathways in these neurological disorders.

Key words: Immune mechanisms, Parkinson's disesae, α-Syn, Ciita, TNF, epilepsy, Syn2, IL-6

Language: English **ISSN and key title**: 1652-8220

ISBN: 978-91-8021-600-5

Recipient's notes **Number of pages**: 134

Immune Mechanisms in Parkinson's Disease and Epilepsy

Preclinical Findings and Clinical Perspectives

Filip Fredlund

LUND
UNIVERSITY

Faculty of Medicine
Department of Experimental Medical Science
ISBN 978-91-8021-600-5
ISSN 1652-8220

Printed in Sweden by Media-Tryck, Lund University
Lund 2024

Till min familj

Feed my will to feel this moment
Urging me to cross the line
Reaching out to embrace the random
Reaching out to embrace whatever may come
- Tool

Table of Contents

Abstract

Parkinson's disease (PD) and epilepsy are neurological disorders in which immune reactions are believed to contribute to disease susceptibility and progression. Despite differing manifestations, both conditions share neuroinflammatory features such as glia cell activation, proinflammatory cytokine production, and leukocyte infiltration. However, the precise role of immune reactions in disease susceptibility and progression remains unclear. Currently, only symptomatic treatments exist for both disorders, highlighting the need for new therapeutic targets that address the underlying causes. This thesis investigates immune mechanisms in PD and epilepsy using preclinical *in vivo* models with the aim to enhance the understanding of disease susceptibility and progression.

We used a combination of recombinant adeno-associated virus mediated α-Synuclein (α-Syn) overexpression in the substantia nigra and striatal seeding of α-Syn preformed fibrils to model α-Syn-induced pathology, neuroinflammation, and neurodegeneration of PD. We demonstrate that allelic variants of the class II transactivator (*Ciita*), the master regulator of major histocompatibility complex class II expression, affect susceptibility and progression of α-Syn-induced neurodegeneration, motor impairment, and α-Syn pathological spread. Immunohistochemical and flow cytometry analyses revealed that reduced *Ciita* levels were associated with more inflammatory-prone microglia both in naïve rats and in a region-dependent manner in rats exposed to exogenous α-Syn. Additionally, reduced *Ciita* levels were associated with elevated soluble tumor necrosis factor (sTNF) levels in serum. However, inhibiting sTNF did not protect against α-Syn-induced neurodegeneration, neuroinflammation, or α-Syn pathology, suggesting that chronic microglial activity, rather than sTNF, drives PD pathology.

To investigate the role of immune reactions in epilepsy development we explored systemic interleukin-6 receptor antibody (IL-6R ab) treatment to block IL-6 signaling in synapsin 2 knockout mice, which develop epileptic seizures from around two months of age. Initiating IL-6R ab treatment before seizure onset significantly reduced the frequency of handling-induced seizures and delayed seizure development without affecting synaptic protein levels or neuroinflammation. These results suggest that systemic immunomodulation can mitigate epilepsy development, although the exact mechanisms remain unclear.

Overall, this thesis underscores the importance of genetic and immunological factors in the pathogenesis of PD and epilepsy and suggests potential immunomodulatory strategies for their treatment. Future studies should continue to explore the therapeutic potential of targeting specific immune pathways in these neurological disorders.

Lay summary

Parkinson's disease and epilepsy are two common neurological disorders that affect millions of people worldwide. Parkinson's disease may be caused by combination of genes and environmental exposures. It is known for causing characteristic slow movement, tremors, and stiffness, consequences of the dysfunction and death of brain cells producing the signaling molecule dopamine. Epilepsy can be caused by a wide variety of factors, from genetic mutations to head trauma, and is defined by recurrent seizures. Seizures may look very different, but can be the loss of consciousness and involuntary muscle spasms. The currently available treatments for both conditions only treat symptoms and do not affect the disease progression. Both Parkinson's disease and epilepsy share a connection with the immune system and inflammation, which is explored in this thesis. Understanding how inflammation affects these diseases could help develop better treatments that target the underlying causes rather than just alleviating symptoms.

This thesis studies immune mechanisms involved in Parkinson's disease and epilepsy using animal models. Parkinson-like disease was induced in rats by exposing their brains to a protein called alpha-Synuclein, which helped us to study the role of different genes and immune responses. We found that variations in a gene called *Ciita*, which controls immune responses, affected several aspects of the mimicked Parkinson's disease. Specifically, lower levels of *Ciita* made microglia, the brain's immune cells, more prone to inflammation and increased the levels of a protein called tumor necrosis factor (TNF) in the blood. However, blocking TNF did not prevent brain cells from dying and did not reduce the inflammatory response, suggesting that continuous microglial activity, rather than TNF, drives Parkinson's disease progression.

For epilepsy, we studied a mouse model that lacks a protein called synapsin 2. In humans, mutations in the synapsin genes can cause inherited epilepsy. Mice lacking synapsin 2 develop epileptic seizures from around two months of age. We treated these mice with an antibody that blocks the action of interleukin-6, a protein involved in inflammation, before seizures began. Although we failed to identify the mechanism involved, this treatment reduced the occurrence and delayed the onset of epileptic seizures. These findings indicate that targeting interleukin-6 can mitigate seizure development, although the exact mechanisms underlaying the observation remain unclear.

The findings in this thesis highlight the complex role of the immune system in both Parkinson's disease and epilepsy and suggest that immune mechanisms could be an important target for the development of new therapeutic options. Future studies should continue to explore immune reactions to better understand their role in Parkinson's disease and epilepsy and to develop more effective therapies.

Populärvetenskaplig sammanfattning

Parkinsons sjukdom och epilepsi är två vanliga neurologiska sjukdomar som drabbar miljontals människor världen över. Parkinson kan orsakas av en kombination av genetik och miljöfaktorer. Parkinsons sjukdom yttrar sig i långsamma rörelser, skakningar och/eller stelhet, vilket är en följd av dysfunktion och förlust av nervceller i hjärnan som producerar signalämnet dopamin. Epilepsi kan orsakas av flera olika faktorer, från genetiska mutationer till hjärnskador, och karaktäriseras av återkommande epileptiska anfall, till exempel krampanfall. Nuvarande behandlingsalternativ för dessa sjukdomar behandlar endast symptomen och påverkar inte sjukdomsförloppet. Gemensamt för båda sjukdomarna är att de har en koppling till immunsystemet och inflammation. Att förstå hur inflammation påverkar dessa sjukdomar kan därför hjälpa till att utveckla bättre behandlingar som riktar sig mot de underliggande orsakerna och inte bara lindrar symptomen.

Denna avhandling studerar immunologiska mekanismer involverade i Parkinsons sjukdom och epilepsi med hjälp av djurmodeller. För att modellera Parkinson-lik sjukdom exponerade vi råttor för ett protein, som heter alfa-Synuclein, inuti deras hjärnor. Denna modell efterliknar sjukdomens progression och möjliggör för oss att studera olika geners och immunreaktioners roll. Vi fann att variationer i en gen kallad *Ciita*, som kontrollerar immunsvar, påverkar hur känslig hjärnan är för mottaglighet och progression av Parkinson-lik sjukdom. Specifikt visade det sig att lägre nivåer av *Ciita* gör mikroglia, hjärnans immunceller, mer benägna att orsaka inflammation och ökade nivåerna av ett protein kallat TNF i blodet. Att blockera TNF förhindrade dock inte det Parkinson-lika sjukdomsförloppet, vilket tyder på att kontinuerlig mikrogliaaktivitet, snarare än TNF, driver progressionen av Parkinsons sjukdom.

För epilepsi studerade vi en musmodell som saknar ett protein kallat synapsin 2. Genetiska mutationer av synapsin hos människan kan orsaka epilepsi. Dessa möss drabbas av epileptiska anfall från två månaders ålder. Vi behandlade mössen med en antikropp som blockerar effekten av interleukin-6, ett protein involverat i inflammation, innan anfallen började. Vi kunde inte påvisa vilken eller vilka mekanismer som låg till grund till förändringen, men behandlingen fördröjde utvecklingen av och minskade antalet epileptiska anfall. Dessa resultat tyder på att behandling mot interleukin-6 kan mildra utvecklingen av epileptiska anfall, även om de exakta mekanismerna fortfarande är okända.

Sammantaget belyser dessa resultat immunsystemets komplexa roll i både Parkinsons sjukdom och epilepsi. Resultaten visar att riktade behandlingar mot specifika immunmekanismer kan vara av intresse i utvecklingen av nya behandlingsalternativ. Framtida studier bör fortsätta att utforska immunreaktioner för att vi bättre ska förstå deras roll i Parkinsons sjukdom och epilepsi och för att utveckla mer effektiva behandlingar.

List of Papers

Papers included in the thesis

Paper I

The MHC class II transactivator modulates seeded alpha-synuclein pathology and dopaminergic neurodegeneration in an *in vivo* rat model of Parkinson's disease

Jimenez-Ferrer I, **Bäckström F**, Dueñas Rey A, Jewett M, Boza-Serrano A, Luk KC, Deierborg T, Swanberg M.

Brain, Behavior, and Immunity. 91: 369-382, 2021.

Paper II

Ciita Regulates Local and Systemic Immune Responses in a Combined rAAV-α-synuclein and Preformed Fibril-Induced Rat Model for Parkinson's Disease

Fredlund F, Jimenez-Ferrer I, Grabert K, Belfiori LF, Luk KC, Swanberg M.

Journal of Parkinson's Disease. 14(4): 693-711, 2024.

Paper III

Lack of neuroprotection after systemic administration of the soluble TNF inhibitor XPro1595 in an rAAV6-α-Syn+PFFs-induced rat model for Parkinson's disease

Fredlund F, Fryklund C, Trujeque O, Staley HA, Pardo J, Luk KC, Tansey MG, Swanberg M.

Manuscript.

Paper IV

Reduced epilepsy development in synapsin 2 knockout mice with autistic behavior following early systemic treatment with interleukin-6 receptor antibody.

Bäckström F, Ahl M, Wickham J, Ekdahl CT.

Epilepsy Research. 191: 107114, 2023.

Author's contribution to the papers

The research presented in this thesis was conducted in two different research groups at Lund University. The majority of my work was conducted in the Translational Neurogenetics Unit, focusing on Parkinson's disease. My research on preclinical epilepsy and autism spectrum disorder was conducted in the Inflammation and Stemcell Therapy group. Papers I-IV involved contributions from several researchers, with me being the main responsible for Papers II-IV. My contributions in Papers I-IV, using the CRediT author statement, are listed below.

Paper I

Data curation, formal analysis, investigation, visualization, writing the original draft, and reviewing and editing the manuscript.

Paper II

Conceptualization, data curation, formal analysis, funding acquisition, investigation, methodology, project administration, validation, visualization, writing the original draft, and reviewing and editing the manuscript.

Paper III

Conceptualization, data curation, formal analysis, funding acquisition, investigation, methodology, project administration, validation, visualization, writing the original draft, and reviewing and editing the manuscript.

Paper IV

Conceptualization, data curation, formal analysis, funding acquisition, investigation, methodology, software, validation, visualization, writing the original draft, and reviewing and editing the manuscript.

Publications outside of the thesis

Paper I

Nigral transcriptomic profiles in Engrailed-1 hemizygous mouse models of Parkinson's disease reveal upregulation of oxidative phosphorylation-related genes associated with delayed dopaminergic neurodegeneration.

Belfiori LF, Dueñas Rey A, Ralbovszki DM, Jimenez-Ferrer I, **Fredlund F**, Balikai SS, Ahrén D, Atterling Brolin K, Swanberg M.

Frontiers in Aging Neuroscience. 16: 1337365, 2024.

Popularized scientific summary I

Påverkar vårt immunförsvar risken att drabbas av Parkinsons sjukdom?

Bäckström F.

Vetenskap & Hälsa, 2021-06-08.

Popularized scientific summary II

Antigenpresentation kan påverka risk och förlopp av Parkinsons sjukdom.

Bäckström F.

Neurologi i Sverige, 4: 18-21, 2021.

Abbreviations

AEDs	Antiepileptic drugs
AI	Artificial intelligence
APC	Antigen presenting cell
ASD	Autism spectrum disorder
BAMs	Border-associated macrophages
BSA	Bovine serum albumin
C3	Complement component 3
CD	Cluster of differentiation
Ciita/CIITA	Class II transactivator
CNN	Convolutional neural network
CNS	Central nervous system
CSF	Cerebrospinal fluid
DN	Dominant negative
DPBS	Dulbecco's phosphate-buffered saline
EAE	Experimental autoimmune encephalomyelitis
ELISA	Enzyme-linked immunosorbent assay
FLE	Frontal lobe epilepsy
En1	Engrailed-1
GABA	Gamma-aminobutyric acid
GFAP	Glial fibrillary acidic protein
GFP	Green fluorescent protein
HLA	Human leukocyte antigen
Iba1	Ionized calcium-binding adapter molecule 1
IL	Interleukin
IL-6R ab	Interleukin-6 receptor antibody
JAK	Janus kinase
KO	Knockout
LB	Lewy body

LN	Lewy neurite
LPS	Lipopolysaccharide
MHCII	Major histocompatibility complex class II
MS	Multiple sclerosis
ND	Not detected
PC	Principal component
PCA	Principal component analysis
PET	Positron emission tomography
PFFs	Preformed fibrils
PHA	Phytohemagglutinin
PNES	Psychogenic non-epileptic seizures
pS129	Phosphorylated serine residue 129
RA	Rheumatoid arthritis
rAAV	Recombinant adeno-associated virus
ROI	Region of interest
SN	Substantia nigra
SNpc	Substantia nigra pars compacta
SNP	Single nucleotide polymorphism
SRS	Spontaneous recurrent seizures
STAT	Signal transducer and activator of transcription
Syn2	Synapsin II
TLE	Temporal lobe epilepsy
TLR	Toll-like receptor
TNF (tm/s)	Tumor necrosis factor (transmembrane/soluble)
TNFR	Tumor necrosis factor receptor
WPRE	Woodchuck hepatitis virus posttranscriptional regulatory element
wt	Wildtype
α-Syn	α-Synuclein

Introduction

Immune reactions in the central nervous system

The central nervous system (CNS) has historically been considered an immune-privileged site due to the inability of mounting antigen-specific responses following allogenic transplantation into the brain parenchyma (1-3). It was believed that the presence of a physical barrier (blood-brain barrier, BBB), the lack of lymphatic drainage, and the lack of professional antigen presenting cells (APCs) ultimately resulted in the inability of producing immune responses of CNS-derived antigens.

Since the mid-20th century, the concept of the CNS as immune-privileged has been gradually reevaluated, based on the identification of functional lymphatic drainage from the CNS into deep cervical lymph nodes, the presence of immune cells in the meninges with CNS surveillance, and an inflammatory role of glia cells in the CNS, including antigen presentation (2, 3).

The main role of the immune system is to maintain tissue homeostasis and defend against pathogens. Not only is the CNS linked to the peripheral immune system, but neuroimmune interactions are necessary to maintain homeostasis (4). Tissue homeostasis is achieved by clearance of debris, promoting apoptosis of infected or damaged cells, and supporting tissue regeneration. Defense against pathogens is achieved by phagocytic activity, production of cytotoxic substances, and secretion of chemokines and cytokines for immune cell recruitment and coordination of the immune response.

In the context of neurodegenerative disease and neurological conditions such as Parkinson's disease (PD) and epilepsy, there is substantial evidence for neuroinflammatory responses. In the last decade and a half, the involvement of the systemic immune responses and neuroimmune interactions has also become evident (5, 6). Whether the immune responses are a cause or consequence of disease remains to be fully determined.

Microglia

Microglia are the resident macrophages of the brain parenchyma (reviewed in (7)). The origin of microglia was long debated but in 2010 a key paper demonstrated that microglia arise from embryonic yolk sac progenitors that migrate into the CNS

during embryogenesis (8). Microglia have been shown to be self-renewing within the CNS, with limited contribution from infiltrating myeloid-derived macrophages (7). Microglia also have distinct roles during CNS development which includes, but are not limited to, inducing neuronal cell death, support neuronal and oligodendrocyte precursor cell survival, perform synaptic remodeling and pruning, and perform CNS surveillance (7).

Microglia respond to external stimuli through cytokine signaling and pattern recognition receptors (PRRs) which can sense e.g., the presence of lipopolysaccharide (LPS), a pathogen associated molecular pattern (PAMP), or DNA, a danger associated molecular pattern (DAMP), which triggers PRRs ultimately activating microglia and other innate immune cells.

Traditionally, microglia activation states have been divided into two subtypes based on the expression of a few markers. The proinflammatory M1, partly characterized by the release of proinflammatory cytokines interleukin (IL) 6, IL-1β, and tumor necrosis factor (TNF), and the anti-inflammatory M2, characterized by the release of trophic factors such as brain derived neurotrophic factors and tumor growth factor β. The M1/M2 classification has been critiqued to be too simplified (9) but is still used today. Transcriptomic studies have shown that microglia activity is context-dependent and better represented by a spectrum rather than two distinct subtypes (10, 11). Similarly, morphological changes of microglia upon different stimuli can also be classified into a context-dependent multi-spectra (reviewed in (12)).

Assessment of microglia activation by immunohistochemistry (IHC) is commonly done by quantifying certain markers. The most common marker is the ionized calcium-binding adapter molecule 1 (Iba1), which is involved in membrane ruffling, enabling migration capacity of microglia and macrophages, and is upregulated following activation (13). As an APC, microglia also upregulate major histocompatibility complex class II (MHCII) following activation together with co-stimulatory markers such as cluster of differentiation (CD) 80 or 86 (14, 15). Using flow cytometry, microglia can be gated based on their $CD45^{low}$/CD11b+ signature (11). CD45 is a pan leukocyte marker that is expressed in low quantities on microglia whereas CD11b is an integrin expressed on e.g., monocytes, macrophages, and microglia, important for cell migration and adhesion.

Astrocytes

Astrocytes are the most abundant glia cells in the CNS and, like microglia, are intricate to the development and homeostasis of the CNS. Astrocytes regulate the formation, elimination, and maturation of neuronal synapses during development (16). Astrocytes are also crucial for the maintenance and regulation of the BBB and provide neuronal structural support, control neuronal energy supply, and perform neurotransmitter recycling.

Astrocyte are emerging as a key cell type in neuroinflammatory responses. Upon activation following e.g., stroke, infections, epilepsy, or neurodegeneration astrocytes upregulate intermediate filament proteins like glial fibrillary acidic protein (GFAP) and vimentin, and shift from non-reactive astrocytes characterized by thin processes, to reactive, hypertrophic, astrocytes (17, 18). Multiple other markers of activated astrocytes exist, such as the production and secretion of complement component 3 (C3) (19, 20) and even the upregulation of MHCII (21).

Circulating immune cells

Peripheral immune cells in circulation have gained increased interest in the context of neurological conditions and neurodegeneration due to the observation of infiltrating leukocyte cells into the CNS (6, 22).

The immune system is composed of the innate and adaptive immune systems. The innate immune system responds quickly to injury or pathogens. It involves the recognition of PAMPs and DAMPs by PRRs on immune cells like monocytes, macrophages, and dendritic cells. This response includes phagocytosis, secretion of antimicrobials by granulocytes, and release of complement factors.

The adaptive immune system, characterized by immunological memory, mounts rapid and highly specific responses upon repeated pathogen exposures. Key adaptive immune cells are lymphocytes, including B and T cells. B lymphocytes can act as APCs and present antigens on MHCII molecules to T lymphocytes. With certain cytokine signals, B lymphocytes differentiate into antibody-producing plasma cells.

T lymphocytes are divided into CD4+ and CD8+ subsets. CD8+ T cells, or cytotoxic T cells, recognize infected or defect cells through MHCI-mediated interactions and induce apoptosis. CD4+ T cells, or helper T cells, interact with antigens presented on MHCII molecules and differentiate into various helper subsets, producing cytokines that regulate and direct immune responses.

Cytokines, signaling pathways and cell-cell communication

Cytokines are a vast category of small proteins important for cell-cell communication with diverse and context-dependent functions (23, 24). Chemokines act by directing migration of cells to sites of injury or during developments whereas interferons (e.g., IFN-γ) and TNF mainly act by inducing inflammation. There are numerous ILs which functions are context dependent but include pro- and anti-inflammatory signaling and promoting differentiation of helper T cells into T cell subsets. In the context of this thesis there are two cytokines of special interest, IL-6 and TNF, that are associated to several neurological disorders, including PD, epilepsy, and autism spectrum disorder (ASD).

Interleukin 6

IL-6 is produced by a wide variety of cells including T lymphocytes, monocytes, macrophages, and microglia. IL-6 signaling occurs mainly through the Janus kinase (JAK)-signal transducer and activator of transcription 3 (STAT3) pathway, and signaling can occur through the classical pathway (**Figure 1A**) or through trans-signaling (**Figure 1B**) (25). In the classical pathway IL-6 binds to its membrane bound receptor, IL-6R, which in turn interacts with glycoprotein 130 (gp130) in a dimer structure. Trans-signaling involves the binding of IL-6 to soluble IL-6R (sIL-6R), and the IL-6/sIL-6R complex subsequently binds to membrane bound gp130, also in a dimer structure. The IL-6/IL-6R/gp130 dimer complex leads to the activation of JAK resulting in phosphorylation of STAT3 with subsequent dimerization and translocation to the nucleus and initiation of transcription of target genes (25).

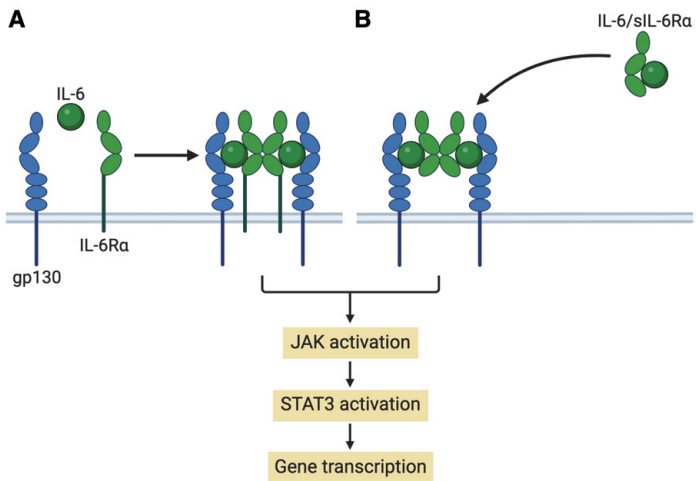

Figure 1. Signaling pathways of IL-6.
(**A**) Classical IL-6 signaling pathway. (**B**) IL-6 trans-signaling pathway. Illustration created using BioRender.com and adapted from (25). **Abbreviations**. IL, interleukin; IL-6Rα, IL-6 receptor; gp130, glycoprotein 130; sIL-6Rα, soluble IL-6Rα; JAK, Janus kinase; STAT3, signal transducer and activator of transcription 3.

IL-6 has vast signaling effects and is involved in regulating B cell survival and differentiation into plasma cells, as well as promoting T lymphocyte survival, proliferation, and differentiation. Additionally, IL-6 signaling can induce the production of chemokines and thus regulate recruitment of immune cells (26). IL-6 is also an inducer of the acute phase response and is elevated in several chronic inflammatory diseases. Consequently, IL-6 signaling has been targeted in inflammatory diseases and an IL-6 receptor antibody (tocilizumab) is approved for treatment of rheumatoid arthritis (RA), Castleman disease, and was most recently

approved for treatment of COVID-19 (27). The role of IL-6 in CNS disorders are emerging and findings suggest that elevated IL-6 levels in CNS decreases hippocampal neurogenesis, affect synaptic connections, and can cause hippocampal hyperexcitability (6).

Tumor necrosis factor

TNF is important for homeostatic functions and considered the prototypic proinflammatory cytokine, which is quickly produced following pathogen invasion or tissue damage (28). TNF is mainly produced by monocytes and tissue macrophages e.g., microglia in the brain parenchyma. TNF levels are associated to inflammatory diseases including RA, psoriasis, and irritable bowel disease (IBD), for which anti-TNF therapies are used today (28). The expectations of anti-TNF therapies in CNS diseases took a rapid turn during clinical trials of multiple sclerosis (MS) when it was shown that anti-TNF therapy could exacerbate, rather than reduce MS severity (29). Subsequent research has identified possible mechanisms involved behind the devastating outcome of the MS trials.

TNF signaling occurs through two distinct TNF receptors (TNFR), TNFR1 and TNFR2 (30, 31). TNF exists in two forms, membrane bound (tmTNF) and soluble (sTNF), both of which signal in a homotrimer configuration. TNFR1 binds both tmTNF whereas TNFR2 only binds tmTNF (**Figure 2**). Both TNFR1 and TNFR2 signaling promotes cell survival, proliferation and induce inflammatory responses including cytokine production (30, 31). Signaling through TNFR1, which is expressed on most cells, can also induce apoptosis and necroptosis (31). In contrast, signaling through TNFR2, which is only expressed on a subset of cell types, including neurons, promotes neuronal survival, tissue regeneration, support oligodendrocyte function and remyelination of demyelinated neurons (30, 31). Therefore, maintaining TNFR2 signaling is thought to be crucial in the context of TNF modulation in the CNS.

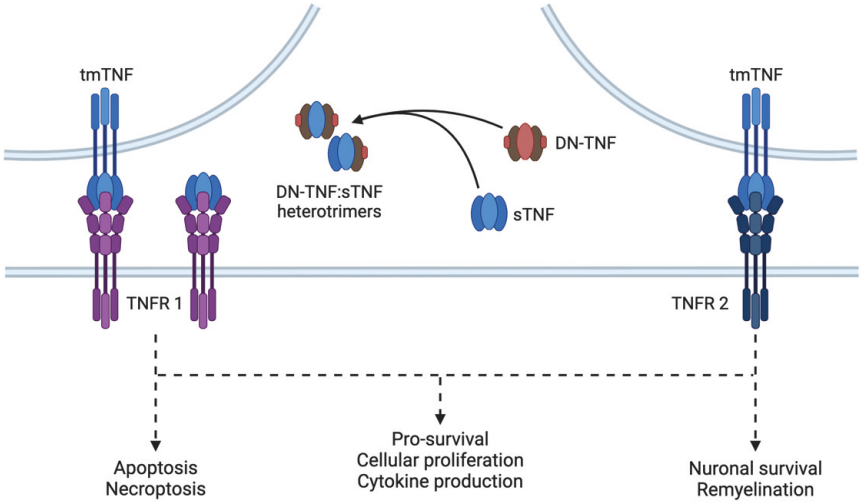

Figure 2. Signaling pathways of TNF and mode of action of DN-TNF variants.
sTNF and tmTNF signals through TNFR1 whereas only tmTNF signals through TNFR2. Dashed lines indicate molecular signaling pathways ultimately affecting homeostatic and immune functions. DN-TNF variants sequesters monomeric sTNF creating heterotrimeric complexes that are unable to bind TNFR1. Illustration created using BioRender.com and adapted from (30, 31). **Abbreviations**. TNF, tumor necrosis factor; tmTNF, membrane bound TNF; sTNF, soluble TNF; DN-TNF, dominant negative TNF; TNFR, TNF receptor.

In 2003, a second-generation TNF inhibitor was developed, utilizing dominant negative TNF (DN-TNF) variants, which works by sequestering sTNF monomers, forming DN-TNF:sTNF heterotrimers which are unable to bind TNFR1, thereby maintaining TNFR2 signaling (**Figure 2**) (32). DN-TNF variants are currently in clinical trials for mild cognitive impairment and early onset Alzheimer's disease.

Parkinson's disease

PD is the second most common age-related neurodegenerative disorder, and with a typical onset around the age of 60 (33). The prevalence is estimated to be around 1% in individuals above the age of 60, and is often reported to be twice as common in men compared to women (33). With an aging population the prevalence of PD increases. According to the World Health Organization, PD prevalence has doubled during the last 25 years and as of 2019 a total of 8.5 million individuals were estimated to have PD.

A core feature of PD is the presence of cardinal motor symptoms which include bradykinesia, resting tremors and/or rigidity, which result from the loss and dysfunction of dopaminergic neurons in the substantia nigra pars compacta (SNpc)

(34). As the disease progresses, motor symptoms worsen and may include postural instability and dysphagia (34). PD patients often have non-motor symptoms in the prodromal phase of PD that include, but are not limited to, sleep behavior disorder, constipation, and hyposmia (34). Non-motor symptoms also worsen with disease progression and can include mild cognitive impairment, hallucinations, and dementia (34).

Current treatment strategies

The available treatments for PD are symptomatic and ultimately focus on replacing or retaining dopamine levels (34). The gold standard treatment is the use of the dopamine precursor L-DOPA which crosses the BBB and is converted to dopamine inside neurons. L-DOPA is often co-administered with inhibitors that prevent the conversion of L-DOPA to dopamine outside of the brain, thereby increasing bioavailability. Other treatment strategies inhibit the clearance of dopamine from the synaptic cleft or use dopamine agonists.

An advanced treatment strategy that treats symptoms, but without the use of pharmaceuticals, is deep brain stimulation. Deep brain stimulation can only be used in patients which response well to L-DOPA, and is often used in advanced stages of disease, e.g., following drug-induced dyskinesia (34).

Over the last decades significant advancements has been made in the field of transplantation of human embryonic stem cell derived dopaminergic neurons into PD patients, and in 2022 first-in-human clinical trial in Europe, STEM-PD, was initiated (35). If the treatment strategy is approved much work remain, e.g., to mitigate neuroimmune interactions, which may reduce the cell survival of the transplanted cells.

Etiology of Parkinson's disease

The etiology of PD is not fully understood. In a minority of cases, termed monogenic PD, the cause can be explained by mutations in certain genes. Monogenic PD only accounts for approximately 3-5% of PD cases, whereas the remaining cases, termed idiopathic, are multifactorial (36).

Monogenic Parkinson's disease

The first report of a monogenic cause of PD was the identification of a missense mutation, A53T, in *SNCA*, encoding α-Syn (37). α-Syn was subsequently reported to be the main component of the pathological inclusions called Lewy bodies (LB) and Lewy neurites (LN) present in post-mortem PD brains (38, 39). Two other missense mutation in *SNCA* have been identified, the A30P (40) and E46K (41). Additionally, duplication (42, 43) and triplication (44) of *SNCA* also cause PD.

There are more than 20 genes linked with monogenic PD, however, replication and validation studies are still lacking for a majority of them (45). In addition to *SNCA* mutations, other well-established genes linked to monogenic PD are *PRKN*, *PINK1*, *DJ-1*, *LRRK2*, and *GBA1* (45). *PRKN*, *PINK1*, and *DJ-1* encode for proteins that are involved in mitochondrial function, whereas *LRRK2* and *GBA1* encode for proteins related to lysosomal trafficking (45). Collectively, this highlights the critical roles of autophagy and mitochondrial function in the pathogenesis of PD.

Idiopathic Parkinson's disease – from an inflammatory point of view

As stated earlier, the majority of PD cases are multifactorial and referred to as idiopathic. In other words, the genetic makeup of an individual together with environmental interactions ultimately determine the risk of developing PD. Several life-style factors have been identified and linked with PD. Common factors that are associated with a decreased risk of PD is the use of tobacco products (e.g., smoking and snus) (46-48) and frequent coffee consumption (46, 49) whereas an increased risk of PD is associated with exposure to pesticides (46, 50, 51).

The largest genome wide association study on PD cases with European ancestry was published in 2019 identifying 90 risk variants (38 of which were novel) explaining 16-36% of the heritable risk of PD. Thus, a considerable amount of genetic risk factors of PD in Europeans remains to be identified. In 2024 a multi-ancestry genome wide association study was published, including genetic data from European, East Asian, Latin American, and African populations confirming 66 risk loci and reporting 12 novel loci (52).

Single nucleotide polymorphisms (SNPs) in the human leukocyte antigen (*HLA*), encoding for MHCII, have been reported in multiple studies to affect PD risk. Studies have reported SNPs in both coding and non-coding regions of *HLA*, indicating that both quality and quantity can affect PD risk (48, 51, 53-55). Additionally, some SNPs are associated with an increased risk of PD whereas others are associated with protective effects. Collectively, the association of common *HLA* variants to PD risk strongly supports a role of the adaptive immune system in susceptibility and/or progression of PD.

Interestingly, *HLA* variant associated with protective effects, *HLA-DRB1* (55), was functionally investigated by Sulzer and colleagues in 2017 (56). Here, it was shown that *HLA-DRB1* was a strong binder of α-Syn epitopes containing serine residue 129 (S129). Phosphorylation of S129 (pS129) on α-Syn is a pathological characteristic of PD (57, 58). Interestingly, the *HLA-DRB1* variant was only a strong binder of unphosphorylated epitopes containing S129 (56). Collectively, this could explain the observed protective effects but requires further investigation (55).

Further support of an inflammatory etiology of PD is the observation that frequent use of ibuprofen, but not aspirin and acetaminophen, slightly reduces the risk of PD (59, 60). However, one might question why long-term frequent use of ibuprofen is

warranted. Is it the ibuprofen, or rather the underlying cause resulting in frequent ibuprofen use, that reduces PD risk?

Pathophysiology

Neurodegeneration

PD is characterized by the loss and dysfunction of dopaminergic neurons in the SNpc ultimately causing an imbalance in the basal ganglia circuitry thereby affecting motor function. The degeneration of dopaminergic neurons is believed to start in the axonal terminals in the striatum, and continue in a retrograde fashion (61, 62). It is often reported that a loss of 80% of striatal dopamine and 60% loss of dopaminergic neurons in SNpc is required for motor symptoms to occur (63). However, reexamination of available data led to conclude that a 50-70% loss of striatal dopamine and 30% loss of dopaminergic neurons in SNpc is sufficient in causing motor symptoms (62, 64, 65)

Degeneration of dopaminergic neurons is not specific for PD but can be triggered by e.g., toxins. Intravenous injection of MPTP, which is converted into MPP+, a selective inhibitor of the mitochondria complex I, causes degeneration of dopaminergic neurons and parkinsonism (66). Dopaminergic neurons in the SNpc are thought to be extra sensitive to mitochondrial dysfunction since they are autonomously active, providing constant basal levels of dopamine in the striatum, which is an energy-demanding process (67)

α-Synuclein pathology

Another hallmark of PD pathology is the accumulation of α-Syn inside neuronal cell bodies (LB) or neurites (LN) (38, 39), which is commonly phosphorylated (pS129 α-Syn) (57, 58). In 2003 a landmark paper proposed a mechanism of α-Syn spreading in PD patients, termed the Braak hypothesis or Braak staging (68). The hypothesis proposed that α-Syn pathology is initiated in the lower brain stem and olfactory bulb, followed by spreading into midbrain and basal forebrain, and finally spreads to limbic and neocortical regions. The Braak staging has received criticism since the proposed pathology staging does not correlate with disease severity, it appears in individuals without PD, and it only applies to a subset of PD cases (69, 70). Convincing evidence of α-Syn propagation was published in 2008 when two independent labs reported findings of LB and LN in transplanted neurons in PD patients (71, 72). The propagation of α-Syn is today well-documented *in vitro* and *in vivo* studies, but the exact role it has on disease initiation or disease progression remain unknown.

The first evidence of an inflammatory component of PD was the identification of MHCII proteins in the SN of post-mortem PD patients (73). In addition to the upregulation of MHCII, the morphology of the identified microglia resembled an activated, ameboid shape (12, 74). Activated microglia have also been shown to be in close proximity to LB and LN pathology, and to produce IL-6 and TNF in the brains of PD patients (75).

Indeed, altered cytokine profiles, represented by elevated TNF levels, in the brain and cerebrospinal fluid (CSF) were first reported in 1994 (76). One year later, increased levels of IL-6 and IL-1β were also reported in the CSF of PD patients (77). Since then, multiple studies have reported cytokine alterations in both CSF and blood, and a recent meta-analysis confirmed elevated levels of IL-1β, IL-6, and sTNF in both CSF and blood (78).

In 2009 came the first evidence of T lymphocyte infiltration into the CNS of PD patients (79) which provided early evidence of the involvement of the adaptive immune system in PD. In 2017 another landmark paper was published when it was shown that PD patients had α-Syn reactive CD4+ T lymphocytes in circulation (56), findings which have been replicated in case studies of two PD patients (80). Additionally, it has been shown that the α-Syn specific T cell response is highest close to PD diagnosis (81). A recent study highlighted the role of a border-associated macrophages (BAMs) in PD, showing that perivascular macrophages are in close proximity to infiltrating T lymphocytes in post-mortem PD brains (82). Collectively, the identification of *HLA* variants affecting PD risk, upregulation of MHCII on CNS-associated macrophages, infiltration of lymphocytes into the CNS, and the identification of α-Syn reactive T cells in PD patients, provide convincing evidence of an adaptive immune component of PD, however, definitive proof of antigen presentation is lacking.

Changes in peripheral immune cells have also been reported in PD. So far, monocytes have received most of the attention. PD patients have been shown to have elevated levels of soluble CD163, which is released from monocytes, and correlates to disease severity (83). *Ex vivo* studies of monocytes isolated from PD patients demonstrated reduced responsiveness following stimulation compared to controls (84). Additionally, MHCII levels on intermediate and non-classical monocytes increase with PD duration (85). Changes associated with monocyte populations in PD also seem to display sexual dimorphism, with more activated monocytes in female compared to male patients (83, 86).

Studies characterizing T cell compartments in PD are inconclusive, with different profiles of T cell subsets being reported (87-92). *Ex vivo* studies have reported functional alterations of T cells, including impaired migratory capacity of CD4+ T cells (93), impaired Treg suppressor function (87), and an association between T cell reactivity and PD severity following phytohemagglutinin (PHA) stimulation

(88). Ultimately, more studies are needed to determine the precise changes, and implication, of T cell subsets in PD.

In 2007 the dual-hit hypothesis was published, suggesting that a neurotropic pathogen can enter the CNS through the vagus nerve or olfactory bulb and initiate α-Syn aggregation, with subsequent spreading according to the Braak staging (94). As of today, no pathogen has been identified to cause idiopathic PD. However, the gut-brain axis has received extensive attention, with a focus on microbiome dysregulation and systemic low-grade chronic inflammation as an initiator and driver of PD (reviewed in (5, 95)). The removal of the appendix, a vestigial organ with abundant α-Syn, has been associated with a reduced PD risk (reviewed in (96)). Additionally, it has been reported that individuals diagnosed with IBD have a 28-30% increased risk of developing PD (97, 98). Interestingly, IBD patients using anti-TNF therapies, was reported to have a 78% reduced PD risk compared to IBD patients not taking anti-TNF treatment (98), supporting a role of systemic inflammation on PD progression.

Models for Parkinson's disease

There are numerous experimental *in vivo* models of PD, some of which are illustrated in **Figure 3**. In the context of this thesis the exogenous α-Syn-induced models are of main interest and subsequently receives the most attention.

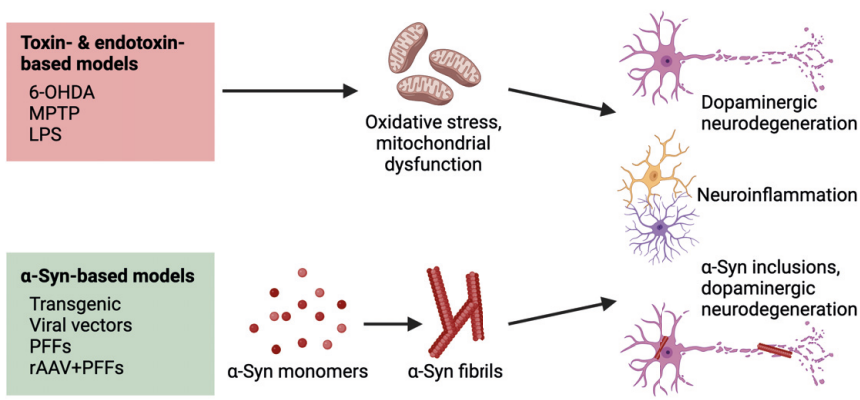

Figure 3. Overview of some of the main *in vivo* models used for experimental PD research. Toxin and endotoxin-based models causes mitochondrial dysfunction and oxidative stress activating microglia cells and causing dopaminergic neurodegeneration. α-Syn-induced models also induce neurodegeneration (to varying degree) and neuroinflammation together with PD-like α-Syn pathology. Illustration created using BioRender.com and adapted from (99). **Abbreviations**. 6-OHDA, 6-hydroxydopamine; MPTP, 1-methyl-4-phenyl-1,2,3,6-tetrahydropyridine; LPS, lipopolysaccharide; α-Syn, α-Synuclein; PFFs, preformed fibrils; rAAV, recombinant adeno-associated virus; PD, Parkinson's disease.

Toxin and endotoxin-induced models – 6-OHDA, MPTP and LPS models

The 6-hydroxydopamine (6-OHDA) model is a reactive oxygen species (ROS)- and mitochondrial dysfunction-induced dopaminergic neurodegenerative model of PD (reviewed in (99)). 6-OHDA is injected, most often unilaterally, into the brain by stereotaxic surgery, targeting either the SN, median forebrain bundle, or the striatum. 6-OHDA is taken up by dopaminergic cells and inducer of ROS. The dopaminergic neurodegeneration subsequently causes a neuroinflammatory response, characterized by microglia activation.

The MPTP model is also a model of mitochondrial dysfunction-induced dopaminergic neurodegeneration (reviewed in (99)). MPTP is systemically administered since it has the ability to cross the BBB. Once inside the CNS, MPTP is converted to MPP+, an inhibitor of complex I, which ultimately results in bilateral dopaminergic neurodegeneration.

The use of endotoxin, or LPS, is a model for inflammatory-induced neurodegeneration (reviewed in (100)). LPS can be administered directly into the CNS, or administered systemically using a single high dose, or repeated injections of low doses. Collectively the LPS administration causes a marked inflammatory response which is sufficient in causing neurodegeneration through ROS-induced mitochondrial dysfunction. Systemic LPS treatment results in significant increase in sTNF (among other cytokines) which reaches the CNS due to impaired BBB integrity.

Transgenic models of Parkinson's disease

The first transgenic mouse models of PD were generated at the beginning of the 21st century, shortly after the identification of α-Syn as a protein of interest in PD. The models created were based on the overexpression of wildtype (wt) or mutated (A53T, A30P, or E46K) α-Syn (reviewed in (101)). Unlike the toxin- or endotoxin-induced models of PD, the transgenic models developed widespread α-Syn pathology. Interestingly, many of the models generated have motor impairments, but no apparent, or limited, dopaminergic neurodegeneration.

Another transgenic mouse model is the hemizygous Engrailed 1 (*En1*$^{+/0}$). EN1 is a homeodomain transcription factor crucial for development of dopaminergic neurons. *En1*$^{+/0}$ on an OF-1 background causes dopaminergic neurodegeneration whereas *En1*$^{+/0}$ on a C57Bl/6J background show sub-clinical dopaminergic neurodegeneration, possibly due to elevated levels of mitochondria-related genes (102).

Viral vector-based a-Syn models

The first recombinant adeno-associated virus (rAAV)-α-Syn mediated rat models were published in 2002. The first study used human α-Syn with A30P mutation

(103), whereas the second study used both the human wt α-Syn and human α-Syn carrying the A53T mutation (104). In both studies the viral vectors were injected into the SNpc. The same year another study using lentiviral constructs, carrying human wt, A30P, or A53T α-Syn, injected into the SNpc of rats was published (105). Collectively, these studies reported important features modelling PD; neuroinflammation, α-Syn inclusions associated with neurodegeneration, including dopaminergic axonal loss in striatum and loss of dopaminergic neurons in SNpc. The latter PD-like events were important in the context of modelling PD, since transgenic mouse models failed to induce dopaminergic neurodegeneration. Additionally, the toxin- and endotoxin-induced models lack α-Syn pathology. With time, rAAV-mediated α-Syn overexpression has been shown more efficiently transduce dopaminergic neurons compared to lentiviral constructs (106) and has become the preferred choice in inducing α-Syn transgene overexpression.

Preformed fibril-induced models

A decade following the first publication of the rAAV-α-Syn-mediated models a new generation of α-Syn models were created based on the findings that that α-Syn pathology seem to spread in a topographical manner (68), and that transplanted neurons in PD got LBs over time (71, 72), further strengthening the evidence of α-Syn propagation. Additionally, α-Syn preformed fibrils (simply referred to as PFFs) could induce LB- and LN-like inclusions in primary neuronal cultures (107, 108) and could be propagated by retrograde transport in neurons (108). The first study using recombinant mouse PFFs was published in 2012, where the authors injected PFFs unilaterally in the dorsal striatum of wt mice (109). Already one month following striatal PFFs injection pS129 α-Syn immunoreactivity could be observed in brain regions anatomically connected to the dorsal striatum, including SNpc, whereas TH+ cell loss in SNpc was not observed until six months post injection (109). Since the first PFFs model was published it quickly became a popular model for PD (99, 110-112). The PFFs-induced models have been shown to recapitulate several key features of PD, including α-Syn inclusions, dopaminergic neurodegeneration, motor impairments, neuroinflammation and the propagation of α-Syn between interconnected brain regions, which is observed in PD. The propagation of α-Syn, and the formation of LB- and LN-like α-Syn inclusions, are features that are less prominent in transgenic or rAAV-mediated models, making the PFFs-induced models unique and suitable for investigating α-Syn propagation. However, a major limitation of the PFFs-induced model is that it is slow-progressing.

By varying the conditions during PFFs production from monomers, different strains of PFFs, with different seeding capacity, can be produced (113). The rationale of α-Syn fibril strains is supported by the observation that different synucleinopathies display α-Syn pathology in various cell types. PD, PD with dementia (PDD) and LB dementia (LBD) primarily show LB and LN inside neurons (38, 39) whereas in

multiple system atrophy (MSA), α-Syn pathology is primarily located inside oligodendrocytes (glial cytoplasmic inclusions) and Schwann cells (114, 115). Isolated α-Syn fibrils from LB or glial cytoplasmic inclusions were also shown to be conformational distinct; fibrils isolated from glial cytoplasmic inclusions was more potent in inducing α-Syn aggregation in primary oligodendrocytes overexpressing α-Syn (116). Indeed, using α-Syn fibrils with varying conformation has been shown to induce distinct synucleonpathies *in vivo* (117, 118).

Combined rAAV-a-Syn+PFFs models

The creation of a model combining rAAV-mediated α-Syn overexpression with seeding of PFFs was published in 2017 (119). The model was created to better recapitulate features of PD (120). In this model, rAAV6-α-Syn was injected into SNpc, followed by the injection of PFFs into SNpc four weeks later (119). The model created robust neuroinflammatory response within ten days following PFFs injection, robust α-Syn pathology, marked dopaminergic neurodegeneration accompanied by motor impairments.

Although α-Syn transgene overexpression can induce pS129 α-Syn inclusions in mice (121, 122), the pS129 α-Syn pathology is less extensive in the rAAV or PFFs models compared to the combined models (119, 120, 123), making the combined model the better choice for studying α-Syn pathology. Additionally, the use of rAAV-α-Syn alone requires expression levels that are approximately five times higher than endogenous α-Syn expression to induce significant neurodegeneration (121, 124, 125), which is not observed in PD. Ultimately, the combined model is more efficient in inducing neurodegeneration, PD-like α-Syn pathology, motor impairments, and neuroinflammatory response, using a reduced rAAV6 titer (119).

The congenic DA.VRA4 rats as a model to study MHCII variability

As stated previously, there is substantial evidence of the involvement of MHCII upregulation in PD and strong evidence for an adaptive immune response during disease progression. Since MHCII links the innate and adaptive immune system it is a protein of marked interest.

The VRA4 locus was identified as regulating MHCII levels in the CNS following ventral root avulsion, a model used to study degeneration of motor neurons (126), by linkage analysis following a cross between the DA and PVG rat strains (127). In a follow-up study the VRA4 locus was fine-mapped and the class II transactivator gene (*Ciita*) was identified to be the candidate gene underlaying altered MHCII levels (128). Additionally, a SNP in the human *CIITA* orthologue, affecting *CIITA* and *HLA* expression levels, was associated with an increased risk of MS, RA and myocardial infarction (128). The DA.VRA4 congenic strain was created by >10 generations of backcrossing of $PVG1^{AV1}$ to a DA background, selecting on carriers of the VRA4 allele from $PVG1^{AV1}$ (129). Thus, the DA.VRA4 congenic strain

carries the VRA4 locus from the PVG strain, but has an identical background genome (>99.9%) to the DA strain. Using the experimental autoimmune encephalomyelitis (EAE) model for MS, the DA.VRA4 congenic rats have been shown to have a milder disease course compared to DA rats (129). In contrast, the DA.VRA4 congenic rats have increased susceptibility, more neuroinflammation, and more neurodegeneration following rAAV6-α-Syn overexpression in SNpc compared to DA rats (130). These findings demonstrate that the effects of *Ciita* variants are context-dependent.

Epilepsy

Epilepsy is defined by two or more unprovoked seizures or one unprovoked seizure with a risk above 60% of a second seizure within ten years (based on e.g., structural lesions) (131). A seizure is defined as excessive and/or abnormal synchronized neuronal activity, and is a symptom of the disease epilepsy. Seizures are often transient, however, seizures occurring for a prolonged period are referred to as status epilepticus, which can be a life-threatening condition (132). The prevalence of epilepsy is around 0.7% (133) and has a bimodal distribution; it is more common in young and elderly individuals (134).

Etiology and classification of epilepsy

The reasons for developing epilepsy are diverse and composed of structural-, metabolic-, infectious-, genetic-, immune-, or unknown etiology (135). The etiologies are complex and can be related to each other. For example, structural etiology can be due to tumors, or trauma to the head, such as traumatic brain injury or stroke, but also due to infectious agents or developmental malformations.

Epilepsies are classified based on the origin, or onset, of the seizure (136) (**Figure 4**). Focal onset seizures are unilateral restricted to smaller region(s) of the brain and can be subdivided into aware or impaired awareness (136). Additionally, subgroups of focal seizures are categorized by the manifestations of motor or non-motor symptoms. In focal seizures symptoms vary greatly depending on the epileptic focus. For example, temporal lobe epilepsies (TLE) with nonmotor symptoms can induce sensations of fear, whereas TLE with motor symptoms may result in automatisms (repetitive movements) of hands and/or face. Focal onset seizures may also evolve, or propagate, to bilateral tonic-clonic seizures (often referred to as secondary generalized seizures).

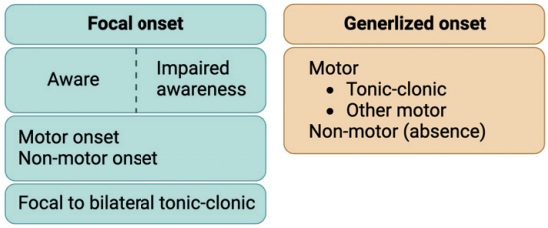

Figure 4. Basic classification of focal and generlized onset of seizure types.
Seizures with a focal onset occur with either impaired or unimpaired awarness, include motor or nonmotor onsets, and include seizures with a primary focal onset but develop into bileteral tonic-cloninc seizures. Generlized seizures are bilateral and involve large regions or the entire brain, and are motor (e.g., tonic-clonic) or non-motor (absence) seizures. Illustration created using BioRender.com and adapted from (136).

Generalized epilepsy is characterized by generalized seizures which occur with impaired awareness, bilateral and involves large portions or the entire brain. Generalized seizures can manifest as either motor or non-motor (absence seizures). Motor seizures, involves motoric movement, e.g., tonic-clonic seizures which are characterized by muscle tonus followed by rhythmic muscle jerks.

Treatment strategies

The first line of treatment for epilepsy is the use of anti-epileptic drugs (AEDs). AEDs are symptomatic, targeting the occurrence of seizures rather than the underlying cause. In addition, 30% of all epilepsy patients are treatment-resistant, defined as the failure to achieve seizure-freedom following trials of more than two adequately chosen AEDs, either in combination or as monotherapies (137).

Available AEDs work by altering neurophysiological functions in the CNS (reviewed in (138)). In general, the modes of actions are to modulate voltage-gated ion channels, increase synaptic inhibition, and/or inhibit synaptic excitation. If AEDs fail there are only a few options left to treat seizures, including dietary change, vagus nerve stimulation, or resective surgery of the epileptic focus (131). Of these, surgical resection is the most successful but only an option for a minority of patients since the epileptic focus have to be well-defined, additionally, the benefit needs to be carefully weighed against the consequence following resection.

Epilepsy and comorbidities

Comorbidities are common in individuals with epilepsy. Approximately 20% of all epilepsy patients are reported to be diagnosed with psychiatric disorders like anxiety and depression, which corresponds to a 2-3 fold increase compared to reference

populations (reviewed in (139)). Another common comorbidity of epilepsy is autism spectrum disorder (ASD), which has been reported to develop in 9% individuals with epilepsy (140). Similarly, epilepsy was reported to develop in 12% of individuals with ASD (140), several folds higher than the 0.7% prevalence in the general population (133). Individuals with epilepsy and/or ASD commonly suffer from sleep disturbances (reviewed in (141)). Common sleep disturbances are prolonged sleep latency (difficulties falling asleep) and/or maintaining sleep (142-144). Individuals with ASD and/or epilepsy commonly suffer from sleep disturbances, such as longer sleep latency and less cohesive sleep (141-150).

Inflammation in the pathophysiology of epilepsy

As illustrated earlier, the etiology of epilepsy is complex and diverse and is often observed together with inflammatory responses. Indeed, individuals with systemic autoimmune disease have a higher risk for epilepsy. A meta-analysis reported that individuals with systemic autoimmune diseases had a 2.5-fold risk of developing epilepsy compared to the reference population, with an elevated risk in individuals below the age of 20 (151).

The process from which a healthy brain is transformed into an epileptic brain is called epileptogenesis, a process which neuroinflammation is a major contributor to (**Figure 5**) (reviewed in (152)). Following an insult to the brain glial cells become activated to perform homeostatic functions such as limitation of damage and tissue regeneration. If the insult fails to be cleared the transient glial activation may become chronic. Chronic glial activation is associated with excessive amounts of proinflammatory cytokine release (e.g., IL-1β, TNF, or IL-6) and damage to the BBB. Chronic astrocyte activation is associated with ionic imbalance, failure to clear excitatory glutamate from the synaptic cleft and decreased production of the inhibitory neurotransmitter gamma-aminobutyric acid (GABA) (152, 153). The excessive production of proinflammatory cytokines by glial cells acts in paracrine and autocrine manners activating more glial cells, additionally, chronic microglia activation can induce neuronal dysfunction and degeneration (152). Collectively, the chronic glial-mediated neuroinflammatory response may induce neurodegeneration and induce hyperexcitability of neurons, leading to seizures, additionally, hyperexcitability can induce microglia activation, and neurodegeneration may activate glial cells through DAMPs (152), ultimately creating a positive feedback loop increasing the risk of seizures (**Figure 5**). Epileptogenesis is thus a complex process which involves neuroinflammatory mechanisms, and targeting the inflammatory response is an appealing strategy for modifying seizure development.

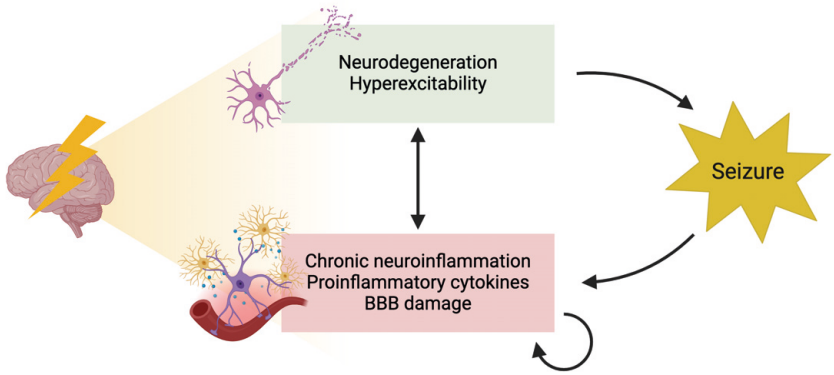

Figure 5. Illustration of epileptogenesis following brain insult resulting in neuroinflammatory response, neurodegeneration, and hyperexcitability, ultimately leading to seizure.
Brain insults may lead to neurodegeneration and neuroinflammation. Chronic neuroinflammation results in BBB damage, execissve cytokine production (e.g., IL-6, IL-1β, and TNF), ionic imbalance, and reduced glutamate uptake. Chronic neuroinflammation results in neurodegenreation and hyperexcitability, which in turn sustain neuroinflammation. Neurodegeneration and hyperexcitability may result in seizures which also increases neuroinflammation. Figure created with BioRender.com and adapted from (152). **Abbreviations**. BBB, blood-brain barrier; IL, interleukin; TNF, tumor necrosis factor.

In experimental models of epilepsy (briefly introduced later) targeting inflammatory processes has indeed been successful, e.g., by inhibition of IL-1 receptor (IL-1R) and toll-like receptor (TLR, a PRR) signaling (reviewed in (154). Cortical injection of LPS into rats can cause epileptiform activity, which could be inhibited by inhibiting TLR-4 signaling (a PRR for LPS), or using an IL-1R antagonist (155). Similarly, another study using lithium-pilocarpine induced epilepsy demonstrated that IL-1R antagonists, blocking IL-1β signaling, protected against BBB breakdown and reduced overall number of rats with SE (156). Additionally, targeting the JAK/STAT3 signaling pathway, of which IL-6 (among other) cytokines signal (**Figure 1**), reduced severity and frequency following pilocarpine-induced epileptic seizures but, surprisingly, without protecting against neurodegeneration (157)

In addition to neuroinflammatory changes, epilepsy is also associated with changes in the peripheral immune system. Infiltration of leukocytes into the CNS and epileptic focus has also been reported in humans and preclinical models of epilepsy (158-160), indicating a role of the peripheral immune system in epilepsy. In experimental epilepsy, pilocarpine-induced BBB disruption, seizures, and neurodegeneration could be protected by blocking leukocyte migration or by depleting neutrophils in mice (159). In contrast, kainate injection into the hippocampus of immunodeficient mice (RAG1 knockout (KO), T- and B-cell deficient) mice caused a delay in neutrophil infiltration into the CNS which exacerbated seizure load and neurodegeneration (158). The RAG1 KO mice also had an earlier onset of spontaneous recurrent seizures indicating a protective, rather

than detrimental, effect of the adaptive immune system in experimental epilepsy (158). In humans, infiltration of lymphocytes is observed in epileptic post-mortem brains (reviewed in (160)). In TLE, CD8+ rather than CD4+ T cells are reported to infiltrate following seizures (158, 160). Due to the heterogeneity of patients, data on peripheral cytokine levels are lacking, however, TLE has been associated with elevated IL-6 levels in blood following seizures in multiple studies (161-163). Collectively, more research is needed to elucidate the role of peripheral immune system on epileptogenesis.

In vivo models for epilepsy

There are numerous *in vivo* models to study epilepsy. In the context of this thesis the genetic *Syn2* KO mouse model is of main interest and the focus of the following section.

Acquired models of epilepsy – induction by chemicals or electricity

Some of the most common models of epilepsy are the kainate- and pilocarpine-induced models. Kainate is a kainate receptor agonist whereas pilocarpine is a muscarinic acetylcholine receptor agonist. Both models can be induced by systemic administration or stereotaxic injections into the brain (reviewed in (164, 165)). Following administration, SE is induced within minutes to hours, a period often accompanied by loss of experimental animals. It takes a few days to several weeks following kainate- or pilocarpine-induced SE (latent period) before rodents develop spontaneous recurrent seizures (SRS).

Another approach to induce seizures by electrical kindling, which is achieved by recurrent electrical stimulation using sub-convulsive current in a specific region of the brain, e.g., the hippocampus. Repeated electrical stimulation reduces the seizure threshold and eventually cause seizures. It has been proposed that the kindling model is better described as a model for epileptogenesis, since the kindling procedure allows for investigation of temporal mechanism during progressive reduction of the seizure threshold (164).

The Synapsin II knockout model of epilepsy and ASD

Synapsins are a family of proteins important for the regulation of neurotransmitter vesicles at the synapses. KO of *Syn1* and *Syn2* but not *Syn3* causes epileptic seizures in mice (166). Additionally, *Syn1* and *Syn2* KO results in ASD-like behavior, with *Syn2* KO showing more severe ASD-like behavior (167, 168). Mutations or SNPs in human *SYN* genes also result in epilepsy and/or ASD (reviewed in (169)). Mutations in the *SYN1* gene, located on the X chromosome, may cause both epilepsy and ASD, depending on mutation (170, 171). Additionally, a SNP in *SYN2* is associated with elevated risk of developing epilepsy (172) whereas loss-of-function

mutations in *SYN2* leads to ASD (173). Collectively, this highlights the relevance of using the *Syn2* KO mouse model to study both epilepsy and ASD-related behavior, which are often observed as comorbidities.

The *Syn2* KO mice develop handling-induced seizures starting around two months of age (174, 175). The seizure semiology (the clinical manifestation of a seizure) of *Syn2* KO mice is orofacial and forelimb twitching followed by truncal tonic flexion, truncal tonic extension, and lastly orofacial and forelimb myoclonus (174, 175). Based on the seizure semiology, the *Syn2* KO mice are suspected to have focal to bilateral tonic-clonic seizures, with a temporal lobe onset. *Ex vivo* recordings of hippocampal slices from *Syn2* KO mice have shown reduced presynaptic asynchronous GABA release, contributing to reduced tonic inhibition, ultimately increasing excitability (176). Additionally, the use of a GABA receptor agonist rescued epileptic seizures in a small cohort of *Syn2* KO mice (176). Because the *Syn2* KO mice develop epileptic seizures starting from around two months of age, it makes them a suitable model to study epileptogenesis. Indeed, *Syn2* KO mice have been shown to have alterations in excitatory/inhibitory (E/I) synaptic proteins during the epileptogenic phase in addition to a more inflammatory prone microglia profile and elevated levels of TNF and IL-6 (175). Collectively, these findings suggest that neuroinflammatory processes may contribute to the epileptogenesis in *Syn2* KO mice.

Association between Parkinson's disease and epilepsy

Due to the diverse etiology of epilepsy, it is commonly observed as a comorbidity to other neurological diseases and conditions. Approximately 10-20% of patients with Alzheimer's disease develop epilepsy, with an elevated risk of seizures in early onset Alzheimer's disease (177). The incidence of epilepsy in PD patients is less studied, however, a retrospective cohort study reported a positive association between epileptic seizures in PD patients (odds ratio of 2.2), with a stronger association in PD patients with dementia (odds ratio of 10) (178).

A recent retrospective cohort study identified epilepsy as a risk factor for PD, findings that were replicated in another data set (179). In a follow-up study the authors found a positive association of AEDs and the risk of PD (180). The authors highlight several key findings which support the hypothesis that AEDs increases PD risk. In rats, chronic carbamazepine and valproate treatment resulted in downregulation of dopaminergic receptors (181, 182). Additionally, a case study of valproate-induced parkinsonism reported that cessation of valproate resulted in remission of symptoms, however, both cases were later diagnosed with PD (183). Thus, it is possible that genetic risk factors of PD, or that prodromal PD, is exacerbated following treatment with AEDs. However, larger replication studies are

still necessary to confirm if the use of AEDs indeed increases PD risk and to exclude the possibility of AEDs inducing parkinsonism.

Commonalities and differences in immune responses between Parkinson's disease and epilepsy

Immune mechanisms play a crucial role in the pathophysiology of both PD and epilepsy. Both diseases are characterized by neuroinflammation, including the activation of glial cells and the production of proinflammatory cytokines, processes associated with neurodegeneration. Additionally, leukocyte infiltration into the CNS is observed in both conditions. Adaptive immune responses may influence disease progression; while autoimmune epilepsy, defined by autoantibodies, is a distinct category (not covered in this thesis), the role of infiltrating adaptive immune cells in some epilepsies, such as TLE, and in PD requires further investigation. Despite several commonalities, questions remain about the exact contribution of immune mechanisms to disease susceptibility and progression. Specifically, the central role of immune responses warrants further investigation into their contribution to epileptogenesis and the susceptibility and progression of PD.

Aims of the thesis

The overall aim of this thesis was to explore immune mechanisms in Parkinson's disease and epilepsy to enhance the understanding of disease susceptibility and progression.

The major aims of the thesis were:

- To investigate how genetic variants of the class II transactivator influence the susceptibility and progression of Parkinson's disease using an *in vivo* model (**Paper I**)
- To characterize immune cell populations and peripheral cytokine levels in an experimental Parkinson's disease model (**Paper II**)
- To study the effects of systemic immunomodulation on Parkinson's disease (**Paper III**) and epilepsy (**Paper IV**) using experimental *in vivo* models

Methodological considerations

The following are considerations of some methodologies used in **Papers I-IV** included in this thesis. For complete details on methodological procedures, readers are encouraged to refer to the full texts of the papers.

All experimental procedures involving laboratory animals was conducted in accordance with ethics permits approved by the local ethics committee in the Malmö – Lund region.

Murine strains used for preclinical research on Parkinson's disease and epilepsy

DA and congenic DA.VRA4 rats

As illustrated in the introduction, the role of immune responses in PD is evident, which makes the DA and the congenic DA.VRA4 strains of particular interest to study idiopathic PD. Collectively, the following findings highlights a role of the adaptive immune response in PD; coding and non-coding *HLA* variants have been associated with PD risk (48, 51, 53-55), T cells infiltrate into the brain parenchyma in PD (79), and the presence of α-Syn reactive T cells in circulation of PD patients (56). The observation of reactive microglia in post-mortem PD brains also strengthens the role of microglia on PD progression (73). Additionally, DA.VRA4 rats have a more activated phenotype of microglia compared to DA rats following nigral rAAV-6-α-Syn injection (130). Collectively, this makes the DA and DA.VRA4 a highly relevant model system to study the effects of *Ciita* variants on PD-like susceptibility and progression.

Throughout **Papers I-III** we used young (~3 months old) male rats at inclusion. These choices hold practical, financial, and ethical importance. Including young rats in the study shortens their time spent in animal facilities, aligning with the 3Rs principle of refinement. PD is more common in males (34, 184), justifying the inclusion of male rats. Using only one sex reduces the total number of rats required, aligning with the 3Rs principle of reduction. However, these choices have limitations. PD is primarily an aging disorder (34), and the validity of studying

relatively young rats can thus be questioned since inflammaging likely plays a pivotal role in disease progression (185). Additionally, the immune system differs between sexes, and recent studies report sexual dimorphisms in circulating monocyte subpopulations in PD (83-86). Therefore, including both sexes in PD research is important. Despite these complexities, the choices made in **Papers I-III** strike a balance between disease relevance, costs, practicality, and ethical considerations.

A common experimental approach to study the role of the immune system in PD models are by genetic manipulation creating KO strains of e.g., MHCII-related genes (186-188). This approach is valid in a context of experimental research as it allows for very specific research questions to be addressed; however, the translatability of such research is limited since mutations in *CIITA* or transcription factors for MHCII causes bare lymphocyte syndrome in humans (189). In other words, the normal function of the immune system has been compromised. The less common, but more elegant, approach is modulating expression levels using short hairpin RNA, e.g., silencing *Ciita* (187). Still, the use of the congenic DA.VRA4 allows for a more physiologically and translationally relevant model, as a normal development and function of the immune system is retained, and human orthologous of *CIITA* alter susceptibility to complex inflammatory disease with adaptive immune components, like RA and MS (128).

Syn2 KO mice

In **Paper IV** we used the *Syn2* KO mouse model to study mild genetic stress-induced seizures and ASD-like behavior (167, 168, 174). The *Syn2* KO mice as a model for both epilepsy and ASD-like behavior has high construct validity as mutations in *Synapsin* genes causes epilepsy and/or ASD (169). The *Syn2* KO mice develop handling-induced seizures starting around two to three months of age, making them suitable for studying epilepsy development. An alternative model is the *Cntnap2* KO mice, which also develop epileptic seizures and ASD-like behavior (190). The *Cntnap2* KO mice also have high construct validity since a nonsense mutation in *CNTNAP2* causes cortical dysplasia, focal epilepsy, and ASD (191). However, *Cntnap2* KO mouse is a model of severe epilepsy associated with cortical dysplasia, with seizures starting around six months of age (190). Therefore, *Syn2* KO mice are preferable for studying milder epilepsy with earlier seizure onset, which also aligns with the ethical principles of the 3Rs refinement, allowing for reduced study durations.

Epilepsy is slightly more common in males compared to females (133). In **Paper IV**, we included both male and female *Syn2* KO mice to better reflect the human situation. While ASD is more commonly diagnosed in men, there is a growing body of evidence suggesting that women with ASD have been misdiagnosed,

underdiagnosed, or overlooked (192-194). Thus, we included *Syn2* KO mice of both sexes in our study to address this potential bias.

Combining nigral rAAV6-α-Syn mediated overexpression with striatal seeding with PFFs to model Parkinson's disease

Considerations of using rAAV6 constructs and their respective controls

Since the first rAAV-α-Syn based models were developed, various constructs with slightly different designs have been published (reviewed in (99, 106, 110, 111, 195, 196)). These designs differ in several aspects; AAV serotype, promotor, and enhancer elements, all of which affect transgene expression efficiency. Additionally, several other factors can influence transgene expression and/or the results, including the choice of murine species, strains, age, the choice of wt or mutant α-Syn transgene (and origin), viral capsid titer (i.e., the number of capsids injected containing the construct), batch effects, and the duration from rAAV injection to phenotyping.

In **Papers I-III** we used an rAAV6 vector designed to enhance α-Syn transgene expression (124). Human α-Syn expression was driven by the synapsin 1 promotor for neuron-specific expression and enhanced with the woodchuck hepatitis virus posttranscriptional regulatory element (WPRE) motif (**Figure 6A**). Indeed, the use of the synapsin 1 promotor and inclusion of WPRE greatly increased the dopaminergic neurodegeneration and caused subsequent motor deficits compared to an rAAV6 construct driving transgene expression using the chicken β-actin promotor without the WPRE following injections into rat SNpc (124).

Control vectors are crucial in rAAV-mediated transgene overexpression studies because rAAV capsids alone can elicit an immune response (106). Proper controls are necessary to assess the specific contribution of the transgene. However, control vectors cannot account for synergistic effects from rAAV injection and α-Syn transgene overexpression. The most common control vector is the rAAV-GFP, allowing for easy visualization by IHC assessment. In **Paper I**, we used an rAAV6-GFP as control vector (**Figure 6B**). However, rAAV-GFP has been shown to induce both neurodegeneration (123, 197, 198) and inflammatory responses (130, 153, 199, 200), which we also observed in **Paper I**.

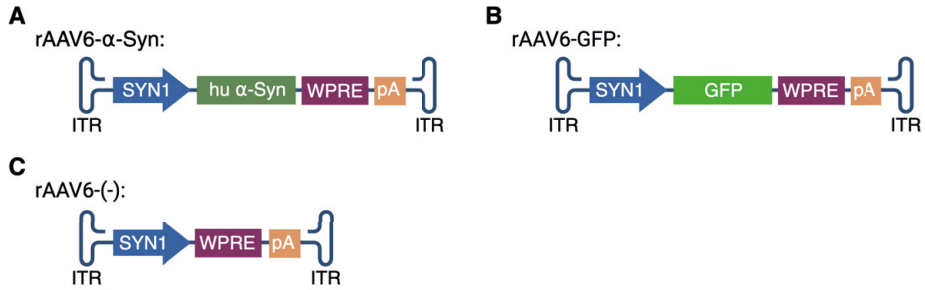

Figure 6. Deisgns of the rAAV6 viral vectors used in Papers I-III.
(**A**) The vector design to overexpress hu α-Syn in SNpc in **Papers I-III**. (**B**) The design of the control vector used in **Paper I**. (**C**) The design of the control vector used in **Paper II**. Illustrations created using BioRender.com. **Abbreviations**. rAAV6, recombinant adeno-associated virus serotype 6; hu, human; α-Syn, α-Synuclein; ITR, internal repeats; SYN1, synapsin 1; WPRE, woodchuck hepatitis virus posttranscriptional regulatory element; pA, poly A tail; GFP, green fluorescent protein; SNpc, substantia nigra pars compacta.

To avoid rAAV6-GFP-induced neuroinflammation and possible neurodegeneration in **Paper II**, we used the rAAV6-α-Syn vector (**Figure 6A**), but with the human α-Syn transgene excised (referred to as rAAV6-(-)) as control (**Figure 6C**). While we did not quantify the response using IHC, qualitative assessments in **Paper II** showed no obvious signs of neurodegeneration following the use of rAAV6-(-). The rAAV6-(-) vector cannot control for a transgene overexpression, however, it still controls for the possible capsid- and vector-induced responses following injection.

Alternative controls for transgene expression include encoding a scrambled protein of similar length to the transgene of interest (e.g., 140 amino acids for full-length α-Syn), which would control for transgene overexpression but complicate IHC visualization. Other suggestions include using non-toxic oligomerizing mammalian proteins like actin and collagen (201). To my knowledge, the use of such controls has never been published. It is important to consider that exogenous collagen injections are used to model RA in rodents, and although these models require genetically susceptible strains and adjuvants to induce prevalent autoimmune responses (202) it is not guaranteed that overexpression of collagen in the CNS would not be immunogenic.

Based on current literature the control vectors used in rAAV-mediated α-Syn overexpression models are suboptimal and requires further development.

Considerations of using PFFs and their respective controls

The PFFs models have been used in a wide variety of ways to study α-Syn propagation (112). Multiple parameters can be varied to affect the results of the studies including origin of PFFs (mouse/rat/human), site of injection, the amount of PFFs injected, and the total time from PFFs injection until phenotyping.

Additionally, murine species, sex, and age are also factors to consider. Another important consideration, is the batch-effect which has been shown to vary greatly highlighting the importance of not using different batches of PFFs within the same experiments. Indeed, by varying the conditions used when creating PFFs, different PFFs strains can be produced (113, 203), which, as described in the introduction, can induce distinct synucleinopathies *in vivo* (117, 118).

A major limitation of the PFFs-induced models is the slow progression, as significant neurodegeneration is often observed starting around six months post injection (99). Even if the slow progression indeed recapitulates the slow progression observed in PD (34), it is less practical, costs more and ultimately require the murine subjects used to be caged for a longer period which is an important consideration from an ethical standpoint.

Proper controls for the PFFs are also an important consideration. In **Paper I** we used BSA to control for PFFs. Although it is difficult to delineate from the results, it is possible that the BSA caused an immune reaction. To avoid this risk, we chose to use vehicle (DPBS) as a control for the PFFs in **Paper II**. Injection of DBPS will not, however, control for the injection of a foreign protein. One might consider the same control as suggested for rAAV-mediated models, oligomeric actin or collagen, but the same caveats as discussed above, remain. Indeed, the most proper control for PFFs is likely the injection of α-Syn monomers, ideally batch-matched to the PFFs injected, which would control for the injection of foreign protein. However, a few studies have reported that vehicle or untreated conditions are comparable to monomers in different experimental setups, both *in vitro* and *in vivo* (21, 109, 204). Collectively, I believe the DPBS to be the better choice over BSA, whereas α-Syn monomers should be selected as the control in future studies.

Considerations of the combined rAAV+PFFs model

The combined rAAV+PFFs model is an attractive model for several reasons; it efficiently recapitulates multiple features of PD; neurodegeneration, α-Syn pathology, and neuroinflammation, over a short period. One of the major benefits with the combined model is the more extensive α-Syn pathology induced compared to the rAAV or PFFs models. Even if α-Syn transgene overexpression (wt and A53T human variants) alone can induce pS129 α-Syn inclusions in mice (121, 122), the pS129 α-Syn pathology more extensive in the combined models (119, 120, 123), thus making the combined model the better choice for studying α-Syn pathology. To this regard we chose to use the combined model in **Papers I-III**. However, we made some minor adjustments compared to the original model (119). We injected the rAAV6 constructs into the SNpc followed by striatal PFFs injections two weeks later (**Figure 7**). The rationale of injecting PFFs into the dorsal striatum was to recapitulate the observed mechanism of α-Syn pathology spreading through retrograde transport (108, 205, 206). By spacing the rAAV6-α-Syn and PFFs

injections two weeks apart, we reasoned that a stable transgene overexpression should have been established, allowing the recipient neurons to transcribe and translate human α-Syn prior to PFFs injection. In **Paper I**, we injected a total of 10 µg of PFFs at two separate locations (5 µg/location) to cover more of the dorsal striatum (**Figure 7B**). In **Papers II** and **III** we chose to reduce the PFFs concentration to 7.5 µg, injected only at one site in the dorsal striatum (**Figure 7C-D**). Since it has been reported that a single dopaminergic neuron in the SNpc can innervate up to an astonishing 5.7% of the striatum volume (207), even a single site injection of PFFs was considered sufficient to affect enough dopaminergic neurons to induce significant neurodegeneration, neuroinflammation, and α-Syn pathology. Indeed, the results of **Papers I** and **III** showed a similar extent of neurodegeneration (discussed later). Details on injection coordinates, rAAV6 titers and PFFs concentrations are specified in **Table 1**.

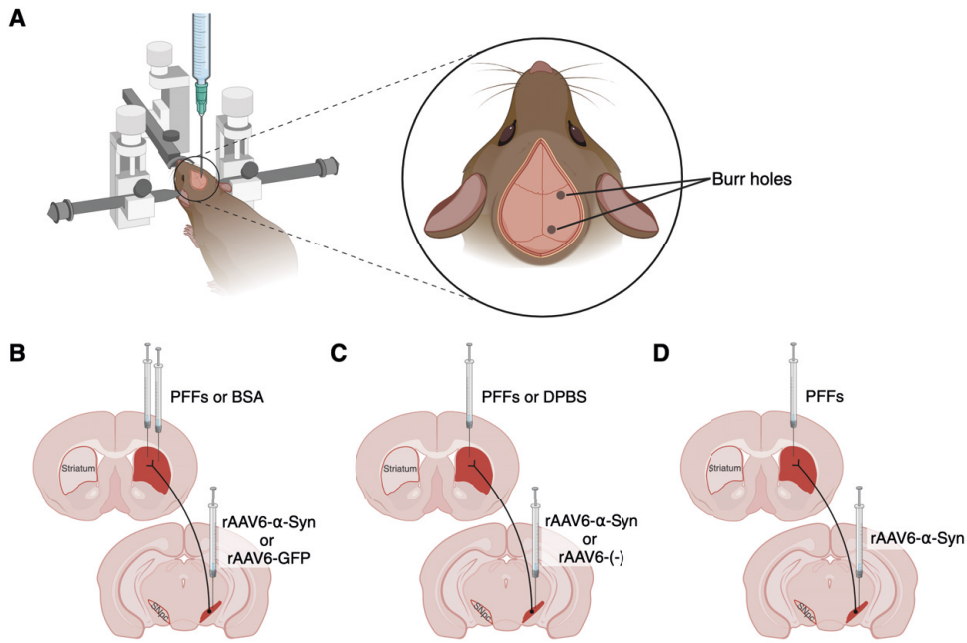

Figure 7. Schematic illustration of stereotaxic surgery, injection sites of rAAV constructs and PFFs, with their respective controls, used in Papers I-III.
(**A**) Illustration of the sterotaxic set-up used for injections of rAAV and PFFs in **Papers I-III** (**B**) In **Paper I** rAAV6-α-Syn or rAAV6-GFP was injected into SNpc followed by two striatal PFFs or BSA injections two weeks later. (**C**) In **Paper II** rAAV6-α-Syn or rAAV6-(-) was injected into SNpc followed by a striatal PFFs or DBPS injection two weeks later. (**D**) In **Paper III** rAAV6-α-Syn was injected into SNpc followed by a striatal PFFs injection two weeks later. Illustrations were created using BioRender.com.
Abbreviations. PFFs, preformed fibrils; BSA, bovine serum albumin; SNpc, substantia nigra pars compacta; rAAV6, recombinant adeno-associated virus serotype 6; α-Syn, α-Synuclein; GFP, green fluorescent protein; DPBS, Dulbecco's phosphate buffered saline.

Table 1. Overview of rAAV6 construct, titers, PFFs amount and stereotaxic coordinates used in Papers I-III

Throughout **Papers I-III** slight modifications were made in the model design. rAAV6-α-Syn titers differ due to the use of different batches in **Paper I** and **Papers II** and **III**. rAAV6 titers were determined by ITR-based qPCR. All injections were made unilateral in the right hemisphere.

Paper	rAAV vector	rAAV titer	SNpc coord.	PFFs amount	Striatum coord.
I	rAAV6-α-Syn	1.02E+10 gc/µl	A/P: -5.3 M/L: ±1.7 D/V: -7.2	5 µg	A/P: +0.1 M/L: ±3.0 D/V: -5.0
	rAAV6-GFP	1.02E+10 gc/µl		5 µg	A/P: -0.4 M/L: ±3.0 D/V: -4.5
II	rAAV6-α-Syn	1.30E+10 gc/µl	A/P: -5.3 M/L: ±1.7 D/V: -7.2	7.5 µg	A/P: -0.4 M/L: ±3.0 D/V: -4.5
	rAAV6-(-)	1.70E+10 gc/µl			
III	rAAV6-α-Syn	1.30E+10 gc/µl	A/P: -5.3 M/L: ±1.7 D/V: -7.2	7.5 µg	A/P: -0.4 M/L: ±3.0 D/V: -4.5

Abbreviations. rAAV6, recombinante adeno-associated virus serotype 6; PFFs, preformed fibrils; α-Syn, α-Synuclein; SNpc, substantia nigra pars compacta; coord., Bregma coordinates; gc, genomic copies; A/P; anterior/posterior; M/L, medial/lateral; D/V, dorsal/ventral;GFP, green fluorescent protein.

Throughout **Papers I-III** we used human α-Syn, both as a transgene and PFFs. Previous work has reported that species homology is essential in inducing efficient PD-like pathology following PFFs injection. Using human PFFs in mice is suboptimal compared to using mouse PFFs (208, 209). To my knowledge, the optimal inducer of α-Syn pathology in rats has yet to be assessed, however a study from 2021 reported that mouse, rather than rat, PFFs were a more potent inducer of α-Syn pathology, but similar in inducing neurodegeneration (210). Therefore, it is possible that either mouse or human PFFs are the best options for efficient PD-like pathology in rats. The lack of studies using rAAV-mediated murine-derived α-Syn overexpression further support the choice of exclusively using human α-Syn, both as PFFs and transgene.

It has recently been shown that sequential rAAV and PFFs injections is not necessary to induce a potent PD-like model (123). The authors demonstrate that features of neurodegeneration, neuroinflammation, motor deficits, and α-Syn pathology are similar following sequential or simultaneous rAAV and PFFs SNpc injections in rats (123). In contrast, comparing sequential or simultaneous injections of rAAV-α-Syn and PFFs into the SNpc of mice, showed that the simultaneous injections were more potent in inducing neurodegeneration and motor deficits, however, this is unpublished data that is only commented on in a review (120). Collectively, these findings suggest that combining the injections of rAAV and PFFs into SNpc is the superior alternative since it requires only one stereotaxic injection, avoiding immune responses following physical damage caused by two injections, more time efficient, and is better form an ethical point of view. Indeed, future studies should consider using the simultaneous rAAV+PFFs model instead.

Lastly, based on findings in **Paper III**, it is possible that systematic errors were introduced during stereotaxic injections. The peak TH+ axonal fiber density loss observed in **Paper III** was more caudal to the intended PFFs injection coordinate. Indeed, needle tracts in the midbrain also suggest that injections were placed more caudal than intended (data not shown). A possible cause is that the stereotaxic coordinates have been based on SD rats, whereas we use rats of DA background throughout **Papers I-III**. The DA strain is significantly smaller compared to the SD rats, based on growth curves provided by Janvier labs SD males weights approximately twice as much compared to DA males at 12 weeks of age. Indeed, it is possible that the DA rat brains are smaller which would result in more caudal injections relative to Bregma. This calls for the attention of producing strain-specific brain atlases to improve reproducibility of results across strains. Indeed, the first brain atlas of athymic nude rats was recently published (211).

Experimental designs

Papers I-III | Experimental designs to study the effects of *Ciita* variants on experimental Parkinson's disease

The experimental designs used to study the role of *Ciita* variants in the context of PD-like pathology were similar in the general induction of the model, but differed depending on the research questions. It is crucial to note that throughout this thesis, all time points for **Papers I-III** are set following rAAV6 injection into SNpc, PFFs were always injected two weeks later.

In **Paper I** the aim was to study *Ciita* variants in the context of susceptibility and disease progression following α-Syn-induced PD-like pathology, assessing the contribution of substrate (rAAV-α-Syn) versus seed (PFFs), ultimately resulting in a total of six groups, and a total of 60 rats (10 rats per group) (**Figure 8**). The main considerations regarding the experimental design for **Paper I** have been discussed previously (the use of appropriate controls). Improvements are always possible and in retrospect the inclusion of naïve rats would have been interesting to gain more knowledge on region-dependent immune markers prior to the induction of the model.

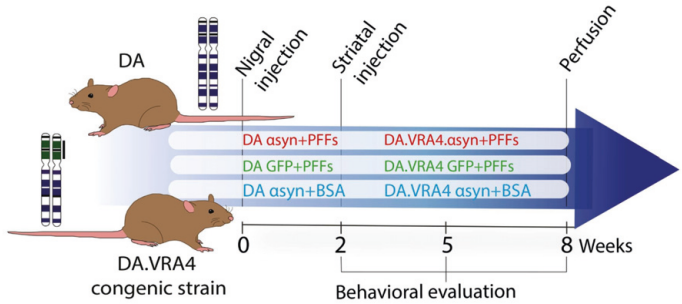

Figure 8. Experimental design of Paper I.
DA rats and congenic DA.VRA4 with naturally occuring *Ciita* variants were unilaterally injected in SNpc with rAAV6-α-Syn or rAAV6-GFP followed by unilateral injections of PFFs or BSA, two weeks later. Behavior (stepping test) was evaluated at three timepoints during the study. Rats were euthanised at the eight-week timepoint and brains collected for IHC analyses. **Abbreviations**. α-Syn/αsyn, α-Synuclein; PFFs, preformed fibrils; GFP, green fluorescent protein; BSA, bovine serum albumin; SNpc, substantia nigra pars compacta; rAAV6, recombinant adeno-associated virus serotype 6.

In **Paper II** the aim was to characterize the effects of *Ciita* variants on major immune cell population in naïve rats, and in rats following rAAV6-α-Syn+PFFs injection at two different timepoints using flow cytometry (**Figure 9**). CSF and serum cytokines were also investigated over time. A total of 77 rats was included and distributed in ten groups, of 6-9 rats per group. The major considerations regarding **Paper II** are related to the flow cytometry experiments; antibody panel used and the choice of analyzing cells isolated from entire brain hemispheres, which are discussed later.

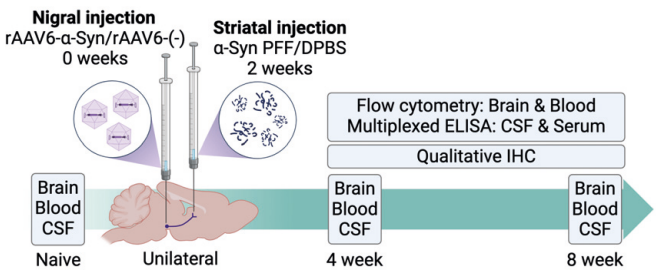

Figure 9. Experimental design of Paper II.
Unilateral PD-like pathology was induced by rAAV6-α-Syn injection in SNpc followed by striatal injection of PFFs two weeks later. Brain,blood, and CSF was collected in naïve rats, as well as four- and eight weeks following rAAV6 injection. Brain (hemispheres) and blood was analyzed by flow cytometry and serum and CSF assessed by multiplxed ELISA. The model was assessed by qualitative IHC. Illustration was created using BioRender.com. **Abbreviations**. rAAV6, recombinant adeno-associated virus serotype 6; α-Syn, α-Synuclein; PFF/PFFs, preformed fibrils; DPBS, Dulbecco's phosphate buffered saline; ELISA, enzyme-linked immunosorbent assay; CSF, cerebrospinal fluid; IHC, immunohistochemistry; PD, Parkinson's disease; SNpc, substantia nigra pars compacta.

In **Paper III** we followed up on findings from **Paper II** showing that congenic DA.VRA4 rats had consistently higher sTNF levels in serum. Here, we aimed to investigate if sTNF inhibition, using the DN-TNF variant XPro1595, would protect against α-Syn-induced PD-like pathology in DA.VRA4 congenic rats. Rats were treated subcutaneous with 10 mg/kg of XPro1595 (or saline as control) every third day, starting from week one (**Figure 10**). A total of 20 rats was included and equally divided into the two groups. Based on the results from **Paper III** it is possible that the sTNF inhibition treatment should have started before or at the time of rAAV6-α-Syn (discussed in more detail later). Additionally, controls for the rAAV6-α-Syn vector and PFFs would have been beneficial to strengthen the conclusions based on α-Syn specific responses. We are currently working on including the two DA.VRA4 rAAV-(-)+DPBS controls from the eight-week time point that were saved for IHC analyses from **Paper II**.

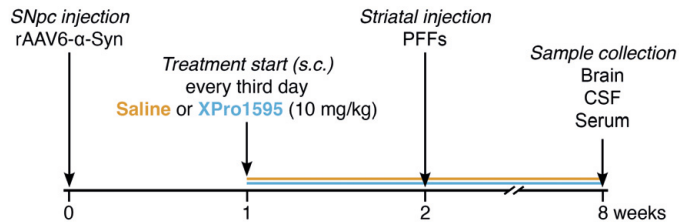

Figure 10. Experimental design of Paper III.
Unilateral PD-like pathology was induced by rAAV6-α-Syn injection in SNpc followed by striatal injection of PFFs two weeks later. Systemic sTNF treatment using XPro1595 was started at the one week timepoint. Rats were euthanised at eigtht weeks following rAAV-α-Syn injection and brains were collected for IHC analyses. CSF and serum was collected for assessment of XPro1595 and cytokine levels. **Abbreviations**. SNpc, substantia nigra pars compacta; rAAV6, recombinant adeno-associated virus serotype 6; α-Syn, α-Synuclein; s.c., subcutaneous; PFFs, preformed fibrils; CSF, cerebrospinal fluid; PD, Parkinson's disease; sTNF, soluble tumor necrosis factor; IHC, immunohistochemistry.

Paper IV | Experimental design to study the role of systemic IL-6R antibody treatment in *Syn2* KO mice with seizures and ASD-like behavior

In **Paper IV** the aim was to study the impact of systemic IL-6R ab treatment in *Syn2* KO mice initiated before, or after, epilepsy debut, and to evaluate behaviors related to spatial memory and anxiety (**Figure 11**). *Syn2* KO mice received weekly i.p. injections of IL-6R ab (200-250 µg corresponding to ~8-10 mg/kg) or vehicle (saline) as control. In the original study design only two groups were included, the "Early (early & late beh)" and "Late (late beh)" (**Figure 11**). However, since the *Syn2* KO mice develop stress-induced seizures, which are induced by handling, the behavioral tests are confounders possibly influencing seizure frequency and development. Several scenarios are possible in regards to the confounding effects.

The mice may become more stressed due to the increased frequency of animal-experimenter interactions necessary to perform behavioral tests (212). In contrast, it is also possible that the mice become habituated to the experimenter, ultimately inducing less stress and therefore developing fewer handling-induced seizures. One might even consider some of the tests (e.g., social interaction, Barnes maze, or the Y-maze) used in **Paper IV** as environmental enrichments. Indeed, environmental enrichments encouraging physical exercise (e.g., running wheels and/or tunnels) have been shown to reduce seizure burden in genetic and chemically-induced murine epilepsy models (213-218). Due to the likely confounding effects a third group receiving IL-6R ab treatment prior to seizure debut was included, but without performing any behavioral tests. A total of 117 *Syn2* KO mice and 13 C57Bl/6J mice was included in the study. C57Bl/6J mice were used in the social interaction test and as controls for actigraphy measurements.

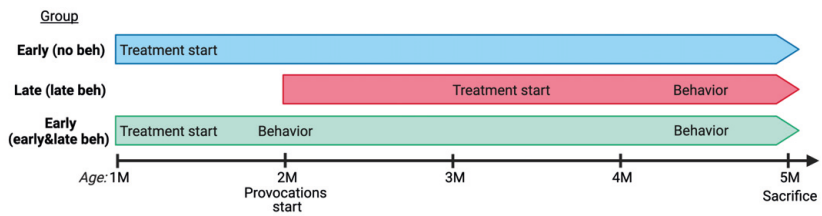

Figure 11. Experimental design of Paper IV.
Three different groups were included in **Paper IV**. Two groups were systemically treated with IL-6R ab starting at one months of age, prior to seizure debut (Early groups). In another group, IL-6R ab treatment started after seizure debut, around thre months of age (Late group). Behavioral tests to investigate social interaction, memory, and anxiety was evaluated in one "Early" and the "Late" group. Vehicle (saline) was used as a control for IL-6R ab treatment.

The steps taken to minimize confounders in **Paper IV** were warranted and ultimately led to high-quality data (25 saline versus 30 IL-6R ab treated) to evaluate the effects of IL-6R ab treatment on seizure development. In retrospect, behavioral testing requiring substantial animal-experiment interactions should have been avoided, or alternatively, the number of behavioral tests reduced.

Behavioral analyses

In **Paper I** motor deficits were evaluated whereas in **Paper IV** several behaviors were investigated, including; social interaction, spatial memory, anxiety and depression-like behavior, and actigraphy measurements.

To avoid biases and increased variations introduced by a researcher scoring behaviors manually, I implemented, when possible, the use of automated behavioral

analyses using the AnyMaze software. The AnyMaze software was used to perform automated analyses of the Barnes maze, Y-maze, open field, and forced swim test in **Paper IV**. A general limitation of the spatial memory tests and the anxiety- and depressive-like behavioral tests used in **Paper IV** is that they have, to my knowledge, not yet been used to study the behavior of *Syn2* KO mice compared to C57Bl/6J mice. Thus, we cannot be certain that the observed alterations in synaptic proteins and inflammation in the temporal lobe regions of *Syn2* KO mice (175) causes deficits in spatial learning and memory retention or that they recapitulate the observed comorbidity of anxiety disorders present in individuals with epilepsy or ASD (219, 220).

Stepping test

In **Paper I** we used the stepping test to assess motor deficits following rAAV6-α-Syn+PFFs injections. The stepping test was created to meet the need of a test to assess spontaneous, rather than drug-induced (e.g., amphetamine- or apomorphine-induced rotations), motor behavior (221). Five years later the cylinder test was published (222), which is another common test for spontaneous motor behavior in rodents. The stepping test requires substantial animal-experimenter interaction to yield high-quality results, animals are pre-habituated and trained for three consecutive days, which is not required in the cylinder test. Therefore, the cylinder test may be the preferred choice of the two tests. However, the stepping test was shown to be less variable compared to the cylinder test following combined rAAV-α-Syn and PFFs injections (119). Consequently, the stepping test was used in **Paper I**.

Motor behaviors were not investigated in **Papers II** and **III**. For **Paper II** we reasoned that it would not give us any additional insights since the test had already been conducted at different time points in **Paper I**. In **Paper III** it would have been of great importance to follow up and include motor assessment if the sTNF inhibitor had shown any protective effects on neurodegeneration.

Social interaction

ASD is characterized by impaired social behavior. The *Syn2* KO mice model has been shown to display social impairments in several different sociability tests (167, 168). To assess the effect from systemic IL-6R ab treatment on sociability of *Syn2* KO mice we used an adapted protocol from (223, 224). In short, the test subject was put in its home cage, alone, and an unfamiliar C57Bl/6J female intruder was introduced to the cage and social interactions (mainly sniffing and/or following in close proximity) were recorded over a three-minute period. The advantage with this approach is that it is fast to perform but there are limitations. One of the major limitations was the inclusion of both male and female *Syn2* KO mice whilst only

using female C57Bl/6J intruders. The reason was to avoid fighting amongst unfamiliar male mice. However, the estrus cycle of the female intruder or female test subjects were not assessed, which could have added to the variation. It has been shown that the estrus cycle does not influence sniffing behavior in the social interaction test in the BTBR mouse model of ASD behavior (225). Studies investigating the effects of the estrus cycle of females on sniffing behavior of *Syn2* KO mice have, to my knowledge, not been published. Another more sensitive approach that tests both sociability and social novelty is the three-chamber social interaction test (226), however, it is more time-consuming than the social interaction test used in **Paper IV**.

Spatial memory tests

Two different tests to assess spatial memory were used in **Paper IV**, the Barnes maze and the Y-maze. Although it has yet to be confirmed by EEG recordings, based on the seizure semiology of the *Syn2* KO mice, we suspect they have secondary generalized seizures with a primary focus in the temporal lobe. The seizures of *Syn2* KO mice start with orofacial twitching, indicative of primary focal TLE with secondary tonic-clonic seizures.

Barnes maze

The Barnes maze is a test for spatial learning and short- and long-term memory retention, processes that requires a functional hippocampus. Indeed, experimental models with hippocampal deficits show impaired performance in the Barnes maze (227-229). In **Paper IV** we used an adapted protocol previously published (230) and analyses was performed using the AnyMaze software. The Barnes maze is time-consuming and consists of a habituation period (day one), spatial acquisition period (from day one until day four) which is repeated two to three times/day, and probe trials on the fifth and twelfth days. The protocol used in **Paper IV** was thorough, however, a possible limitation was the inclusion of both male and females. It has been shown that male mice perform better in the Barnes maze compared to females (reviewed in (231), thus, the inclusion of both sexes may have increased the variation in **Paper IV**. However, we did not detect any sex-dependent performances in the Barnes maze during the acquisition period or probe trials (data not shown).

Y-maze

The Y-maze is a test for spatial short-term memory (232). In **Paper IV** we used the AnyMaze software to track mice during the eight minutes spent in the Y-maze during testing. The percentage of spontaneous alterations, defined as consecutive entries of all three arms, was calculated using **Equation 1** (233).

$$\%\ spontaneous\ alterations = \frac{n_{spontaneous\ alterations}}{n_{arm\ entries}-2} \times 100 \qquad (1)$$

The use of AnyMaze not only removed the need of an investigator to define if a mouse has entered an arm or not, but also allowed for collection of data for the total distance travelled during the test. Ultimately, this allowed us to perform quality control of the data according to Miedel et al. (233). To assess if the systemic IL-6R ab treatment induced any hypo- or hyperdynamic locomotion, the percentage of spontaneous alterations was correlated to the total distance travelled and number of arm entries during the test. Additionally, a one-way ANOVA was performed to ensure that no specific arm in the Y-maze was visited more frequently. The quality control revealed no such hypo- or hyperdynamic locomotion or biases to any arms (data not shown). Collectively, the implementation of automated video analyses using the AnyMaze software allowed for proper quality control to ensure high quality data.

Anxiety and depression-like tests

Individuals diagnosed with epilepsy or ASD often have comorbid anxiety and/or depressive disorders (139, 219, 220). Anxiety and depression are complex psychiatric disorders. As researchers we do not have the means to understand the murine species emotions, but instead have to rely on anxiety- and depression-like behaviors. Multiple tests of anxiety score the aversion of open spaces e.g., the elevated plus maze, elevated zero maze, light-dark box, or the open field test (reviewed in (234)). A test to assess the "state of despair" (depressive-like) is by quantifying immobility in the forced swim test (235, 236). In **Paper IV** we used the open field and forced swim test to assess the effects of IL-6R ab treatment on anxiety- and depressive-like behaviors.

Open field

The AnyMaze software was used to automatically track the behavior of the mice in the open field arena. The mice were put in the arena for ten minutes, and the last eight minutes were used for analysis. The arena was divided into three zones; corners, walls, and center. The use of automated tracking allowed for the collection of data including total distance and velocity. Total distance was investigated to determine similar locomotor activity between IL-6R ab and saline-treated *Syn2* KO mice (data not shown). The time spent and velocity in zones was investigated. *Syn2* KO mice have been shown to travel similar distances to C57Bl/6J mice in the open field (167), however the time or velocity in zones (e.g., the center) has, to my knowledge, not yet been compared between *Syn2* KO and wt mice. The implementation of automatic tracking of the test subjects allowed for collection of reliable data for parameters like distance travelled and velocity in defined zones, which is, according to me, superior to manual investigations of the open field test.

Forced swim test

The AnyMaze software was used to track and register immobility during the forced swim test. The mice were put in a large glass cylinder (20 cm diameter) containing ~20°C water. The mice were recorded for six minutes, the last four minutes were used for analysis to minimize analysis of hyperactive locomotion. A limitation of using the AnyMaze software for immobility tracking in the forced swim test was the biased registration of mobility when the mice were moving along the x-axis (side to side), whereas mobility of the mouse along the z-axis (away from or towards the camera) was generally scored as immobility according to the software. One might consider recording the cylinder using cameras set perpendicular from each other, on a horizontal plane, to better identify the true time of immobility.

Preclinical actigraphy measurements

Individuals diagnosed with ASD and/or epilepsy commonly suffer from sleep disturbances (141, 142, 145, 146). To this end we wanted to evaluate if *Syn2* KO mice would be a suitable model for sleep disturbances observed in patients. Five months old *Syn2* KO or C57Bl/6J mice were individually housed in a cage surrounded by two IR frames, the lower frame recorded general locomotor activity and the upper frame registered rearing events in one-minute bins. Recordings were done over a 72-hour period. The raw data was manipulated using R and a five-minute rolling average was applied to general locomotor activity to reduce noise. Parameters like sleep latency and periods of activity during lights-ON were extracted and used for analysis. Thresholds for assumed sleep was determined by assessing all recordings in a blinded manner. An ethical consideration of the approach used in **Paper IV** is the need of single housed mice to record data, a procedure that ideally should be avoided due to the social nature of mice. In contrast, to yield robust data larger groups and longer recordings would be necessary (discussed later). Due to the sensitive recording equipment used in **Paper IV**, the approach of using one-minute bins (which is what is used for human actigraphy measurements) resulted in noisy data. One might consider analyzing the actigraphy measurements using larger bins or apply a rolling average of a larger interval to better visualize general patterns of activity (e.g., hypo- or hyperactivity) during a 24-hour period. In a study of *Cntnap2* KO mice and rats, actigraphy measurements were binned in 1-hour intervals, which was sufficient in visualizing general patterns of hypo- and hyperactivity (237).

Enzyme-linked immunosorbent assay

To analyze cytokines involved in inflammatory responses we exclusively used electrochemiluminescence enzyme-linked immunosorbent assay (ELISA) from MSD (multi- or single-plex), which allows for cytokine detection in the pg/ml range. The cytokines analyzed in **Papers I-IV** are summarized in **Table 2**.

Table 2. Overview of cytokines, sample types, and dilutions used in Papers I-IV
Total protein to analyze cytokine in brain tissue in **Paper IV** was determined using BCA. All MSD plates were read using the MESO QuickPlex SQ 120 analyzer.

Paper	Sample type	Dilution/ amount	Cytokine(s)	Catalog number
I	Serum	2-fold	IFN-γ, IL-1β, IL-2, IL-4, IL-5, IL-6, IL-10, IL-12p70, KC/GRO, TNF	K15048D
II	Serum	4-fold	IFN-γ, IL-1β, IL-4, IL-5, IL-6, IL-10, IL-13, KC/GRO, TNF	K15059D
	CSF	2-fold		
III	Serum	200-fold	TNF (calibrators exchanged to allow for quantification of XPro1595 levels)	K151QWD
	CSF	neat		
IV	Serum	2-fold	IL-6	K152QXD
	Cortex Hippocampus	200 µg	IFN-γ, IL-1β, IL-2, IL-4, IL-5, IL-6, IL-10, IL-12p70, KC/GRO, TNF	K15048D

Abbreviations. IFN-γ, interferon γ; IL, interleukin; KC/GRO, keratinocyte chemoattractant/growth-regulated oncogene; TNF, tumor necrosis factor; CSF, cerebrospinal fluid.

In **Paper I** the ELISA kit used was designed for mice samples, as this was the kit that was available at the time of analysis. In **Papers II** and **IV** kits intended for the correct species were used. In **Paper III** a kit intended to measure TNF levels in human samples were used to quantify XPro1595 levels in serum and CSF using an adapted protocol.

In **Papers II** and **IV**, the analyses of cytokines were challenging since the majority of cytokine levels investigated was low. The levels of most cytokines were below the lower limit of quantification and outside the linear range, ultimately contributing to increased variation. In many cases the cytokine levels were observed just above, or even below (not detected, ND), the lower limit of detection. In **Papers II** and **IV** ND values were treated with different approaches. In **Paper IV** ND values were excluded, ultimately skewing data towards detected values and introducing biases. In **Paper II** ND values were replaced with the lowest quantifiable values, a procedure that was done if there was only one sample/group with ND values. If more than one sample had ND values, the group data was not used for comparison to avoid reporting results based on assumption. An improved approach to the ones used in this thesis would have been to replace only a fraction of ND values (e.g., accepting only one ND value/group, similar to **Paper II**) with the lower limit of detection divided by two. We are currently analyzing cytokine data in **Paper III**, and to reduce the number of samples that would be ND, we chose to run serum and

CSF samples neat. However, even if samples were run neat, the majority of cytokine values were still below the lower limit of quantification (data not shown).

Flow cytometry analyses to characterize immune cell populations in blood and brain

In **Paper II** we used flow cytometry to characterize major immune cell populations in blood and brain samples with an aim of investigating the effects of allelic *Ciita* variants in naïve rats, and following rAAV6-α-Syn+PFFs injections at four- and eight-week time points. Flow cytometry is an efficient method that allows for thorough characterization of cell populations. However, there are many factors to consider to obtain high-quality data.

Mononuclear cell isolation from brain homogenates

In short, saline-perfused brains were collected into RPMI 1640 medium and immediately stored at 4°C. The cerebellum was removed and hemispheres separated and homogenized using a dounce homogenizer in Hank's balanced salt solution. Homogenized samples were passed through a 100 µm cell strainer. Brain mononuclear cells were subsequently isolated using two-layer density gradient separation (11, 238).

In addition to practical reasons, the relatively low cell numbers prompted us to not explore the option of analyzing brain regions separately. I aimed to analyze around 10,000 cells of interest to yield robust data on various cell populations. With the cell isolation protocol used in **Paper II** the cell numbers would have been far below 10,000 events, and therefore more uncertain, if we would have analyzed brain regions, e.g., striatum and ventral midbrain, separately. However, we did not use any enzymatic dissociation of myelin. By adding a cocktail of enzymes (collagenase I, Dnase I, dispase and TLCK) myelin can efficiently be dissociated, ultimately increasing cell yield. Using enzymatic dissociation for one hour increased the yield of microglia by 40% compared to not using any enzymatic dissociation (238). Therefore, the inclusion of enzyme dissociation might have enabled us to explore relatively robust data collected from brain regions as well. However, for the protocol used in **Paper II** it would not have been practically viable to include more processing steps due to time constraints.

Antibody panel to investigate immune cell populations

The antibody panel used in **Paper II** was designed to cover major immune cell populations and to work in both brain and blood (**Table 3**). The antibody panel used allowed for investigation of T cells (including CD4+ and CD8+ subsets), myeloid cells, and microglia. Additionally, MHCII and CD86 was included to analyze markers important for antigen presentation (15).

Table 3. Antibody panel for flow cytometry experiments in Paper II.
Details on antibodies used for flow cytometry experiments in **Paper II**. All samples were recorded on an LSR Fortessa.

Antigen/ Target	Species specificity	Fluorochrome/ Conjugation	Clone	Isotype/ Host	Dilution	Company
CD45	Rat	APC-eFluor 780	OX1	Mouse IgG1, κ	1:100	Invitrogen (47-0461-82)
CD3	Rat	BV421	1F4	Mouse IgM, κ	1:200	BD Horizon (563948)
CD4	Rat	BV605	OX-35	Mouse IgG2a, κ	1:200	BD OptiBuild (740369)
CD8a	Rat	PE-Cy7	OX8	Mouse IgG1, κ	1:200	Invitrogen (25-0084-82)
CD11b	Rat	PE	WT.5	Mouse IgA, κ	1:200	BD Pharmingen (562105)
MHCII RT1B	Rat	Alexa Fluor 647	OX-6	Mouse IgG1, κ	1:400	Bio-Rad (MCA46A647)
CD86	Rat	BV711	24F	Mouse IgG1, κ	1:100	BD OptiBuild (743215)
Viability/ dsDNA	-	DRAQ7	-	-	1:1,000	Invitrogen (D15106)

Abbreviations. CD, cluster of differentiation; MHCII, major histocompatability complex II; dsDNA, double-stranded DNA.

Even if the antibody panel used in **Paper II** worked well with multiple sample types it has limitations. It would have been more interesting to focus the analyses of blood samples on e.g., monocyte subsets, rather than a broad myeloid cell population since alterations in monocyte subsets, including changes in MHCII levels, have been implicated in PD (85, 87). Additionally, an antibody panel specifically for brain samples could allow for more detailed analyses of microglia or include analysis of BAMs in the brain parenchyma. Indeed, BAMs have become highly interesting in the context of PD as it was recently suggested to be a main driver of α-Syn-induced neuroinflammation (82). In an early version of the antibody panel used in **Paper II**, an antibody for CD68, a marker for activated macrophages or microglia, was included. Since CD68 is an intracellular marker, fixation with PFA and subsequent permeabilization is required. Fixation, permeabilization, with subsequent washes added too much time to the protocol and therefore had to be excluded.

All samples in **Paper II** were processed within hours of collection and analyzed fresh, to obtain high quality, reproducible data. Due to practical reasons only four to six rats could be recorded at each session. It would have been beneficial to analyze all samples at once as it would reduce inter-recording variation and allow for direct comparisons of e.g., MFI-values without the need for normalization. However, since flow cytometry recordings of all samples occurred over several months multiple factors need to be considered to optimize any procedure to analyze cells at a later timepoint. Antibody staining and post-fixing using PFA was not an option since it is a method that can be used for short-term, but not long-term, storage. An alternative would be to freeze down freshly isolated cells. However, cryopreservation has been shown to alter cell surface markers when comparing fresh and cryopreserved samples of renal cell carcinoma and colorectal carcinoma analyzed using CyTOF (239). Thus, extensive validation would have been necessary to guarantee high-quality data from frozen cells analyzed by flow cytometry.

There are numerous limitations with the flow cytometry experiments and antibody panel design used in **Paper II**. Ultimately the protocol was necessary to be feasible for one experimenter to perform during a day, from tissue collection to recording. I believe the protocol used in **Paper II** struck a balance between practicality and quality of data.

Immunohistochemistry

Throughout this thesis both fluorescent and DAB staining were done to visualize proteins of interest. Readers are referred to **Papers I-IV** for detailed protocols. All primary antibodies used in this thesis are listed in **Table 4**.

Table 4. List of antibodies used in Papers I-IV
List of antibodies with details and dilution used for each paper. If clone is not specified the antibody is polyclonal.

Antigen	Clone	Host	Company	Catalog number	Dilution	Paper(s)
CD68	FA-11	Rat	Bio-Rad	MCA1957	1:500	IV
C3	11H9	Rat	Abcam	Ab11862	1:50	IV
GFAP	-	Rabbit	Agilent	Z0334	1:1,000	III & IV
GFP	-	Chicken	Abcam	Ab13970	1:1,000	I
Human α-Syn	211	Mouse	Santa Cruz	Sc-12767	1:1,000	I-III
Iba1	-	Chicken	Abcam	Ab139590	1:1,000	I
Iba1	-	Rabbit	Fujifilm Wako	019-19741	1:1,000	III
					1:500	IV
MHCII	OX-6	Mouse	Abcam	Ab23990	1:500	I, II
pS129 α-Syn	EP1536Y	Rabbit	Abcam	Ab51253	1:2,000	I-III
TH	-	Rabbit	Millipore	AB152	1:1,000	I-III

Abbreviations. CD, cluster of differentiation; C3, complement component 3; GFAP, glial fibrillary acidic protein; GFP, green fluorescent protein; α-Syn, α-Synuclein; Iba1, ionized calcium-binding adapter molecule 1; MHCII, major histocompatability complex II; pS129, phosphorylated serine residue 129; TH, tyrosine hydroxylase.

Image analyses

Development of deep CNN models for image analyses

In **Paper III** we developed three AI models using the aiforia platform. All images were acquired at 20x with extended focal imaging using an Olympus VS-120 virtual slide scanner and images were uploaded to the aiforia cloud. A brief overview of the AI models can be found in **Table 5**.

Table 5. AI models used for IHC analysis in Paper III
Summary of the AI training and performance of the three models developed for IHC analysis. For layers with object & IS, precision, recall and F1 scores refer to performance of object detection (metrics not available for IS).

Model (iterations)	Layer type	Complexity	Annotations	Precision (%)	Recall (%)	F1 score (%)
TH+ SNpc cell (700)	Object	Very Complex	269 objects across 56 regions	92.31	98.14	95.14
TH+ axonal swelling (1,000)	Region (parent)	Very Complex	114	100	99.94	99.97
	Object & IS (child)	Intermediate (object) & Complex (IS)	405 objects across 224 regions	97.67	95.45	96.55
Iba1+ cell (2,193)	Region (parent)	Very Complex	41	99.49	98.14	98.81
	Object & IS (child)	Intermediate (object) & Ultra Complex (IS)	235 objects across 231 regions	98.94	91.18	94.40

Abbreviations. AI, Artifical intelligence; IHC, immunohistochemistry; IS, instance segmentation; TH, tyrosine hydroxylase; SNpc, substantia nigra pars compacta; Iba1, ionized calcium-binding adapter molecule 1.

The TH+ SNpc cell model was trained (using AI engine version 5) to recognize TH+ cells in SNpc. Both the TH+ axonal swelling and Iba1+ cell models were trained using AI engine version 7. These models included a parent layer, trained to identify brain tissue, and a child layer which was trained to identify TH+ axonal swellings (approximately >3 μm in diameter) or Iba1+ cells. The identification of brain tissue allowed for thorough normalization to the region of interest (ROI) area. The child layers were also trained using instance segmentation, and the perimeter of each object (TH+ swelling or Iba1+ cell) was manually traced. The inclusion of instance segmentation allowed for more parameters to be analyzed, such as area, perimeter, length, and width. The developed models are discussed in more detail below.

Quantifying dopaminergic neurodegeneration

In **Papers I-III** TH has been used as a marker for dopaminergic neurons. TH is a specific marker for dopaminergic neurons, as it converts L-tyrosine to L-DOPA inside the neurons, however, TH has been shown to be downregulated prior to neurodegenerative events following rAAV-α-Syn-induced neurodegeneration (197), resulting in a false perception of neurodegeneration. In this regard the superior option would be to use VMAT2, another marker specific for dopaminergic neurons, which is not, to my knowledge, downregulated prior to neurodegeneration. Quantification of TH+ cells were only done in **Papers I** and **III**, based on $1/6^{th}$ of evenly distributed coronal sections of 40 μm thickness.

Quantifying TH+ cells in SNpc – stereology versus deep CNN models

The gold standard for quantifying dopaminergic neurons in SNpc is through unbiased stereology using the optical fractionator principle (240). In short, the optical fractionator principle estimates the total number of cells based on systematically randomly dispersed virtual counting spaces, evenly distributed across the entire volume of interest, which is manually annotated. In **Paper I** we used the MBF stereological investigator software to estimate the numbers of TH+ cells in SNpc by a researcher blinded to the treatment conditions and strains. The major limitation using unbiased stereology is that it is a very time-consuming undertaking, several hours are required to quantify TH+ cell counts in the entire SNpc of a rat.

In **Paper III** we instead trained a deep CNN, using the aiforia platform, to automatically count every TH+ neuron in manually annotated SNpc regions, taking only a few minutes to quantify all cells in the selected sections. The researchers were blinded to treatment conditions in **Paper III** as well.

We have not compared the TH+ cell estimates in the SNpc by unbiased stereology and our AI model using the same sections. However, a paper from 2018 compared mouse and rat stereological counts using MBF stereological investigator (same software used in **Paper I**) to their trained CNN algorithm developed using the Fimmic platform (renamed to aiforia in 2018). The authors reported strikingly similar TH+ cell estimates from stereology and CNN quantification in both species (241). The authors manually annotated a total of 1,254 TH+ cell bodies in SNpc to train their CNN model (241). In the model developed in **Paper III** we annotated only 269 TH+ cells, however, it is important to note that the AI engine has been improved "under the hood" over time, ultimately resulting in reduced efforts necessary from investigators to train high-quality CNN models.

Collectively, the use of CNN-assisted quantification significantly reduces the time needed to produce good unbiased estimates of TH+ cell counts in SNpc, making it the preferred choice over unbiased stereology. Additionally, the developed CNN model can be readily used for future projects, and does not necessarily need to be re-trained. Further optimizations to save time are possible. The time-limiting procedure in **Paper III** was acquiring the images using an Olympus VS-120 virtual scanner. The set-up only allowed for batch scans of six glass slides and following image acquisition, the slides need to be manually changed and a new batch initiated by an investigator. The use of a proper slide scanner would allow for the scanning of entire projects overnight.

Determining TH+ fiber density in dorsal striatum

To quantify axonal loss in the dorsal striatum the staining intensity of TH in the ipsilateral hemisphere is compared to the non-injected contralateral hemisphere, which is assumed to have 100% of TH+ axonal fibers intact. All analyses on TH+ fiber density was done using Fiji.

The approaches used in **Papers I** and **III** to measure TH+ fiber density differed slightly. In **Paper I** 2x images were acquired using an Olympus BX53 microscope and converted to 8-bit grey-scale images. OD values were obtained using Rodbard calibration curve. The OD values for dorsal striatum were obtained and adjusted for background staining taken from corpus callosum. In **Paper III** 10x images were acquired using an Olympus VS-120 virtual slide scanner and converted to 8-bit grey-scale images. The inverted mgv in dorsal striatum was recorded and adjusted for background staining from cortex. Although the approach using global calibration based on the Rodbard calibration curve (**Paper I**) might yield results that are more comparable between experiments, the use of modern microscopes does not warrant a use of such an approach since illumination sources are stable over time. Variations from DAB immunostaining procedures likely contributed more to the variability compared to the illumination sources. Additionally, the 10x magnification used to acquire dorsal striatum images in **Paper III** is not necessary. Indeed, 2x (like in **Paper I**) or 4x magnification is enough to quantify TH fiber density.

Microglia activation

Microglia were quantified in a blinded manner by IHC in **Papers I, III** and **IV**. Multiple different approaches were used to assess microglia activation, including morphological changes (**Papers I, II** and **III**), MHCII levels (**Paper I**), and CD68 levels (**Paper IV**). MHCII and CD68 levels are currently being evaluated in **Paper III** as well. It is important to note that the markers used to assess microglia are not exclusively expressed by microglia cells. Iba1, MHCII and CD68 are markers that are also expressed on macrophages, which can infiltrate the CNS during inflammation (200). Additionally, MHCII can be expressed on astrocytes as well (21). To ensure specific analyses on microglia TMEM119 may be best available marker of activation (242).

Quantifying microglia morphologies – manual assessment versus CNN-assisted quantification

In **Paper IV** microglia (Iba1+ cells) morphologies in the hippocampus were scored based on three categories; ramified, intermediate, and round/ameboid, a scoring system that was adapted from (74). Others have used four categories to distinguish microglia morphologies; resting/ramified, hyper-ramified/activated, reactive, and ameboid (199). The most obvious limitation using a manual assessment of Iba1+ cells into categories is to achieve consistency when the morphology shifts along a spectrum rather than existing in fixed categories (12). Additionally, the scoring of microglia along a spectrum from resting to ameboid may already be outdated as microglia morphologies vary greatly depending on stimuli (12). Another limitation of the approach used to quantify microglia in **Paper IV** is not employing unbiased stereology using the optical fractionator to estimate the total number of Iba1+ cells

throughout the hippocampus (240). However, as stated previously, unbiased stereology is a very time-consuming undertaking. In **Paper IV** three coronal sections between the Bregma coordinates -1.46 and -2.18 were used. The majority of sections matched on coordinates or differed only slightly (data not shown), thereby minimizing the effect of hippocampal size along the rostro-caudal axis.

In **Paper III** we opted to develop a deep CNN to analyze Iba1+ cells in dorsal striatum and in SN. In short, $1/12^{th}$ of all coronal sections were stained for the Iba1 marker. Coronal sections were matched on their relative Bregma coordinates along the rostro-caudal axis; 1.2, 0.36, -0.4, -1.2 and -2.04, and the dorsal striatum was analyzed. For SN analyses all sections available between the Bregma coordinates -4.56 and -6.6 were included. As specified in **Table 5**, 235 manual annotations of Iba1+ cells with instance segmentation were enough to develop a versatile model with good performance. There are no standard methods to quantify microglia morphology and thus it is not as straightforward to evaluate the performance of the developed CNN, as in the case for TH+ cells in SNpc previously discussed. Some examples of approaches are to count Iba1+ cells in the field of view in a subset of sections (e.g., $1/8^{th}$) (243), measure the OD of CD11b+ staining in an ROI (123), or use unbiased stereology of CD11b+ cells in ROI (130). The latter approach is probably the most accurate but also time-consuming. Based on the available data comparing CNN models to unbiased stereology of TH+ cells, there is no reason to believe that a CNN model would perform worse than unbiased stereology for microglia quantification. Additionally, using a CNN model with instance segmentation of Iba1+ cells allowed for more complex analyses at a cellular level, and thus has the ability to set strict guidelines to determine e.g., a morphology category. As discussed below, the Iba1+ cell area was shown to be the best measurement for microglia activation (reduced area = more activated), however, the "hyper-ramified" state of microglia has a larger cell area compared to both resting and reactive microglia, thus, the CNN might have missed these subtle cellular changes. However, as previously mentioned, further development of the CNN model is possible and should be revisited for future projects.

Collectively, the different strategies of quantifying morphologies are vast and include several key aspects to consider. To ensure high-quality data I believe manual investigations should be minimized and instead be automated as much as possible to reduce biases and variation. Additionally, time is another important factor to consider. Considering both of these parameters the development of CNN models is the superior choice as it is fast and consistent.

Quantification of MHCII immunoreactivity

Upon activation both microglia and astrocytes can upregulate MHCII. However, based on the morphology of the MHCII+ cells investigated; it is probable that the cells investigated were mostly microglia. The number of MHCII+ cells in dorsal striatum and in the SN was assessed using a semi-quantitative approach in **Paper I**.

Four sections from dorsal striatum and four from SN were used to count all MCHII+ cells in the ROI. Images were acquired using an Olympus BX53 at 20x and the number of MHCII+ cells were counted using Fiji. This is a relatively fast approach to acquire data; however, it is not always easy to distinguish between activated microglia cells in close proximity, thus, the approach used in **Paper I** runs the risk of underestimating the number of MHCII+ cells. Another approach is to score the staining intensity according to an arbitrary scale (186), however, this approach runs a higher risk of introducing variation due to the difficulties of manually scoring categories of a continuous spectrum. In **Paper III** we are currently investigating MHCII+ signal and chose to investigate the percentage positive MHCII area normalized to ROI. This approach lets us investigate continuous data but is also very sensitive resulting in increased variability. Indeed, one might consider developing more sophisticated methods using CNN models to quantify the MHCII signal.

Quantification of CD68 immunoreactivity

Although CD68 is expressed at low levels in resting microglia, it is upregulated following activation. In **Paper IV** we manually counted the number of Iba+/CD68+ cells in the hippocampus to complement the morphology scoring. The same limitations as previously discussed, when scoring IHC immunostainings manually, apply here as well. Since CD68 is expressed at low levels in resting microglia, an arbitrary threshold was set to determine if a cell was double positive in **Paper IV**, which may have increased the variation in the results. In **Paper III** investigation of CD68 immunoreactivity is ongoing, and here the same approach as for MHCII is being used; determining the CD68+ area normalized to the ROI. The approach used in **Paper IV** is the more thorough of the two, but based on the available data in **Paper III** (discussed below), we do not think it is warranted to analyze the CD68 (or MHCII) immunoreactivity with the same finesse. Quantification was done by a blinded researcher in both papers.

Assessing phosphorylated α-Syn

A pathological hallmark of PD is the presence of pS129 α-Syn inside LB and LN (57, 58). To this end, we assessed the load of pS129 α-Syn in **Papers I** and **III**.

In **Paper I** the pS129 α-Syn load was extensively quantified, by two independent researchers in a blinded manner, throughout the brain using an adapted scale previously described (209). The scale ranged from 0-5 to represent the severity of pathology (from no pathology to severe pathology). This approach is very thorough, but time-consuming. Additionally, a limitation of using a global scale while investigating multiple brain areas is the restriction it causes on certain regions. An alternative would be to set separate scoring scales for each region analyzed, based on the available material, ultimately increasing the resolution of the pathology for each region. As previously discussed, the use of manual scoring is problematic and

introduces variation as decisions might drift. However, the scoring was based on two independent researchers which effectively will reduce the variation.

In **Paper III** a much more crude but simpler approach was used to assess pS129 α-Syn pathology; measuring the percentage of pS129 α-Syn positive area, normalized to each ROI, which does not require manual assessment. Of the two methods the one used in **Paper I** is more precise but requires more manual labor. An alternative method would be a combination of the two approaches, analyzing the percent area occupied by pS129 α-Syn in interconnected brain regions (244). Indeed, further optimizations could also be made by developing CNN models to quantify α-Syn pathology throughout the brain.

Astrocyte analyses

The astrocyte response was investigated in **Papers III** and **IV** using similar approaches. Astrocytes were visualized by GFAP, which is upregulated following activation (18). The percentage of GFAP+ area normalized to the ROI was calculated in the dorsal striatum, the SN (**Paper III**) or in hippocampal sub-regions (**Paper IV**). This approach is relatively fast and minimizes the use of manual investigations. Another common approach to quantify astrocyte activation is to measure the GFAP intensity (243). Following activation astrocytes changes morphology and they can start to overlap, thus making quantification of GFAP+ cell numbers challenging without using confocal microscopy or 3D renderings (245).

To complement the analysis of GFAP+ area in **Paper IV** we also performed evaluation of GFAP+/C3+ area. We opted to use C3 since it has been shown to be upregulated in astrocytes following activation (20, 246).

Statistical analyses and presentation of data

Throughout this thesis a significance level of 5% was used. All statistical analyses in **Papers I**, **II** and **IV** were done using GraphPad Prism. All statistical analyses in **Paper III** were performed in R. The use of statistical software with user friendly interface, like GraphPad Prism, is appealing since it is easy to use. However, the use of R (or e.g., Python) to handle data and perform statistical analyses is superior to GraphPad Prism according to me. The main advantage is that R allows for data manipulation while only reading raw data, whereas data manipulation is usually done in Excel prior to cut-and-paste into GraphPad Prism. Thus, the risk of errors introduced during data manipulation is reduced while using R.

Assessing data distribution of small sample sizes

In **Papers II-IV** the distribution of data was assessed by Q-Q plots of the residuals. This is a relatively easy way of assessing the distribution of data in small data sets, which are common in preclinical research. Histograms or density plots can be used if sample sizes are large enough, however, with 10-20 observations, Q-Q plots of the residuals are an easier method to determine the distribution. In **Figure 12** simulated data is presented to illustrate how the number of observations affect the shape of the distribution and how corresponding Q-Q plots of residuals can look from a normal distribution of varied sample sizes. There are statistical tests, like the Kolmogorov-Smirnov test, to determine if data are parametrically distributed. However, these tests are sensitive to small sample sizes ($n \approx 10$) and outliers, thus rendering them virtually useless in preclinical settings.

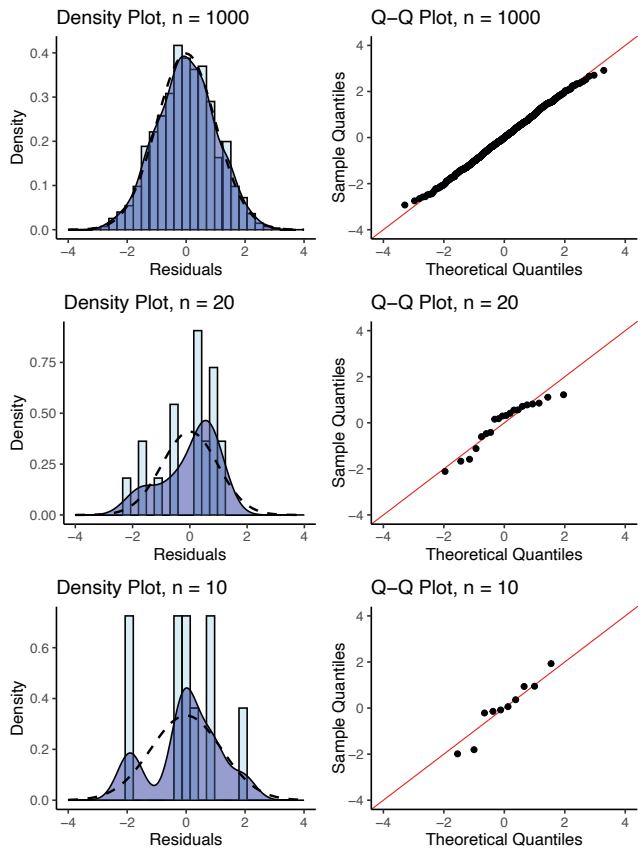

Figure 12. Simulation of histograms and Q-Q plots of residuals based on various samples sizes taken from parametric distrubtions.

Dashed line in the left columns represent a perfect parametric distribution. The histograms and density plots represent simulated parametric distributions based on sample sizes of n = 1000, 20, and 10 (from top to bottom). Right column shows the respective Q-Q plot of residuals from each simulation.
Abbreviations. Q-Q, quantile-quantile.

Presentation of summary statistics

Throughout this thesis the summary statistics are presented in different ways. In **Paper I** data was presented using mean ± SEM, without showing individual data points. This approach is not intuitive for readers since there is no information about the spread of data, only a mean and the precision of said mean. In my opinion this approach should be avoided. I argue for a more transparent presentation of data, and in **Papers II-IV** this was adjusted for. In **Papers II-IV** the mean ± SD with individual data points is shown for data with a parametric distribution, whereas in **Papers III** and **IV** median with IQR and individual data points are shown for non-parametric data. Indeed, since SD is a measure of data variability it is more transparent and provides information that is more intuitive for readers. However, another approach for parametric data would be to plot the mean ± 95% CI, since the 95% CI is both a measurement of the precision of the mean (or rather an uncertainty measurement of the mean) and the data variability. Indeed, the use of mean ± 95% CI with individual data points should be considered as a standard for data presentation.

Summary of results and discussion

The following are summaries of the results and discussions from **Papers I-IV** included in this thesis. For complete details, readers are encouraged to refer to the full texts of the papers.

Papers I-III | Genetic variants of the class II transactivator impacts systemic and local immune responses, susceptibility, and progression of experimental Parkinson's disease

The connection between PD and inflammation is evident, although the sequence of events and specific contributions to disease susceptibility and progression remain largely unknown. In **Papers I-III**, we focused on the link between the innate and adaptive immune systems by investigating how allelic variants of *Ciita* influence the susceptibility and progression of rAAV6-α-Syn+PFFs-induced PD-like pathology. In **Paper I**, we discovered that reduced *Ciita* levels were associated with more widespread α-Syn pathology, more activated microglia, and enhanced motor impairments following PD-like pathology. To determine if these effects were due to changes in brain-resident or peripheral immune cells, we conducted an immune characterization of naïve rats and rats with α-Syn-induced PD-like pathology, four- and eight-weeks post-SNpc injection (**Paper II**). Altered *Ciita* levels were associated with only minor changes in immune cell populations, but with consistently elevated sTNF serum levels. Consequently, in **Paper III**, we used a sTNF inhibitor to investigate if sTNF neutralization would protect against α-Syn-induced neurodegeneration, α-Syn pathology and neuroinflammation in DA.VRA4 rats. This protective effect was not observed.

Throughout **Papers I-III**, we used a combination of unilateral human α-Syn transgene overexpression in the SNpc and striatal seeding of human PFFs to model PD (described in more detail under methodological considerations). In all three papers, stable human α-Syn overexpression was observed (**Figure 13**). It is important to note that the reduced signal intensity in **Figure 13B** was due to

technical issues during IHC procedure (specifically with an avidin/biotin complex kit) and not inherent to transgene expression.

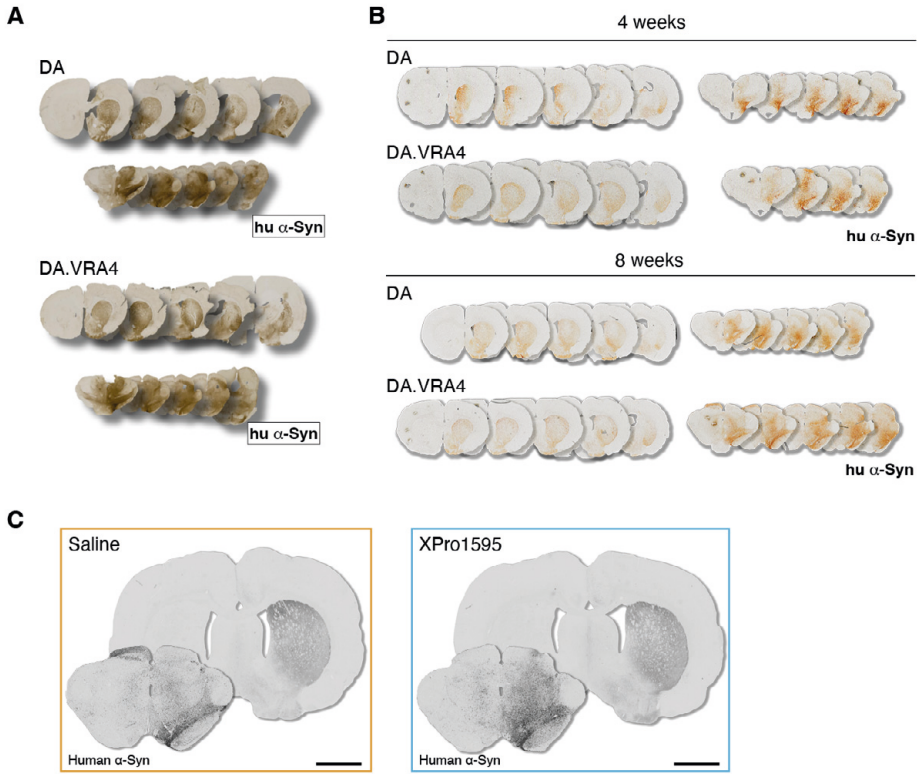

Figure 13. Representative images of human α-Syn expression following injections of rAAV6-α-Syn and PFFs in Papers I-III.
(A) Human α-Syn transgene expression in DA (top) and DA.VRA4 (bottom) eight weeks post injection into SNpc (**Paper I**). **(B)** Human α-Syn transgene expression in DA and DA.VRA4 rats four (top) and eight (bottom) weeks post injection into SNpc (**Paper II**). **(C)** Human α-Syn transgene expression in DA.VRA4 rats treated with saline (left) or the sTNF inhibitor XPro1595 (right) eight weeks post injection into SNpc (**Paper III**). Scale bar = 2 mm. **Abbreviations.** hu α-Syn, human α-Synuclein; rAAV6, recombinant adeno-associated virus serotype 6; PFFs, preformed fibrils; SNpc, substantia nigra pars compacta; sTNF, soluble tumor necrosis factor.

Paper I | *Ciita* variants affect susceptibility and progression of rAAV6-α-Syn+PFFs induced Parkinson-like pathology

The congenic DA.VRA4 strain exhibits more activated microglia, indicated by morphology and relative MHCII+ cell numbers, without a change in overall microglia numbers in the striatum or SN, compared to DA rats in response to rAAV6-mediated α-Syn overexpression (130). Additionally, DA.VRA4 rats

showed a reduction of TH+ fiber density in the dorsal striatum and also developed motor impairments, none of which was observed in DA rats (130).

To investigate if allelic variants of *Ciita* would impact α-Syn pathological spread, we used the combined rAAV6-α-Syn+PFFs model, which efficiently induces α-Syn pathology, neurodegeneration, and neuroinflammatory response (99, 119, 120, 123).

Allelic Ciita variants are associated with increased susceptibility to α-Syn-induced neurodegeneration and motor impairments

First, we confirmed that combined injections of rAAV6-α-Syn+PFFs caused dopaminergic neurodegeneration (**Figure 14A-C**). Although the combined model caused a reduction in striatal TH+ fiber density in both DA and DA.VRA4 (relative to the contralateral hemisphere), the loss was more pronounced in the DA.VRA4 strain (**Figure 14B**). rAAV6-α-Syn+PFFs injections reduced the number of TH+ cells in the SNpc in both strains, however, rAAV6-α-Syn+BSA and rAAV6-GFP+PFFs was enough to cause dopaminergic neurodegeneration in DA.VRA4 but not in DA rats, indicating enhanced susceptibility to α-Syn/PFFs-induced neurodegeneration (**Figure 14C**). The more extensive neurodegeneration observed in DA.VRA4 rats was also reflected by motor impairments following rAAV6-α-Syn+PFFs injections, which caused significant forelimb akinesia only in DA.VRA4 rats (**Figure 14D**). Collectively, these findings show that allelic variants of *Ciita* regulate susceptibility to α-Syn-induced PD-like neurodegeneration, which is in line with a previous study using rAAV6-α-Syn only (130).

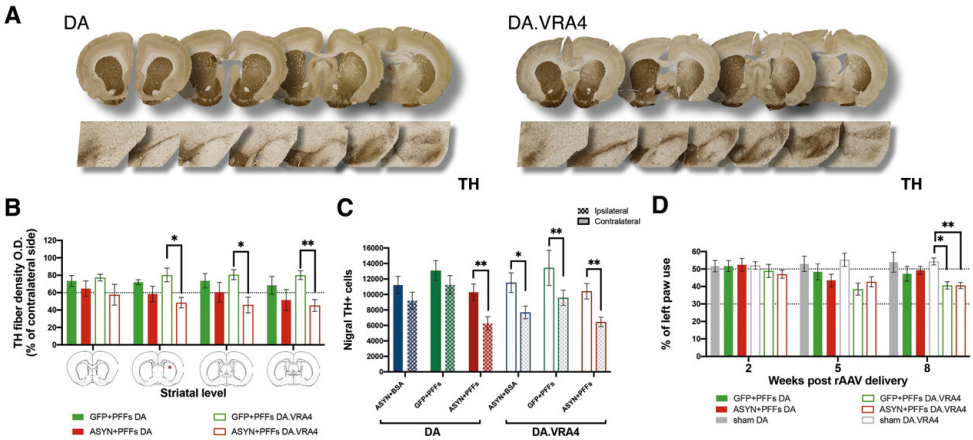

Figure 14. DA.VRA4 rats with reduced *Ciita* levels are more susceptible to α-Syn-induced neurodegeneration.

(A) Representative images of TH+ signal in striatum and SNpc following combined rAAV6-α-Syn+PFFs injections in DA (left) and DA.VRA4 (right) rats. **(B)** Quantification of TH+ fiber density (relative to non-injected contralateral hemisphere) in the dorsal striatum following rAAV6-α-Syn+PFFs or rAAV-GFP+PFFs injection. **(C)** Stereological estimates of TH+ neurons in SNpc in contralateral and ipsilateral hemispheres following rAAV6-α-Syn+BSA, rAAV-GFP+PFFs, and combined rAAV6-α-Syn+PFFs injections. **(D)** Quantification of forelimb akinesia from the stepping test in DA and DA.VRA4 rats following rAAV6-α-Syn+PFFs, rAAV6-GFP+PFFs, or sham controls. Data is presented as mean ± SEM. Statistical analyses was performed using two-way ANOVA with Tukey's HSD post-hoc test. *p < 0.05, **p < 0.01. **Abbreviations.** TH, tyrosine hydroxylase; O.D., optical density; GFP, green fluorescent protein, PFFs, preformed fibrils, ASYN/α-Syn, α-Synuclein; BSA, bovine serum albumin; rAAV6, *Ciita*, class II transactivator; SNpc, substantia nigra pars compacta; rAAV6, recombinant adeno-associated virus serotype 6; SEM, standard error of the mean; ANOVA, analysis of variance; HSD, honestly signficant difference.

Microglia activation is region-dependent in rats with allelic Ciita variants following rAAV6-α-Syn+PFFs injections

Next, we investigated the *Ciita*-dependent MHCII expression on microglia following rAAV-α-Syn+PFFs. MHCII+ cells were visible throughout multiple brain regions but the highest immunoreactivity was observed in the striatum and SNpc (**Paper I**). The number of MHCII+ cells did not differ between strains in the SNpc but it was higher in the DA.VRA4 compared to DA in the dorsal striatum following rAAV-α-Syn+PFFs (**Figure 15A**), despite the allelic *Ciita* variants in the DA.VRA4 strain resulting in reduced *Ciita* and MCHII expression (128, 129). Our observation is in line with previous findings showing an increased number of MHCII+ cells in the dorsal striatum, but not SNpc, in DA.VRA4 rats compared to DA following α-Syn transgene overexpression (130). The MHCII+ cells observed in **Paper I** exhibited a morphology associated with an activated state, being hypertrophic and even ameboid (130, 199). Additionally, pS129 α-Syn inclusions were observed within Iba1/MHCII double-positive cells in the striatum of both DA and DA.VRA4 rats (**Figure 15B**). This finding is also supported by previous research showing that

reactive microglia correlate with pS129 α-Syn inclusions in TH+ SNpc cells following striatal PFFs injection (247).

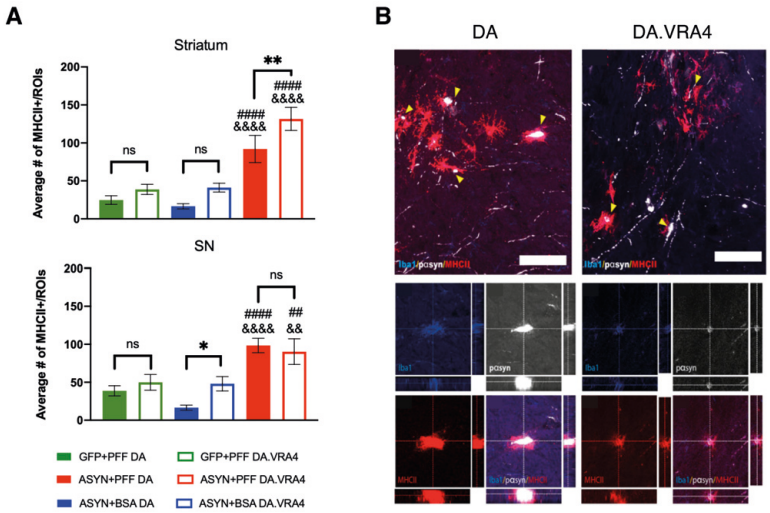

Figure 15. MHCII+ microglia increase in response to rAAV6-α-Syn+PFFs injection and associate with pS129 α-Syn.
(A) Stereological quantification of MHCII+ cells in dorsal striatum (top) and SN (bottom) following rAAV6-α-Syn+BSA, rAAV6-GFP+PFFs, and combined rAAV6-α-Syn+PFFs injections. Data presented as mean ± SEM. Statistical analyses was performed by two-way ANOVA with Tukey's HSD post-hoc test. *p < 0.05, **/##/&&p < 0.01, ####/&&&&p < 0.0001. "&" denotes differences within DA strains and "#" denotes differences within DA.VRA4 strains. **(B)** Iba1/MHCII double positive cells in striatum are in close proximity and/or contain pS129 α-Syn following rAAV6-α-Syn+PFFs injections in both DA and DA.VRA4 rats. Scale bar = 100 µm. **Abbreviations**. MHCII, major histocompatability complex class II; ROI, regions of interest; ns, non significant; SN, substantia nigra; GFP, green fluorescent protein; PFF/PFFs, preformed fibrils; ASYN/α-Syn, α-Synunclein; BSA, bovine serum albumin; Iba1, ionized calcium-binding adapter molecule 1; pαsyn/pS129 α-Syn, α-Synuclein phosphorylated at Serine resiude 129; rAAV6, recombinant adeno-associated virus serotype 6; SEM, standard error of the mean; ANOVA, analysis of variance; HSD, honestly significant difference.

Pathological α-Syn spread is exacerbated in DA.VRA4 rats with reduced Ciita levels following combined injections of rAAV6-α-Syn and PFFs

To determine if allelic variants of *Ciita* would impact the pathological spread of α-Syn, we investigated pS129 α-Syn along the rostro-caudal axis in DA and DA.VRA4 rats (**Figure 16A**). The extent of pS129 α-Syn inclusions was scored using an adapted scoring-system from Rey et al. (209). Although some pS129 α-Syn pathology was observed in all groups, it was most evident following combined rAAV6-α-Syn+PFFs injections, where DA.VRA4 had more severe and widespread pathology compared to DA rats (**Figure 16B**).

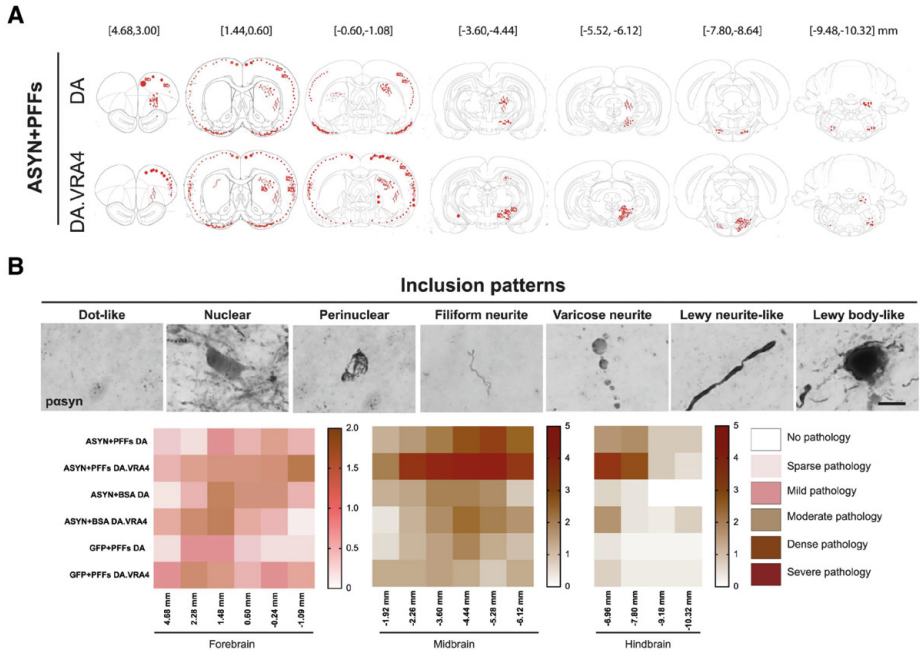

Figure 16. Pathological pS129 α-Syn is observed throughout the rostro-caudal axis and is more evident in DA.VRA4 rats following rAAV6-α-Syn+PFFs injections.
(A) Representative illustration of the pS129 α-Syn load present in one DA (top) and one DA.VRA4 (bottom) rat following rAAV6-α-Syn+PFFs injection. **(B)** Representative images of different inclusion patters of pS129 α-Syn (top), scale bar = 10 µm. Heat-map showing the severity of pS129 α-Syn pathology along the rostro-caudal axis in all groups (bottom). **Abbreviations**. ASYN/α-Syn, α-Synuclein; PFFs, preformed fibrils; pαsyn/pS129 α-Syn, α-Synuclein phosphorylated at Serine resiude 129; BSA, bovine serum albumin; GFP, green fluorescent protein; rAAV6, recombinant adeno-associated virus serotype 6.

Summary of findings in Paper I

In **Paper I**, we confirm and expand on the findings that allelic *Ciita* variants can regulate the susceptibility and progression of PD-like neurodegeneration with subsequent motor impairments following α-Syn-induced PD-like pathology (130). Additionally, we report that the congenic DA.VRA4 strain may have a compensatory mechanism of increasing the number of activated microglia due to reduced *Ciita* and MHCII levels. Previous studies have shown that priming with IL-4, which is associated with anti-inflammatory microglia/macrophages (248, 249), and reduced α-Syn propagation in mice transplanted with α-Syn overexpressing mouse embryonic midbrain neurons (250). This, along with findings that MHCII+ microglia numbers correlate with pS129 α-Syn load in the SNpc following striatal PFFs seeding (247), and that priming microglia with LPS exacerbate α-Syn transfer between neurons (250), strongly suggests that the number of activated microglia could drive α-Syn pathology. In contrast, LPS priming in the 5xFAD mouse model

of Alzheimer's disease enhanced amyloid β internalization in microglia and reduced amyloid β deposits in the prefrontal cortex and dentate gyrus (251), and pharmacological reduction of total microglia numbers exacerbated α-Syn propagation between neurons in an α-Syn cell-to-cell transfer mouse model (250). Collectively, these reports highlight a dual role for microglia, which is context-dependent, in neurodegenerative disease. More studies are necessary to fully elucidate if it is the increased number of reactive microglia that cause more widespread α-Syn pathology in the congenic DA.VRA4 rats compared to DA rats.

In addition to the crucial role that microglia seem to have in PD pathogenesis, multiple studies have highlighted the importance of the peripheral immune system and its impact on PD or PD-like progression (56, 79-82, 200, 252, 253). To what extent allelic variants of *Ciita* affect immune cell populations is limited. A pervious study have shown that DA.VRA4 congenic rats display reduced susceptibility and progression in the EAE model for MS (129), which is driven by adaptive immune responses (254) How allelic *Ciita* variants affect major immune cell populations in naïve rats, or how *Ciita* variants affect peripheral immune responses over time, following α-Syn-induced PD-like pathology, is not known. In **Paper II** we set out to close this knowledge gap by performing immune characterization of the DA and DA.VRA4 strains in naïve rats and by exploring changes in immune responses over time in both strains following rAAV6-α-Syn+PFFs injections.

Paper II | *Ciita* regulates immune profiles in naïve rats and in response to rAAV6-α-Syn+PFFs injections

In **Paper II**, we conducted immune characterization of major immune cell populations in blood and brain using flow cytometry, and measured cytokine levels in CSF and serum using multiplexed electrochemiluminescence ELISA. This characterization was performed on naïve DA and DA.VRA4 rats to identify differences prior to any exogenous α-Syn exposure. Additionally, we investigated two time points following rAAV6-α-Syn+PFFs injections: four weeks after rAAV-α-Syn injection, suspected to be the peak inflammatory response with little or no neurodegeneration present (119), and eight weeks after rAAV-α-Syn injection, the same time point investigated in **Paper I**, with evident neurodegeneration, α-Syn pathology and microglia activation.

Microglia response is highest four weeks after rAAV6-α-Syn nigral injection in the rAAV6-α-Syn+PFFs model

First, we focused on the brain, specifically resident microglia ($CD45^{low}CD11b+$), and infiltrating monocytes/macrophages ($CD45^{high}CD11b+$) (**Figure 17A**). There was no major infiltration of monocytes/macrophages (or T lymphocytes) following human α-Syn exposure in **Paper II**. The MHCII levels were generally lower on

monocytes/macrophages in DA.VRA4 rats compared to DA rats (**Figure 17B**), but did not change in response to exogenous α-Syn exposure.

Relative MHCII levels on microglia were reduced in DA.VRA4 rats compared to DA rats (**Figure 17C**), which was in line with what was observed by IHC analyses in **Paper I**. Both strains showed elevated MHCII levels on microglia following rAAV6-α-Syn+PFFs injections at four- but not eight-weeks post SNpc injection (**Figure 17C**). The percentage of microglia expressing MHCII was higher in naïve DA.VRA4 compared to naïve DA rats, suggesting that the DA.VRA4 rats are more inflammatory-prone during homeostatic conditions (**Figure 17D**). Similarly, to the MHCII levels, the percentage of MHCII+ microglia increased in both strains at four weeks, but returned to baseline levels at the eight-week time point (**Figure 17D**).

The lack of differences in percentage of MHCII+ microglia at eight weeks likely relate to the choice of analyzing entire hemispheres by flow cytometry, potentially diluting region-specific differences in areas such as striatum and midbrain. This reasoning is supported by results in **Paper I**, where we observed region-dependent strain differences in the MHCII+ microglia population. Previous reports also support the rationale of a peak neuroinflammatory response prior to neurodegenerative events following injection of PFFs into striatum (247) and SNpc (204) in rats, in transgenic mice overexpressing human α-Syn under the Thy-1 promotor (255), as well as in rats injected with rAAV-α-Syn and PFFs, spaced four weeks apart, into the SNpc (119). Therefore, it is possible that the microglia response, even if restricted to certain brain areas, was substantial enough to be observed at the four-week time point (suspected peak neuroinflammation), but reduced and diluted enough to no longer be observed at the eight-week time point using flow cytometry.

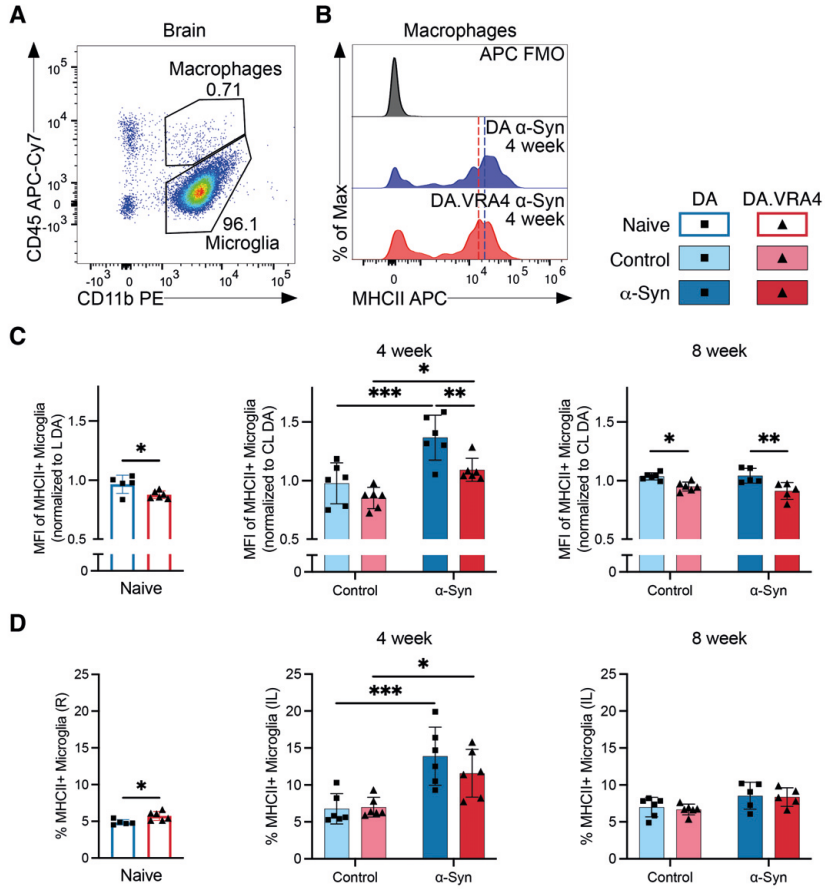

Figure 17. MHCII+ microglia response is highest at 4 weeks after rAAV-α-Syn+PFFs injections. (**A**) Gating of microglia ($CD45^{low}CD11b+$) and infiltrating monocytes/macrophages ($CD45^{high}CD11b+$). (**B**) Representative histogram of MHCII levels on infiltrating monocytes/macrophages four weeks after rAAV-α-Syn+PFFs injection. Approximate MHCII+ MFI-value indicated by dashed vertical lines. (**C**) Quantification of relative MFI-values of MHCII+ microglia. R/IL MFI-values were normalized to mean MHCII+ MFI-values of L/CL hemispheres of DA rats. (**D**) Quantification of the percentage of MHCII+ microglia in R/IL hemispheres. (**C-D**) Data presented as mean ± SD with individual values. Statistical analyses performed using Students t-test for naïve rats and two-way ANOVA with Šídák multiple comparison post-hoc test at the four- and eight-week time points. *p < 0.05, **p < 0.01, ***p < 0.001. **Abbreviations**. CD, cluster of differentiation; FMO, fluorescence minus one; α-Syn, α-Synuclein; MHCII, major histocompatability complex II; MFI, median fluorescent intensity; L, left; CL, contralateral; R, right; IL, ipsilateral; rAAV6, recombinant adeno-associated virus serotype 6; PFFs, preformed fibrils; SD, standard deviation; ANOVA, analysis of variance.

Determining if microglia activity and neuroinflammation peaks prior to neurodegeneration in PD is more challenging (256). Current literature based on positron emission tomography (PET) imaging suggests that microglia activity is widespread and relatively constant during disease progression (257). One study using a PET ligand specific for activated microglia identified differences in

microglia binding potential in multiple brain areas (although not in midbrain or SN) compared to age-matched controls (258). The same study reported that the binding potential remained unchanged in longitudinal investigations and did not increase with disease progression (258). In contrast, another study investigating patients with early PD using the same PET ligand reported a correlation between motor impairments and binding potential in the midbrain compared to controls (259). The same PET ligand has also been criticized and suggested to be inadequate in providing reliable measurements of neuroinflammation in PD patients (260). Despite the different outcomes, which may be due to methodological differences and the inclusion of patients with varying disease severity, most PET imaging studies have reported elevated microglia activity during PD progression compared to healthy controls (257).

In **Paper II**, it is important to note that even if we observe a peak neuroinflammatory reaction at the four-week time point, we have yet to determine if substantial neurodegeneration is present at this stage in the rAAV-α-Syn+PFFs model. In the original model, the authors reported a trend towards TH+ fiber density loss in striatum approximately five weeks after rAAV-α-Syn and ten days after PFFs injection, both injected into the SNpc (119). Based on this, minor neurodegenerative events may have already occurred already at four weeks in the rAAV6-α-Syn+PFFs model used in **Paper II**. Additionally, the choice of analyzing cells isolated from entire hemispheres by flow cytometry may have diluted any infiltration of lymphocytes or macrophages, which has been observed experimental models and in post-mortem PD brains (79, 82, 200, 261).

Minor changes in peripheral immune cell populations are observed following exposure to exogenous α-Syn

In addition to the infiltration of peripheral immune cells into the CNS, changes in circulating immune cells have been reported in PD. However, studies characterizing T cell compartments in PD are inconclusive, with different profiles of T cell subsets being reported (87-92). In **Paper II**, we detected only minor changes of T cells. Naïve DA.VRA4 rats had reduced CD4/CD8 ratio compared to DA rats. In response to exogenous α-Syn, only DA rats showed a reduced ratio compared to control, with no difference between strains.

In humans, *ex vivo* studies have reported functional alterations of T cells, including impaired migratory capacity of CD4+ T cells (93), impaired Treg suppressor function (87), and an association between T cell reactivity and PD severity following PHA stimulation (88). Whether T cell function is altered following combined rAAV-α-Syn+PFFs injection or regulated by *Ciita* requires further investigation, by e.g., PHA stimulation or ELISpot.

The percentage of circulating myeloid cells (CD45+CD11b+) (**Figure 18A**) did not differ between DA and DA.VRA4 rats. However, the percentage of myeloid cells

expressing MHCII was higher in naïve DA.VRA4 rats compared to DA rats, indicating a more inflammatory-prone naïve profile (**Figure 18B**). The number of MHCII+ myeloid cells did not change in response to rAAV6-α-Syn+PFFs injection at any time point investigated (**Figure 18B**). In contrast, MHCII MFI-levels increased at eight weeks in both strains compared to their respective controls (**Figure 18C**). As expected, the general trend showed reduced relative MHCII levels on circulating myeloid cells in DA.VRA4 rats compared to DA rats (**Figure 18C**).

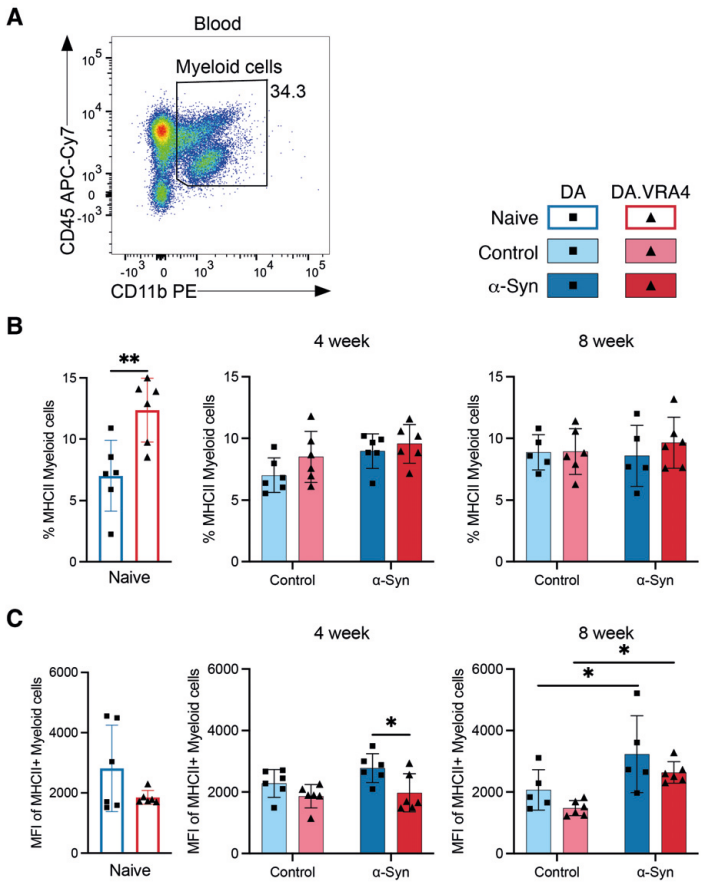

Figure 18. MHCII levels are highest eight weeks following rAAV6-α-Syn+PFFs injection in both DA and DA.VRA4 rats.

(**A**) Myeloid cells were gated as CD45+CD11b+ cells. (**B**) Quantification of percentage of MHCII+ myeloid cells. (**C**) Quantification of MFI-values of MHCII+ myeloid cells. (**B-C**) Data presented as mean ± SD with individual values. Statistical analyses performed using Students t-test for naïve rats and two-way ANOVA with Šídák multiple comparison post-hoc test at the four- and eight-week time points. *p < 0.05, **p < 0.01. **Abbreviations**. CD, cluster of differentiation; α-Syn, α-Synuclein; MHCII, major histocompatability complex II; MFI, median fluorescent intensity; rAAV6, recombinant adeno-associated virus serotype 6; PFFs, preformed fibrils; SD, standard deviation; ANOVA, analysis of variance.

These results align with findings in PD, where elevated MHCII levels on intermediate and non-classical monocytes have been observed in late, and not early, PD (85). However, we investigated the general myeloid cell population, which includes monocytes and granulocytes (mainly neutrophils), hindering separate analyses of these populations and their subpopulations (discussed in methodological considerations). Alterations in monocyte subpopulations in PD have been reported, including reduced activity based on soluble CD163 levels (84). Furthermore, sexual dimorphism in monocyte populations has been observed in several studies, highlighting the importance of sex in PD progression (83-86). Throughout **Paper I-III** we used only male rats, hindering the possibility of identifying sex-dependent differences.

Fewer studies have investigated neutrophils in PD. One study reported an overall reduction of both lymphocytes and monocytes, but not in neutrophils, in idiopathic PD compared to healthy controls (262). Additionally, the neutrophil-to-lymphocyte ratio, a marker of systemic inflammation (263), has been reported to be higher in PD patients compared to healthy controls (262, 264). To determine if *Ciita* levels affect neutrophil or monocyte subpopulations requires further investigation, ideally including both males and females to account for potential sex differences in the rat model as well.

Allelic Ciita variants in congenic DA.VRA4 rats are associated with consistently higher levels of sTNF in serum

Altered cytokine levels are also implicated in PD and have been identified in several studies. A meta-analysis reported increased levels of several cytokines in blood from PD patients, including IL-6, sTNF, IL-1β, CRP, IL-2, RANTES, and IL-10 (265). Another study of 230 newly diagnosed PD patients reported elevated levels of sTNF, IL-1β, IL-2, and IL-10 (266). Studies on cytokine levels in CSF from PD patients are few, and available data is limited. A meta-analysis from 2018 reported increased levels of IL-1β, IL-6 and TGF-β (267). The most recent meta-analysis however, reported elevated levels of IL-1β, IL-6, and sTNF in both CSF and blood (78)

To further characterize how *Ciita* variants affect the peripheral immune response following rAAV6-α-Syn+PFFs injections, we investigated nine cytokines in serum and CSF (specified in methodological considerations). Most cytokines analyzed in **Paper II** were unaffected by both exogenous α-Syn and *Ciita* variants, and the levels observed were generally low, outside of the linear range. At the eight-week time point, CSF IL-10 levels were higher in DA.VRA4 rats compared to DA rats following rAAV-α-Syn+PFFs injections, and the levels were undetectable in the control groups (**Figure 19A**). In contrast, IL-6 levels in CSF were regulated by exogenous α-Syn and increased in both strains compared to their respective controls at the eight-week time point (**Figure 19B**). IL-10 and IL-6 levels in CSF did not differ between naïve rats or in any groups at the four-week time point. It is somewhat

surprising that we observe elevated CSF IL-6 levels at the eight-week, and not four-week, time point when microglia activity was highest. It is possible that there is an inflammatory response following the physical damage after striatal PFFs injection, which occurred two weeks prior to the four-week time point, which may have interfered with any specific response, albeit IL-6 or any other cytokine examined, towards exogenous α-Syn.

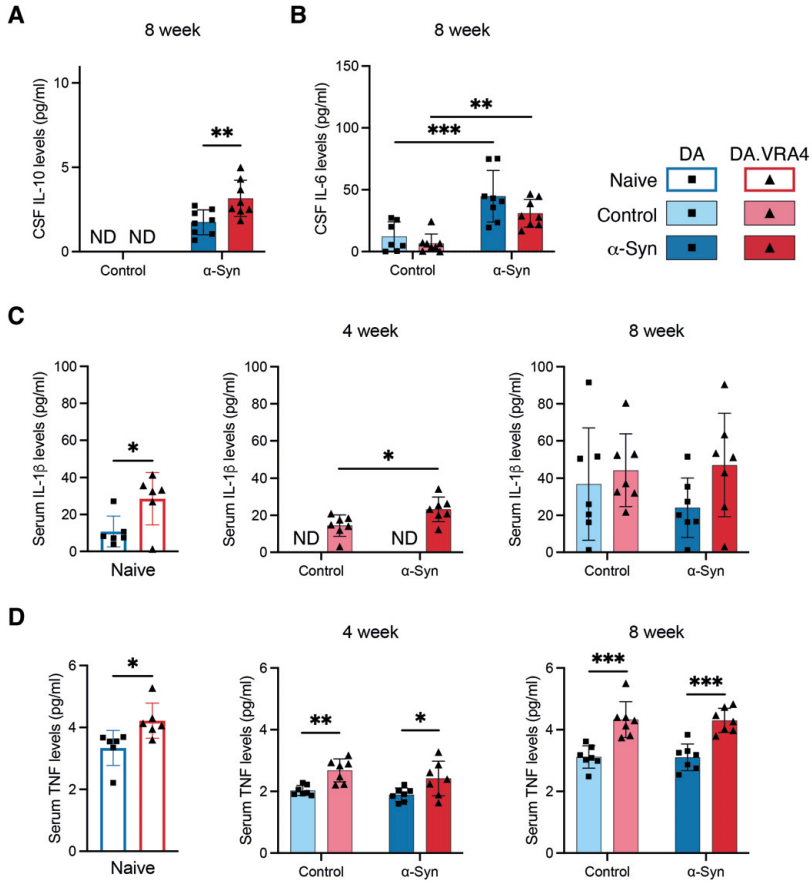

Figure 19. DA.VRA4 rats have consistently higher sTNF levels in serum compared to DA rats. (**A**) Quantification of IL-10 levels in CSF eight weeks following rAAV6-α-Syn+PFFs injections. (**B**) Quantification of IL-6 levels in CSF at the eight week time point. (**C**) Quantification of IL-1β serum levels in naïve rats or following injections of rAAV6-α-Syn+PFFs. (**D**) Quantification of sTNF levels in serum in DA and DA.VRA4 rats. (**A-D**) Data presented as mean ± SD with individual values. Statistical analyses performed using Students t-test for naïve rats and two-way ANOVA with Šídák multiple comparison post-hoc test at the four- and eight-week time points. *p < 0.05, **p < 0.01, ***p < 0.001. **Abbreviations**. CSF, cerebrospinal fluid; IL, interleukin; ND, not detected; α-Syn, α-Synuclein; TNF/sTNF, soluble tumor necrosis factor; rAAV6, recombinant adeno-associated virus serotype 6; PFFs, preformed fibrils; SD, standard deviation; ANOVA, analysis of variance.

IL-1β levels in serum were *Ciita*-dependent, with naïve DA.VRA4 rats having higher levels compared to DA rats (**Figure 19C**). Additionally, IL-1β levels increased in DA.VRA4 rats in response to rAAV6-α-Syn+PFFs injections at four weeks, whereas the levels were undetectable for DA rats (**Figure 19C**). Although IL-1β levels were detectable at eight weeks in all groups, no differences were observed. Interestingly, sTNF serum levels were regulated by *Ciita* variants, with DA.VRA4 rats constitutively having higher sTNF levels compared to DA rats, which remained unaltered following exogenous α-Syn (**Figure 19D**).

Available data on blood and CSF cytokine levels in α-Syn-induced models are lacking. Following striatal injection of PFFs in mice, one study reported no change in serum cytokine levels (268). Most studies have investigated cytokines in brain homogenates, rather than in CSF and/or blood, reporting slightly different outcomes. Eight weeks following striatal PFFs injection in mice TNF levels were elevated in striatal tissue (269). Increased levels of TNF, ICAM-1, IL-1α, and IL-6 in SN was observed two weeks following nigral rAAV-mediated α-Syn overexpression in mice (270). In contrast, another study, also utilizing nigral rAAV-mediated α-Syn overexpression in mice, reported no cytokine alterations in SN but instead elevated levels of IL-1β, IFN-γ, and TNF in striatum eight weeks post injection (271). Indeed, investigating region-specific cytokine responses in brain homogenates could be help explain why allelic *Ciita* variants alter susceptibility and progression to α-Syn-induced PD-like pathology.

Summary of findings in Paper II

In **Paper II**, we demonstrate using flow cytometry and electrochemiluminescence ELISA that *Ciita* variants regulate baseline immune profiles and cytokine levels. DA.VRA4 rats, with lower levels of *Ciita,* exhibited more inflammatory-prone myeloid cells in circulation and microglia in the brain, as indicated by elevated MHCII-levels. Additionally, DA.VRA4 rats had higher levels of both IL-1β and sTNF in serum. We also observed that the microglia response peaks prior to major neurodegenerative events, whereas the increase in MHCII levels on myeloid cells occurred later. The impact of myeloid cells in the rAAV6-α-Syn+PFFs model is still to be determined. It is possible that the altered immune profiles observed at baseline in DA.VRA4 rats contribute to the increased susceptibility to exogenous α-Syn, reported in **Paper I,** which includes motor impairments, neurodegeneration and α-Syn pathological spread.

Based on our findings in **Paper I** and **II**, we hypothesize that the increased numbers of activated microglia affect both susceptibility and progression of PD-like pathology. This rationale is supported by evidence that MHCII KO protects against nigral α-Syn overexpression-induced microglia activation and neurodegeneration in mice (186). However, a more recent study suggests that CNS-resident BAMs, rather than microglia, are the main contributors to α-Syn-induced neuroinflammation and neurodegeneration (82).

In our proposed model (**Figure 20**), processed α-Syn peptides are presented to CD4+ T lymphocytes in the CNS, initiating an adaptive immune response. Indeed, α-Syn reactive T cells have been observed in PD patients (56, 80, 81). Elevated sTNF levels may increase the number of nigral astrocytes and microglia, exacerbating dopaminergic neurodegeneration. Multiple studies using toxin- or endotoxin-induced neurodegeneration have shown that inhibiting sTNF mitigates neuroinflammatory responses and protects against dopaminergic neurodegeneration (243, 272-274). In **Paper III**, we chose to further investigate role of sTNF on susceptibility and progression following rAAV6-α-Syn+PFFs-induced PD-like pathology in DA.VRA4 rats using a DN-TNF protein which sequesters sTNF (32).

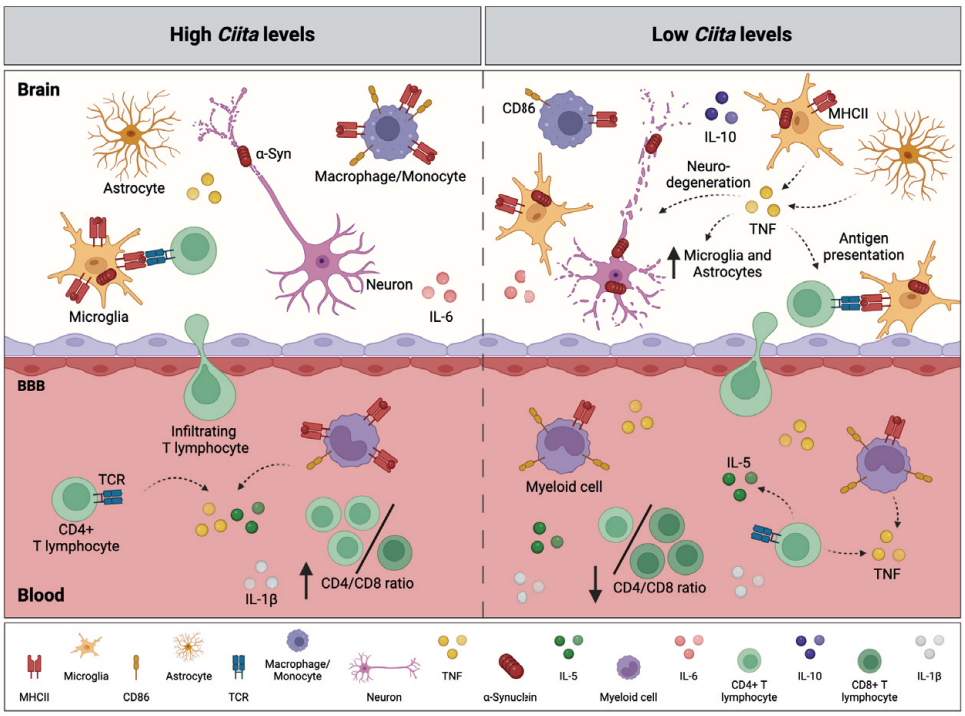

Figure 20. Hypothesis for how *Ciita* variants regulates baseline immune populations, cytokine levels, α-Syn propagation and susceptibilty to PD-like neurodegeneration.
Summary of main findings from **Paper I** and **II**. Dashwed arrows indicate possible sources and/or mechanisms based on litterature. Created with BioRender.com. **Abbreviations**. Ciita, class II transactivator; α-Syn, α-Synuclein; IL, interleukin; BBB, blood brain barrier; TCR, T cell receptor; CD, cluster of differentiation; MHCII, major histocompatability complex II; TNF, tumor necrosis factor.

Paper III | Inhibition of sTNF is not protective against rAAV6-α-Syn+PFFs induced Parkinson's disease-like neurodegeneration, pathology or neuroinflammation

In **Paper III** we set out to determine the role of sTNF on susceptibility and progression following unilateral rAAV6-α-Syn+PFFs injections in DA.VRA4 rats with allelic *Ciita* variants. We used a DN-TNF variant, XPro1595, to inhibit soluble but not membrane bound TNF (32, 243). Dopaminergic neurodegeneration, α-Syn pathology and neuroinflammation was evaluated eight weeks after rAAV6-α-Syn+PFFs injections, the earliest time point with significant neurodegeneration, observed in **Paper I**.

Systemic treatment of XPro1595 can reach the CNS in sufficient concentrations to neutralize native sTNF (243, 275). In **Paper III**, we confirmed that XPro1595 levels reached the CNS in comparable concentrations to previous studies (243, 275).

Systemic sTNF inhibition does not protect against rAAV6-α-Syn+PFFs induced neurodegeneration

Dopaminergic neurodegeneration was evaluated by investigating TH+ cells in SNpc, TH+ fiber density in dorsal striatum, and TH+ axonal swellings in dorsal striatum, as a sign of early axonal pathology. We trained a CNN algorithm to quantify TH+ cells in the SNpc, an approach that has been shown to be comparable to conventional stereology (241). The loss of TH+ cells in SNpc was similar between controls and XPro1595 treated rats with a 32-35% loss of TH+ cells compared to the contralateral side (**Figure 21A**). Similarly, the TH+ fiber density, as a measurement of axonal loss, was similar in both groups along the rostro-caudal axis, showing a mean reduction of 25-50% depending on the coronal coordinate (**Figure 21B**). The neurodegenerative events observed in **Paper III** were similar to what was observed in the DA.VRA4 rats in **Paper I**, where there was an approximate 40% loss of TH+ cells in SNpc and 50% loss of TH+ fibers in dorsal striatum. The slightly more pronounced neurodegeneration observed in **Paper I** is likely due to methodological differences, including more PFFs injected and stronger human α-Syn expression (**Figure 13A** versus **C**).

To assess axonal swellings, we trained an AI model to identify larger TH+ axonal swellings, approximately >3 µm in diameter, a size that were almost completely devoid in contralateral dorsal striatum (**Figure 21C**). The quantification revealed similar size distributions in both ipsilateral and contralateral hemispheres around 10 μm^2, although there were substantially more swellings in the ipsilateral hemispheres versus contralateral in both groups ($p < 0.001$, chi-squared goodness-of-fit test) (**Figure 21D**). After correcting for the size of the dorsal striatum regions and the number of TH+ cells remaining, there was no difference observed between saline and XPro1595 treated rats (**Figure 21E**).

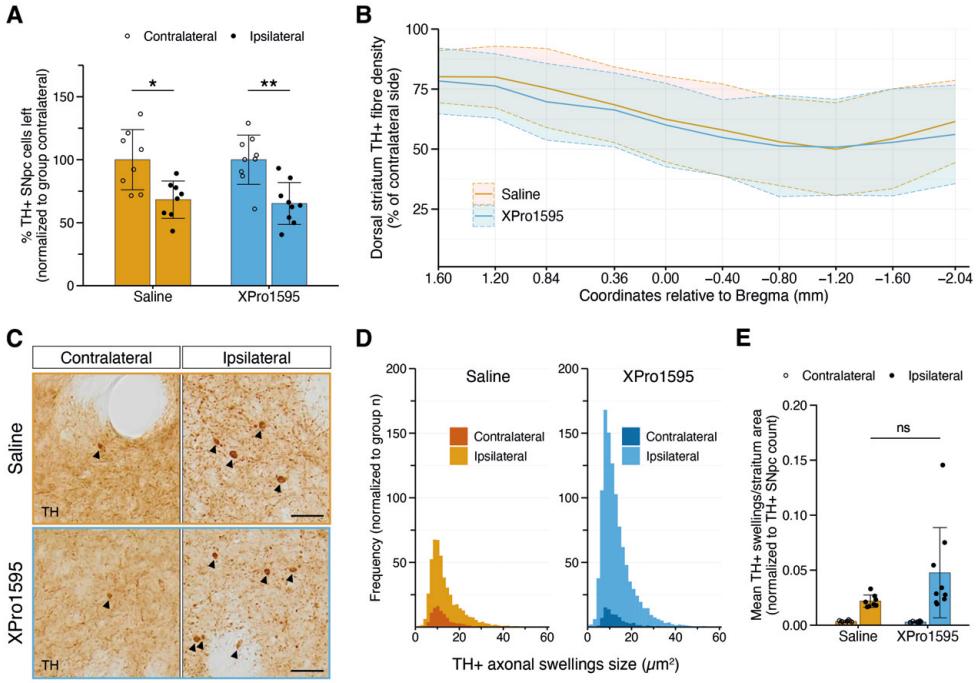

Figure 21. sTNF inhibition using XPro1595 does not protect against neurodegeneration following unilateral rAAV6-α-Syn+PFFs injections.

(**A**) Quantification of percentage TH+ cells left in the SNpc (relative to group contralateral). Statistical analysis perfomred using two-way ANOVA with Tukey's HSD post-hoc test. * $p < 0.05$, ** $p < 0.01$. (**B**) Remaining TH+ fiber density, relative to contralateral hemisphere, in the dorsal striatum along the rostro-caudal axis. Mean ± SD is shown. (**C**) Representative images of TH+ axonal swellings in the dorsal striatum. Axonal swellings identified by the CNN algorithm are indicated by arrowheads. Scale bar = 25 µm. (**D**) Histogram of TH+ axonal swelling frequencies across sizes. Statistical analysis performed using chi-squared goodness-of-fit test to compare ipsilateral and contralateral dorsal striatum in both groups ($p < 0.001$ in both groups). (**E**) Quantification of normalized TH+ axonal swellings. Unpaired student's t-test was used to compare ipsilateral hemispheres between treatments. (**A** and **E**) Data presented as mean ± SD with individual values. **Abbreviations**. TH, tyrosine hydroxylase; SNpc, substantia nigra pars compacta; ns, non-significant; rAAV6, recombinant adeno-associated virus serotype 6; α-Syn, α-Synuclein; PFFs, preformed fibrils; ANOVA, analysis of variance; HSD, honestly significant difference; SD, standard deviation; CNN, convolutional neural network.

Pathological α-Syn load following sTNF inhibition is unaltered in the rAAV6-α-Syn+PFFs model

Since DA.VRA4 rats, with reduced *Ciita* levels, showed extensive and widespread pS129 α-Syn pathology in response to human α-Syn (**Paper I**) and had elevated sTNF serum levels (**Paper II**) we wanted to test if sTNF inhibition would affect the extent of pS129 α-Syn pathology. In the ipsilateral dorsal striatum, the morphology of the pS129 α-Syn inclusions was similar in both saline- and XPro1595 treated rats, appearing as puncta or neurite-like (**Figure 22A**). The percent positive pS129 α-Syn area was unaffected by XPro1595 treatment (**Figure 22B**).

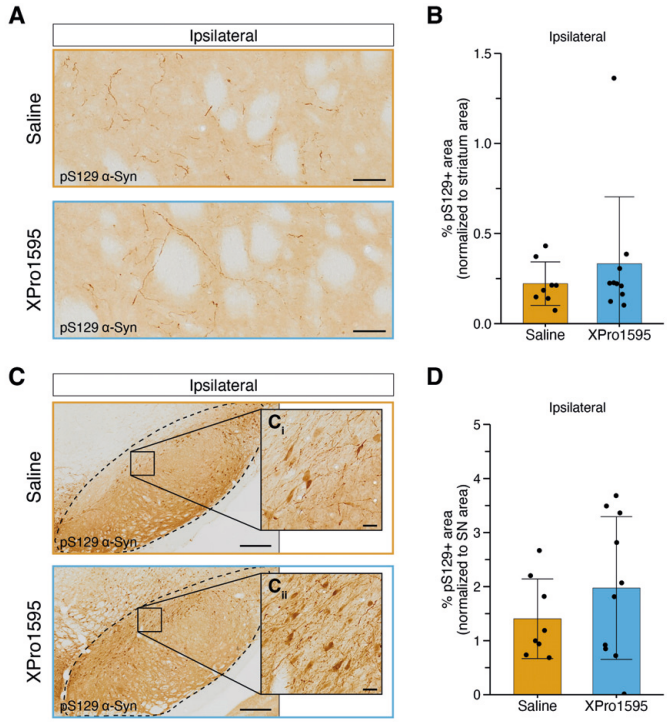

Figure 22. pS129 α-Syn pathological load is unaffected by systemic sTNF inhibition following rAAV6-α-Syn+PFFs injections.
(**A**) Representative image of pS129 α-Syn immunoreactiviy in the dorsal striatum of saline (top) and XPro1595 (bottom) treated rats. Scale bar = 50 µm. (**B**) Quantification of pS129 α-Syn positive area normalized to dorsal striatum area analyzed. (**C**) Representative image of pS129 α-Syn immunoreactiviy in SN of saline (top) and XPro1595 (bottom) treated rats. Scale bar = 300 µm. Scale bar in $\mathbf{C_i}$ and $\mathbf{C_{ii}}$ = 25 µm. (**D**) Quantification of pS129 α-Syn positive area normalized to SN area analyzed. (**B** and **D**) Data presented as mean ± SD with individual values. Unpaired Students t-test was used to compare groups. **Abbreviations**. pS129, phosphorylated serine residue 129; α-Syn, α-Synuclein; SN, substantia nigra; sTNF, soluble tumor necrosis factor; rAAV6, recombinant adeno-associated virus serotype 6; PFFs, preformed fibrils; SD, standard deviation.

Similar to striatum, the morphology of pS129 α-Syn inclusions in ipsilateral SN were comparable between treatment groups although more prominent, including puncta, neurite-like and present in the cytoplasm (**Figure 22C**). No difference in pS129 α-Syn immunoreactivity was observed between groups (**Figure 22D**).

It is worth noting that the rat with most pS129 α-Syn immunoreactivity in striatum (and also with extensive pathology in SN) in the XPro1595 group also accounted for almost one third of all TH+ axonal swellings in the XPro1595 treated rats, but displayed only mild neurodegeneration (data not shown). This is purely observational and may be due to methodological or biological variation, however, it may also be due to an effect from the XPro1595 treatment, ultimately delaying

neurodegenerative events even in the context of pronounced pS129 α-Syn pathology and early signs of neuronal stress.

Astrocyte response is region-dependent and unaffected by sTNF inhibition following nigral α-Syn overexpression combined with striatal seeding with PFFs

In **Paper I** and **II** we did not analyzed astrocytes following exogenous α-Syn exposure, and we do not know if *Ciita* variants affect astrocyte reactivity in our PD model. Since activated astrocytes are observed in post mortem PD brains, indicating a role in disease progression (276), and that sTNF inhibition reduced astrocyte reactivity following 6-OHDA (243), we also examined astrocyte reactivity in SN and striatum in **Paper III**.

Following unilateral rAAV6-α-Syn+PFFs injections there was a distinct increase in GFAP immunoreactivity, representing activated astrocytes, in the dorsal striatum. Quantification of GFAP+ area showed that systemic sTNF inhibition was ineffective in mitigating astrogliosis (**Figure 23A**).

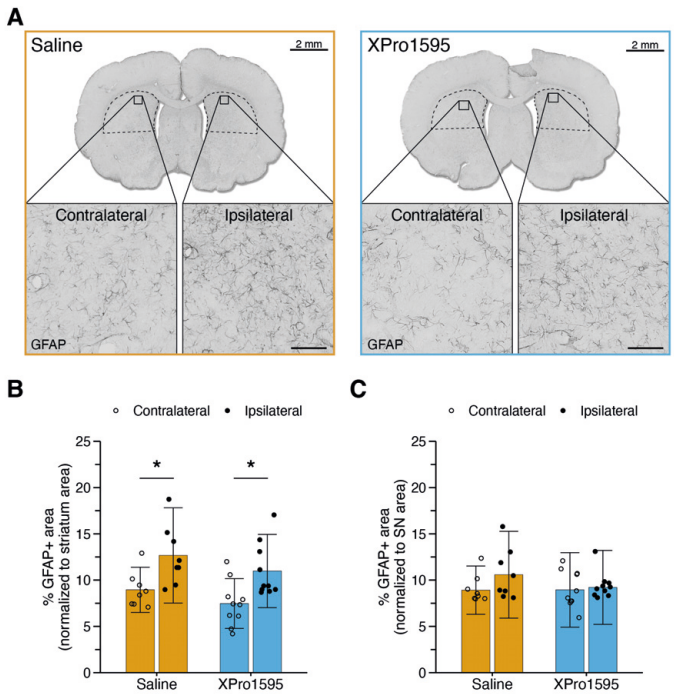

Figure 23. Astrogliosis is region-dependent following rAAV6-α-Syn+PFFs.
(**A**) Representative images of GFAP immunoreactivity in the dorsal striatum in saline (left) and XPro1595 (right) treated rats. Scale bar = 80 µm, unless otherwise stated. (**B**) Quantification of normalized GFAP+ area in dorsal striatum. (**C**) Quantification of normalized GFAP+ area in SN. (**B** and **C**) Data presented as mean ± SD with individual values. Statistical analyses performed using the two-way ANOVA with Tukey HSD post-hoc test. *p < 0.05.

In contrast, no clear difference was observed in the SN between contra- and ipsilateral hemispheres following rAAV6-α-Syn+PFFs injections (**Figure 23B**), suggesting a region-dependent upregulation of GFAP eight weeks after rAAV6-α-Syn+PFFs exposure. Multiple studies have reported astrogliosis in SN using experimental models of PD, including 6-OHDA injections in rats (243), striatal PFFs injection in mice (268), and following inoculation of LB extract in SNpc in mice (277). Available studies investigating astrocyte reactivity following combined rAAV-mediated α-Syn overexpression and PFFs injection are lacking. It is possible that astrocyte reactivity in the SN peaks prior to neurodegeneration, similar to the microglia.

The aim of **Paper III** was to specifically investigate the effects of sTNF inhibition following exposure to exogenous α-Syn, therefore further investigation is necessary to fully elucidate the role of astrocytes following rAAV6-α-Syn+PFFs injections. However, CIITA has been shown to regulate MHCII expression on astrocytes (278, 279), and been suggested to have a role in antigen presentation in an EAE mouse model of MS (280). Recently, astrocytes were reported to have antigen presentation capacity in PD, and *ex vivo* analyses of primary microglia and astrocytes showed that astrocytes expressed co-stimulatory markers necessary for antigen presentation following exposure to PFFs, which was not observed in microglia cultures (21). Indeed, being the most abundant cell type in the CNS, astrocytes are likely to play a role in PD progression, but further investigation is required to delineate the exact role (281).

Microglia analysis using deep CNN reveal region-dependent activation which is unaltered following systemic sTNF treatment

Finally, we investigated the microglia response in detail utilizing CNN algorithms trained with supervised learning. The developed AI model efficiently identified Iba+ cells in both striatum (**Figure 24A**) and SN (**Figure 24B**). PCA of all analyzed Iba1+ cells revealed area to be the main contributor to PC1 in both datasets from striatum (**Figure 24C**) and SN (**Figure 24D**). When each region, i.e., hemispheric dorsal striatum or SN, was analyzed separately, Iba1+ cell counts clearly distinguished contralateral and ipsilateral hemispheres in dorsal striatum (**Figure 24E**) but not SN (**Figure 24F**). Conventional analyses confirmed a higher Iba1+ cell count and reduced cell area following unilateral rAAV6-α-Syn+PFFs injections in the ipsilateral compared to contralateral hemisphere (**Figure 24G** and **H**). In contrast, two-way ANOVA revealed no hemisphere effect on Iba1+ cell count in SN whereas the cell area was significantly reduced following exposure to exogenous α-Syn (**Figure 24I** and **J**). Throughout the analyses of microglia characteristics, systemic XPro1595 treatment failed to mitigate the microglia response, suggesting that sTNF inhibition does not protect against microglia activity following rAAV6-α-Syn+PFFs.

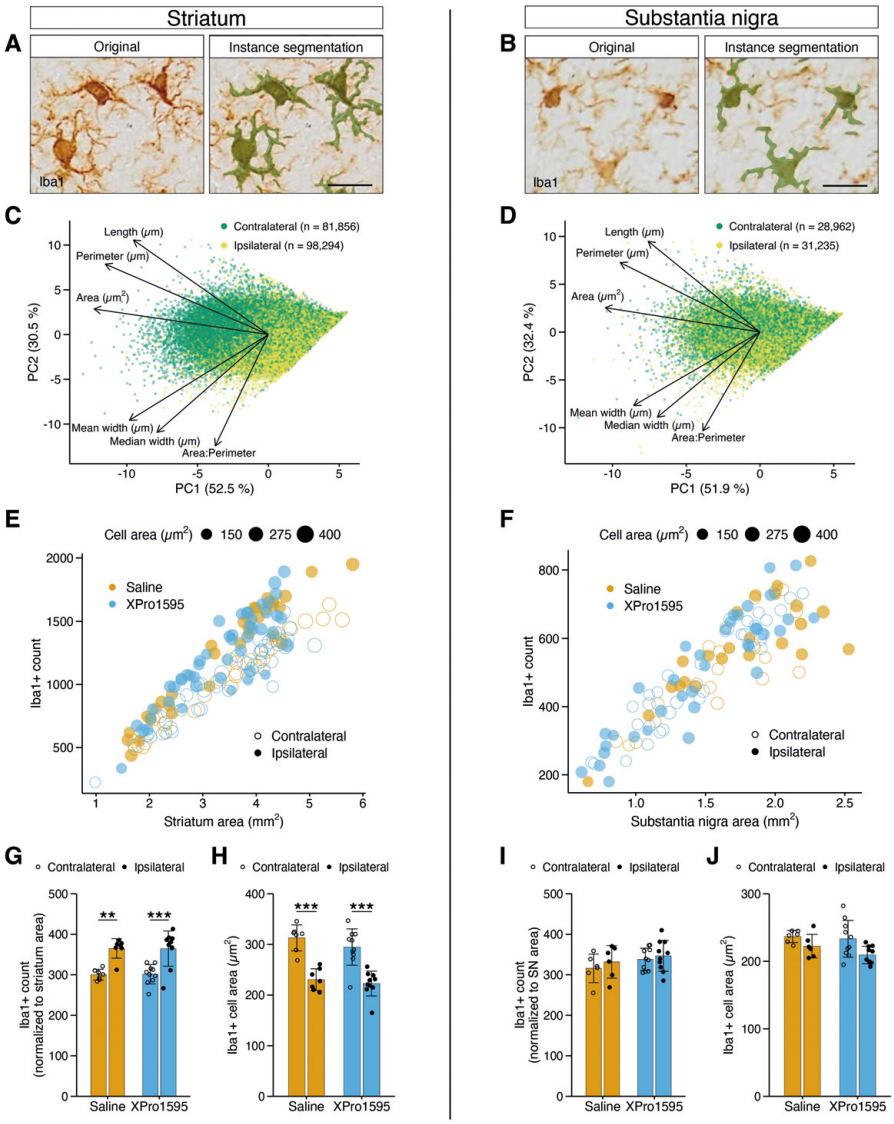

Figure 24. Detailed analyses of Iba1+ cells using CNN algorithms reveal region-dependent microglia characteristics and show no effect of sTNF inhibition following rAAV6-α-Syn+PFFs. (**A** and **B**) Representative image of Iba1+ cells and the detection by the CNN algorithm in striatum and SN. Scale bar = 20 µm. (**C** and **D**) PCA biplot with variable loadings in striatum and SN. (**E** and **F**) Scatter plots showing Iba1+ cell counts for each ROI analyzed in striatum and SN. (**G** and **I**) Quantification of normalized Iba1+ cell counts in striatum and SN. (**H** and **J**) Quantification of mean Iba1+ cell area in striatum and SN. (**G-J**) Data presented as mean ± SD with individual values. Statistical analyses was performed with two-way ANOVA and Tukey's HSD post-hoc test. **p < 0.01, ***p < 0.001. **Abbreviations**. Iba1, ionized calcium-binding adapter molecule 1; PC, principle component; SN, substantia nigra; CNN, convolutional neural network; sTNF, soluble tumor necrosis factor; rAAV6, recombinant adeno-associated virus serotype 6; α-Syn, α-Synuclein; PFFs, preformed fibrils; PCA, principle component analysis; ROI, region of interest; SD, standard deviation; ANOVA, analysis of variance; HSD, honestly significant difference.

Summary of findings in Paper III

In **Paper III**, we report that sTNF inhibition fails to exert neuroprotective effects and in mitigating the neuroinflammatory response following unilateral injection of rAAV6-α-Syn combined with striatal seeding with PFFs. We chose to initiate sTNF inhibition one week following injection of rAAV6-α-Syn into SNpc, and one week prior to striatal PFFs seeding based on the following rationale;

i) Initiation of XPro1595 treatment is required at least three days following 6-OHDA induced neurodegeneration to be neuroprotective (243). Therefore, an early treatment start is required.

ii) The rAAV6-α-Syn vector used in **Paper III** was injected at a low titer and overexpress human α-Syn which is combined with injection of PFFs, made from human α-Syn, which is less potent compared to using murine-derived α-Syn in a murine model system (208).

iii) XPro1595 treatment was initiated early, prior to striatal injection of PFFs, and before the rapid onset of α-Syn pathology, neurodegeneration, and neuroinflammation (99, 120).

Further investigation, initiating sTNF inhibition at, or even before, the time of rAAV6-α-Syn delivery to the SNpc is required to establish if the treatment-window was missed. However, based on the available results from **Paper III**, the consistently elevated sTNF levels associated with allelic *Ciita* variants (**Paper II**), are not central in the increased susceptibility and PD-like disease progression (**Paper I**).

Summary of findings in Paper I-III

Although the overall numbers of microglia are unaffected by allelic *Ciita* variants, the baseline state of microglia are more inflammatory-prone, indicated by an increase in MHCII+ microglia throughout the brain (**Paper II**). Following α-Syn-induced PD-like pathology, the difference in activated microglia between DA.VRA4 and DA rats becomes region-dependent, restricted to the striatum, and not SNpc (**Paper I**). We hypothesize that the reduction of *Ciita* is compensated by an increased number of MHCII+ microglia (**Paper II**), making the DA.VRA4 strain more susceptible to α-Syn-indued PD-like pathology (**Paper I**). The DA.VRA4 rats also had consistently elevated sTNF levels in serum (**Paper II**). Although sTNF levels did not change in response to rAAV6-α-Syn+PFFs injections, we investigated whether elevated sTNF levels impact PD-like disease susceptibility and progression following rAAV6-α-Syn+PFFs injection (**Paper III**). We found no protective effects using the sTNF inhibitor XPro1595 on α-Syn-induced neurodegeneration, pathology or neuroinflammation indicating that sTNF levels are not central to the

increased susceptibility and progression of PD-like pathology in the DA.VRA4 rats (**Paper III**).

The collective findings in **Paper I-III** suggest that the chronic ongoing neuroinflammatory response, mainly attributed to microglia activity and numbers, rather than sTNF, is a driving force of PD-like pathology.

Paper IV | Systemic immunomodulation targeting IL-6 signaling in synapsin 2 knockout mice delays epilepsy development but does not affect synaptic protein levels or behavior

Like PD, both ASD and epilepsy are accompanied by inflammatory responses, including elevated IL-6 levels (6, 282, 283). Individuals with ASD have over ten times the risk of developing epilepsy compared to the general population (140). There can be various reasons why an individual develops ASD and/or epilepsy, genetic mutations in synaptic proteins (including synapsins) are one of them. In **Paper IV** we use a *Syn2* KO mouse model that displays ASD-like behavior, with most mice developing epileptic seizures around two to three months of age. Additionally, *Syn2* KO mice have elevated levels of IL-6 in brain tissue before developing epileptic seizures (175).

Accordingly, in **Paper IV**, we aimed to determine if systemic treatment with an IL-6 receptor (IL-6R) antibody (ab), blocking IL-6 signaling, could affect epilepsy development and alter cognitive and ASD-like behaviors. Following systemic IL-6R ab treatment, starting before seizure onset, we observed reduced seizure development in *Syn2* KO mice; however, we did not identify the mechanism behind this observation. Additionally, we found that systemic IL-6R ab treatment did not affect ASD-related or cognitive behaviors.

Systemic IL-6R ab treatment initiated before seizure debut delays epilepsy development in Syn2 KO mice

Animal-experimenter interaction impact stress levels of rodents in preclinical research (212). Since *Syn2* KO mice have handling-induced seizures, the increased animal-experimenter interaction necessary for behavioral tests can confound the investigation of seizure parameters. Therefore, we evaluated seizure development in a cohort of *Syn2* KO mice that were not subjected to behavioral testing. Systemic IL-6R ab treatment, starting before seizure onset, reduced the overall seizure frequency seizures over a four-month period (**Figure 25A**). The number of *Syn2* KO mice that developed handling-induced seizures were also reduced from 80% to

50% following IL-6R ab treatment (**Figure 25B**). Additionally, the cumulative seizure load, i.e., the sum of epileptic seizures during the study duration, clearly separated the control and IL-6R ab groups, further illustrating delayed seizure development (**Figure 25C**).

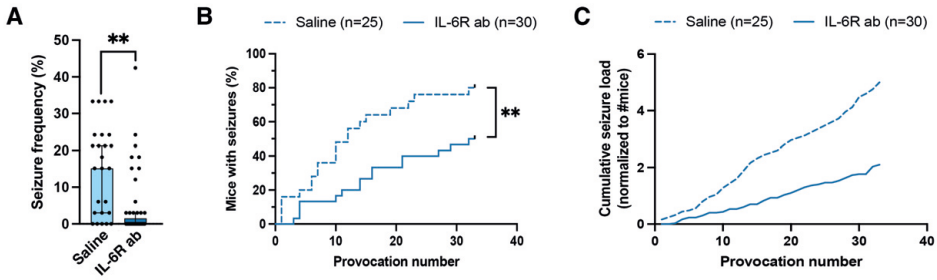

Figure 25. Deleyed seizure development following early systemic IL-6R ab treatment.
(**A**) Seizure frequency in *Syn2* KO mice following five months of systemic saline or IL-6R ab treatment. Data presented as median ± IQR with individual values. Statistical analysis was performed using the Mann-Whitney U test. **p < 0.01. (**B**) Kaplan-Meier plot showing the percentage of mice that developed seizures at each provocation. Statistical analysis was performed using the log-rank test. **p < 0.001. (**C**) Line graph depicting cumulative seizure load against provocation events. **Abbreviations**. IL-6R ab, interleukin 6 receptor antibody; KO, knockout; IQR, interquartile range.

Microglia morphology in hippocampus is unaffected by systemic IL-6R ab treatment

Syn2 KO mice have slightly more activated microglia, determined by morphology, in the ML and GCL (175). To assess the effect of systemic IL-6R ab treatment on microglia activity in the hippocampus (**Figure 26A**), we quantified microglia based on three morphology categories; ramified, intermediate, and round/ameboid (74, 175). Systemic IL-6R ab treatment did not affect microglia morphology in the ML or GCL (**Figure 26B**) or in any other hippocampal regions analyzed. Additionally, the number of Iba1+/CD68+ or GFAP+/C3+ cells (**Figure 26C**), representing activated macrophages or astrocytes, respectively, was also unaffected. Collectively these findings suggest that systemic IL-6R ab fails to reverse the region-specific inflammatory-prone microglia observed in the *Syn2* KO mice.

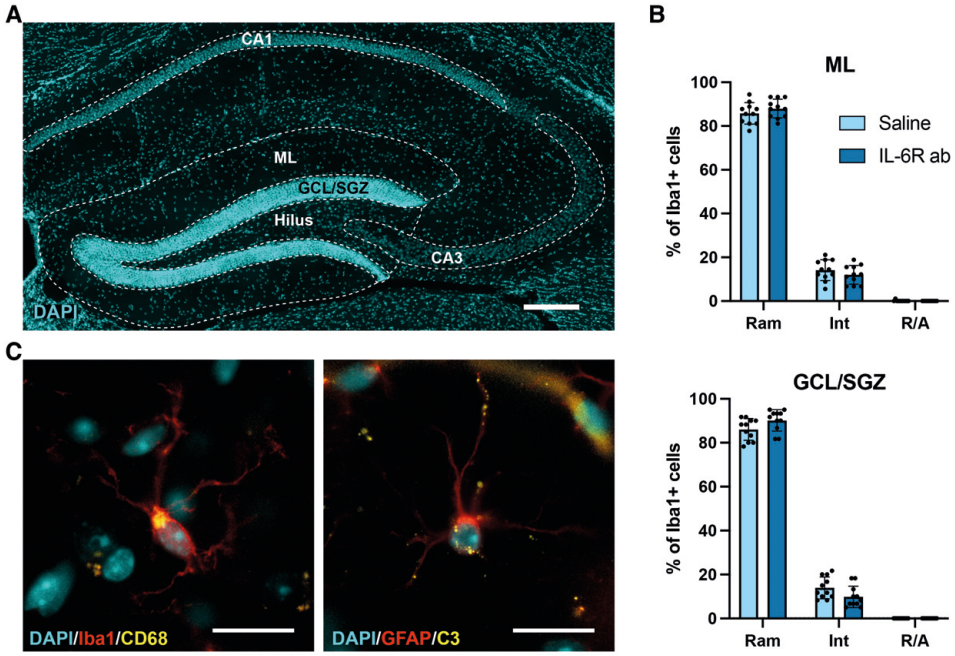

Figure 26. Early systemic IL-6R ab treatment does not affect microglia or astrocyte activation states.

(**A**) Overview of a DAPI stained mouse hippocampal formation and indication of ROI analyzed in **Paper IV**. (**B**) Quantification of microglia morphology in the ML (top) and GCL/SGZ (bottom) in saline- and IL-6R ab-treated *Syn2* KO mice. Mean ± SD with individual values are shown. (**C**) Representative image of an Iba1+/CD68+ microglia (left) and GFAP+/C3+ astrocyte. **Abbreviations**. ML, molecular layer; GCL, granular cell layer; SGZ, subgranular zone; Iba1, ionized calcium-binding adapter molecule 1; IL-6R ab, interleukin 6 receptor antibody; Ram, ramified; Int, intermediate; R/A, round/ameboid; GFAP, glial fibrillary acidic protein; C3, complement component 3.

Changes in synaptic proteins that could underly E/I imbalance in Syn2 KO mice are unaffected by IL-6R ab treatment

In addition to altered region-dependent microglia activity in the hippocampal formation, *Syn2* KO mice also exhibit altered levels of synaptic proteins specific for both inhibitory and excitatory synapses (175). These changes could cause an E/I imbalance, which is observed in epilepsy (284). Additionally, inflammatory reactions can cause changes in synaptic protein expression, potentially leading to E/I imbalance (176, 285, 286). Following early systemic IL-6R ab treatment, synaptic protein levels in *Syn2* KO mice were unaltered in cortex, hippocampus and sub-cortex. We investigated the synaptic proteins PSD-95 and NL-1, located at excitatory synapses, and gephyrin and NL-2, located at inhibitory synapses.

Based on the findings in **Paper IV**, blocking IL-6 signaling is sufficient to delay seizure development in *Syn2* KO mice without affecting region-dependent

inflammatory alterations in microglia or synaptic proteins levels. Interestingly, voluntary running of *Syn2* KO mice, initiated prior to seizure onset, has also been shown to delay seizure development without affecting microglia or astrocyte activity (215). IL-6 signaling occurs through the JAK-STAT signaling cascade, which includes phosphorylation of STAT3 (26). Inhibition of STAT3 phosphorylation, using a small molecule inhibitor that can cross the BBB and exert its effect directly in the CNS, reduced the severity of spontaneous seizures following pilocarpine-induced status epilepticus, without affecting neurodegeneration in rats (157). Although the pilocarpine-induced model of acquired epilepsy is more severe than the *Syn2* KO model, the results clearly demonstrate that modulating cytokine signaling in the periphery and/or the CNS can affect seizure development. In **Paper IV**, we did not determine if the IL-6R ab reaches the CNS. Even if epilepsy can disrupt the BBB (287), it is not known if the BBB is disrupted in *Syn2* KO mice. Further investigation is necessary to delineate how systemic IL-6R ab treatment exerts its effect on seizure development and whether the effect is related to direct or indirect actions of IL-6R ab reaching the CNS.

IL-6R ab treatment does not affect social interest, anxiety, or spatial memory in Syn2 KO mice

Syn2 KO mice also exhibit ASD-related behaviors, including impaired social interest (167, 168). In **Paper IV** we confirmed reduced social interest in *Syn2* KO mice compared to wt mice. Systemic IL-6R ab treatment did not affect social behavior or repetitive grooming behavior. We also evaluated spatial learning and memory (Y- and Barnes maze), depression-like behavior (forced swim test), and anxiety-like behavior (open field) following systemic IL-6R ab without observing any effects.

Evaluating actigraphy measurements and sleep parameters in wt and Syn2 KO mice

Individuals with ASD and/or epilepsy commonly suffer from sleep disturbances, such as longer sleep latency and less cohesive sleep (141, 142, 145-150). To explore if *Syn2* KO mice also show signs of disturbed sleep patterns, we performed actigraphy measurements on 5-months old *Syn2* KO and wt mice in **Paper IV**. We analyzed several sleep parameters, including sleep latency and sleep disturbances: number of periods awake, time awake, and number of rearing events during the sleep period (lights-ON) (**Figure 27A**). *Syn2* KO mice were, unexpectedly, less active during the sleep lights-ON compared to wt mice, determined by number of rearing events (**Figure 27B and C**). Sleep latency and sleep disturbances did not differ between wt and *Syn2* KO mice (**Figure 27D-F**).

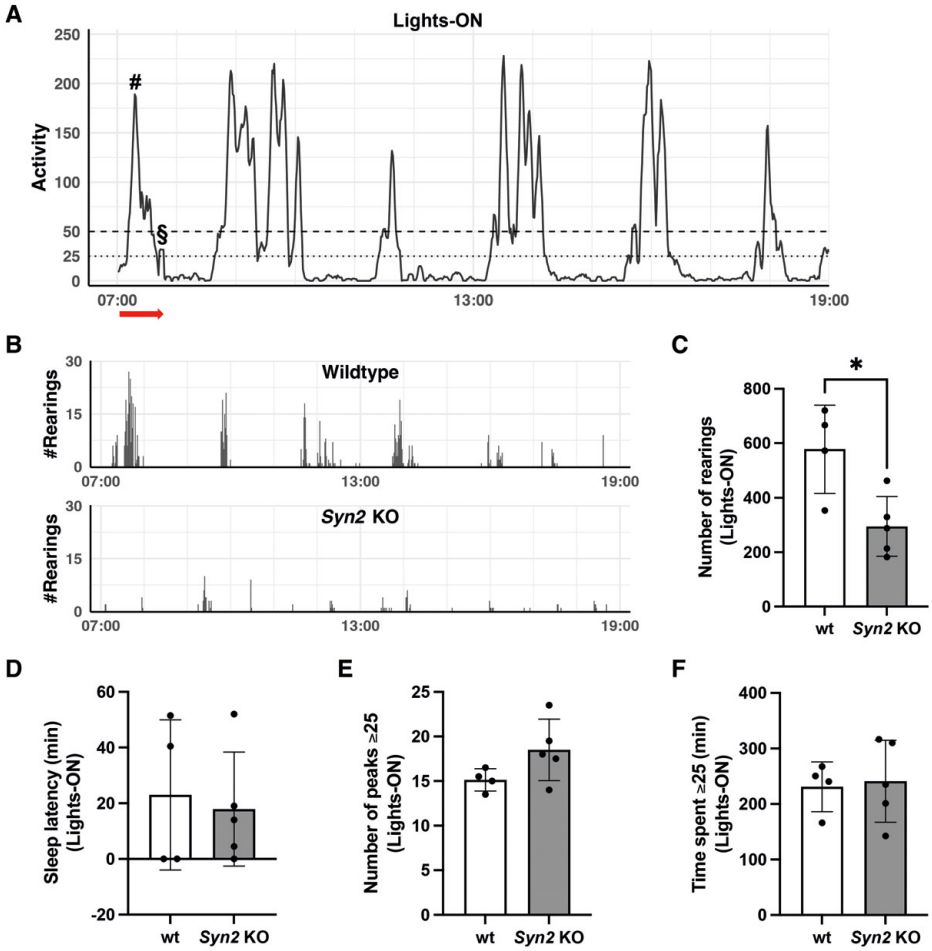

Figure 27. Actigraphy measurment reveal no epilepsy- and ASD-related sleep disturbances in *Syn2* KO mice.

(**A**) Representative 12-hour actigraphy recording showing 5-min rolling average of general locomotor activity from a 5-month old wt mouse. An example of a peak/period ≥ 50 and ≥ 25 (but not 50) is indicated by # and §, respectively. Approximate sleep latency is indicated by a red arrow along the x-axis. (**B**) Representative actigraphy showing rearing events during a 12-hour period for 5-month old wt (top) and *Syn2* KO (bottom) mice. (**C**) Quantification of mean number of rearings during lights-ON. (**D**) Quantification of sleep latency. (**E**) Quantification of the number of peaks/periods exceeding 25 in mean locomotor activity during lights-ON. (**F**) Quantification of time spent exceeding 25 in mean locomotor activity during lights-ON. (**C-F**) Data presented as mean ± SD with individual values. Statistical analyses performed using the Student's t-test. *p < 0.05. **Abbreviations**. KO, knockout; wt, wildtype; ASD, autism spectrum disorder.

In **Paper IV**, only a limited number of mice were used to perform actigraphy measurements over a short period of 72 hours, making subtle changes in sleep patterns difficult to detect due to large variation. Based on the results from **Paper**

IV, it is unclear if the *Syn2* KO mice are suitable as a model for sleep disturbances observed in epilepsy and/or ASD. We are currently conducting follow-up experiments to characterize sleep patterns in wt, *Syn2* KO, and *Cntnap2* KO mice at different ages. Although **Paper IV** is, to my knowledge, the first study to perform actigraphy measurements on *Syn2* KO mice, it has previously been done on *Cntnap2* KO mice and rats (237). The authors showed that *Cntnap2* KO rats are hyperactive during lights-ON, whereas *Cntnap2* KO mice did not differ from their corresponding wt controls, highlighting the importance of considering species-related differences when performing translational research (237).

Immune profiles in children with autism, epilepsy, or autism with comorbid epilepsy

Recognizing the complexities of sleep disturbances in epilepsy and/or ASD, our research has also extended to exploring related physiological factors, such as immune profiles, in affected individuals. Sleep disturbances and immune dysfunctions are frequently observed in children with ASD and/or epilepsy. However, it is not known if immune profiles differ between children with ASD, epilepsy or ASD with comorbid epilepsy. In an ongoing study we aim to explore differences in immune cell profiles and cytokine levels in blood in these children. Additionally, we aim to investigate if sleep patterns alone, or in combination with altered immune profiles, could be used to distinguish children with ASD from children with ASD with comorbid epilepsy. Since this work is ongoing, what follows are presentations of preliminary data of immune profiles in children with ASD, ASD and epilepsy or epilepsy alone.

Cytokine profiles in children with ASD and/or epilepsy do not differ

In ASD alterations in cytokine levels have been reported in several studies, and although there is a heterogeneity in cytokine levels in individuals with ASD, the most recent meta-analysis reports a minor increase in IFN-γ, IL-1β, IL-6, and TNF-α in blood (288). Epilepsies are also a heterogenous group of neurological disorders (135) which makes the identification of biomarkers challenging. It was recently reported that it is possible to distinguish psychogenic non-epileptic seizures (PNES) and epileptic seizures in adults; individuals with temporal and frontal lobe epilepsy showed elevated interictal IL-6 levels whereas the IL-6 levels were unaffected in individual with PNES compared to healthy controls (163). Additionally, postictal changes in cytokine levels, 6 hours following a seizure were sufficient to distinguishing TLE and frontal lobe epilepsy (FLE), where e.g., IL-6 levels were further elevated in TLE but not FLE compared to interictal levels >24 hours after the last seizure (163). Another study also reported elevated IL-6 levels following TLE seizures but only in the immediate postictal state, changes that were not

observed 1 or 24 hours post seizure (289). Interestingly right-TLE was associated with higher IL-6 levels compared to left-TLE (289).

In our study, IL-6 and ICAM-1 levels were comparable between children at the age of 10-14 years old with mild ASD, mild ASD and epilepsy, or epilepsy alone (**Figure 28**), additionally, we found no alteration in any of the other 21 blood biomarkers analyzed; CRP, eotaxin, eotaxin-3, IFN-γ, IL-10, IL-12p70, IL-13, IL-1β, IL-2, IL-4, IL-8, IP-10, MCP-1, MCP-4, MDC, MIP-1α, MIP-1β, SAA, TARC, TNF, and VCAM-1 (data not shown).

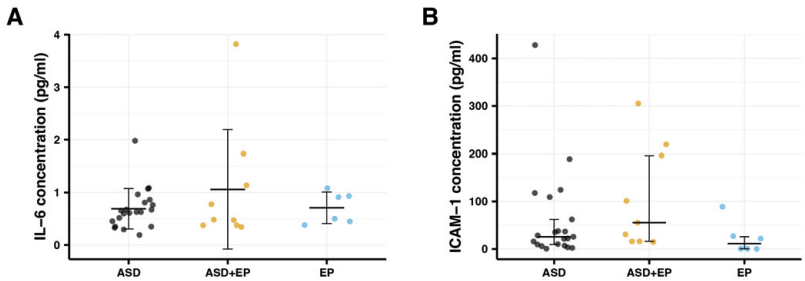

Figure 28. IL-6 and ICAM-1 serum levels do not differ between childredn with ASD, epilepsy, or ASD with comorbid epilepsy
(**A**) Quantification of serum IL-6 levels. Mean ± SD and individail values are shown. (**B**) Quantification of serum ICAM-1 levels. Median and IQR with individual values are shown. **Abbreviations**. IL-6, interleukin 6; ASD, autism spectrum disorder; EP, epilepsy; ICAM-1, intracellular adhesion molecule 1; SD, standard deviation; IQR, interquartile range.

Characterization of lymphocytes in blood show comparable populations in children with ASD and/or epilepsy

To further evaluate immune profiles in ASD, ASD with epilepsy or epilepsy alone, flow cytometry analysis of circulating lymphocytes was performed at the Clinical Immunology and Transfusion Medicine, Skåne University Hospital. The panel consisted of markers specific for general lymphocyte populations, including B cells, CD4+ and CD8+ T cells, as well as the activation of T cells by assessment of the HLA-DR+ subpopulation. Samples did not differ substantially from the reference values, however, minor deviations in lymphocyte concentrations were observed in some samples. It is important to highlight that the reference values are set based on cell concentrations in adults and were not available for children. We could not detect any changes in B or T lymphocytes or HLA-DR levels between the groups (data not shown).

Previous studies have identified changes in leukocyte subsets in both epilepsy and ASD. Functional studies of T cell subsets have shown altered responses in children (2-11 years). Isolated T cells stimulated with PHA demonstrated an alternative

activation profile compared to typically developed peers, with a Th2 skew (290, 291). Another study reported a reduction in Th1 (IL-2 and IFN-γ) and an increase in Th2 (IL-4) cytokines in children (3-7 years) based on flow cytometry analysis of cytokine-positive lymphocytes (292). Conversely, cytokine analysis of post-mortem brain tissue from individuals with ASD (4-37 years) showed a polarization towards Th1 response with elevated IFN-γ but no change in Th2 associated IL-4, IL-5 or IL-10 (293). Analysis of NK cell function revealed dysfunctional cells in children (2-5 years) with ASD, with a more activated profile at baseline but with a defective cytotoxicity following stimulation (294). Additionally, alterations in monocyte activation in children (2-5 years) with ASD, showing stronger activation and cytokine production following TLR2 and TLR4 stimulation, but a reduced response following TLR9 stimulation (295). Most of the aforementioned studies investigating leukocytes in ASD have included young children, often with a median around the age of three. Early ASD diagnoses are often more severe compared to milder cases diagnosed later. In our study, the children had mild ASD diagnoses. It is possible that the immune profiles vary with the severity of the ASD diagnosis.

In epilepsy there are also reports of altered systemic immune populations. A retrospective chart review indicated a higher leukocyte count in generalized compared to focal epilepsies, primarily due to elevated monocyte counts (296). In the immediate postictal state, patients with TLE showed expanded leukocyte, lymphocyte, neutrophil and NK cell counts, with a decrease in the percentage of CD4+ T lymphocytes, alterations which were reverted back to baseline 24 hours post seizure (297). Since seizures affect cytokine levels and possibly leukocyte profiles, this could be a potential confounder in our current study. However, according to medical records and information provided by caregivers, all children with epilepsy included had appropriate seizure control and were presumably seizure-free during blood sampling.

Our preliminary findings suggest no significant differences in immune profiles between children with ASD, ASD and epilepsy or epilepsy alone. However, limitations in our current study may affect the identification of immune profile discrepancies. The study only included 36 children, affecting variability within groups. Additionally, the children with epilepsy had either focal or generalized origin, and due to the low number of participants, sub-group analyses could not be conducted. The lack of age-matched typically developed peers limits our ability to determine changes in immune profiles in ASD, ASD and epilepsy, or epilepsy alone. Although analyses of sleep parameters remain, future studies should include age-matched typically developed peers as controls, expand the number of participants, and focus on specific types of epilepsies and ASD diagnoses to increase the chances of identifying alterations in immune profiles. By addressing these limitations, we can enhance our understanding of the immune mechanisms underlaying these conditions and potentially identify biomarkers for better diagnosis and treatment.

Future perspectives

Parkinson's disease

As PD is a slow, progressive, disorder with a long prodromal phase, the identification of viable biomarkers is key in early intervention that could stop or slow down disease progression. Targeting the immune system is supported by retrospective studies demonstrating a reduced PD risk following long-term ibuprofen use, however, with possible confounders underlying the decreased risk. Additional support for immunomodulation as a promising therapeutic strategy comes from the use of anti-TNF therapies in the context of autoimmune disease (IBD). However, the relevance of this finding to individuals predisposed to PD, but without any inflammatory disease, can be questioned. Still, a prodromal biomarker for PD would allow for clinical trials to evaluate efficacy of currently available immunomodulators on PD progression. There are multiple pathophysiological mechanisms at play in PD; neuroinflammation, α-Syn pathology, and the dopaminergic neurodegeneration. Therefore, the use of combination therapies may have a synergistic effect, targeting immune mechanisms, α-Syn aggregation and/or spread, assuming aggregation is a toxic gain-of-function (298), or restoring monomeric α-Syn, assuming loss-of-function of monomeric α-Syn following aggregation (299), and dopaminergic neurodegeneration.

The development of preventative therapeutics for PD will take time. However, extensive progress is being made in the development of treatment therapies for PD. The current European clinical trial of transplanting human embryonic stem cell derived dopaminergic neurons in PD patients, STEM-PD, is greatly anticipated within the field of PD. Following positive results of primary objective, safety and tolerability, the dose has been increased from a total of 7 to 14 million cells for the remaining four patients in the trial (300). As of writing this, it is too early to assess secondary objectives, cell survival and efficacy. Neuronal survival following grafting is a common problem in transplantation studies. A recent experimental study using human pluripotent stem cell derived dopaminergic neurons showed that using approved anti-TNF therapy significantly reduced degeneration of grafted dopaminergic neurons six months post grafting in mice (301). Thus, the investigation of immune mechanisms in PD is not only important in the exploration of preventative therapies, but also has a key role in treatment strategies.

Indeed, whether the aim is to develop a monotherapy, combination therapy or to prolong grafted dopaminergic neurons, the continued investigation of immune mechanisms in PD is crucial in the search for disease-modifying strategies.

Epilepsy

Due to the complex and heterogenous nature of the disease, the identification of new treatments for epilepsy has been challenging. Further elucidation of the mechanisms underlying epileptogenesis and ictogenesis is crucial for discovering effective treatment options. As demonstrated in this thesis, immune responses may play an essential role in the development of epilepsy, making the immune system a prime target for future research aimed at reducing the incidence of treatment-resistant cases. Another promising direction is the identification of biomarkers, although this has proven difficult due to the disease's variability (302). The observation of elevated levels of IL-6 in serum in TLE, but not in PNES, suggest the potential of serum biomarkers to facilitate appropriate patient care. However, the reliability of systemic markers like IL-6 may be compromised by external factors. Therefore, the development of multimodal biomarker panels, combining multiple different biomarkers, might represent the most promising approach (reviewed in (302)).

In summary, the evident role of neuroinflammatory and inflammatory mechanisms in epilepsies justifies further investigation. This research could uncover new pathways that serve as prognostic or diagnostic biomarkers, or targets for modifying the development of epilepsy.

Concluding remarks

Throughout this thesis immune mechanisms in PD and epilepsy have been explored with an aim of increasing our understanding of disease susceptibility and progression.

The results presented in **Papers I-IV** demonstrate that:

- *Ciita* variants affect susceptibility and progression of experimental PD. Reduced *Ciita* levels were associated with an increased number of activated microglia cells, enhanced neurodegeneration, and more widespread α-Syn pathology following rAAV6-α-Syn+PFFs injection in congenic DA.VRA4 rats.
- *Ciita* variants have minor, but detectable, effects on immune cell profiles in naïve rats. Additionally, variants causing reduced *Ciita* levels were associated with elevated serum sTNF levels, possibly increasing susceptibility of experimental PD.
- Systemic sTNF inhibition, using a DN-TNF variant, reaches the CNS but fails to exert neuroprotective effects, indicating that elevated sTNF levels are not central to PD susceptibility and progression using the rAAV6-α-Syn+PFFs model in congenic DA.VRA4 rats.
- Systemic treatment using an IL-6R ab, blocking IL-6 signaling, during the epileptogenic phase reduced seizure development and frequency in *Syn2* KO mice, without reversing previously published neuroinflammatory or synaptic alterations.

In summary, this thesis provides valuable insights into the complex immune mechanisms involved in PD and epilepsy. Future research may build upon these results to further characterize central immune mechanisms in disease susceptibility and progression, with the hope of identifying targets for disease-modifying therapeutics.

Acknowledgements

I am deeply thankful to my two great supervisors, **Maria** and **Christine**, who have guided me throughout my PhD journey. To Maria, thank you for creating a trusting environment that allowed me to grow not only as a scientist but also on a personal level. My admiration of your leadership style is something I will bring with me for future endeavors. Your consistent support in allowing me to prioritize my family has been invaluable, fueling my will to perform and to learn at work. To Christine, I am very thankful for your continuous support and inspiration. Your dedication to science and willingness to engage in detailed discussions (even hour-long discussion about single samples…) has been a source of motivation.

I would also like to thank the past and present members of the TNG group. Special thanks to **Itzia** for your support in the animal house and lab, and for your substantial contributions to the VRA4 projects, which have laid the foundation for much of my thesis. **Kajsa**, my friend and colleague, thank you for making my time in TNG more enjoyable and for your tips that have made my PhD journey smoother. Thanks to past and present TNG postdocs: **Claes**, thanks for all of the help in the lab the last couple of months, you're a great addition to TNG; **Lautaro**, your approach to science is inspiring, I miss our lab chats and the F1 updates; **Olivia**, thank you for always helping out when I needed an extra pair of hands; **Susanne**, your willingness to go above and beyond to help with all kinds of issues has been deeply appreciated; **Catarina**, thank you for offering your craftsmanship, I wouldn't have been able to finish in time without your help. I would also like to acknowledge all the past and present students of TNG for their contribution to the group.

Matilda, thank you for introducing me to the field of epilepsy and for your support in the animal house and lab. **Marie T** and **Jenny**, having you as colleagues and friends during my PhD has been a great pleasure. Your support has made my time at BMC more enjoyable and memorable. I would also like to thank the members and students of the epilepsy center, past and present. Special thanks to **Eliška**, **My**, **Agnieszka**, and **Camilla** for your assistance in the animal house.

I owe a special thanks to my past and present office mates. **Malin**, thank you for always being there to listen, and **Jana**, for the fun conversations and your assistance with R. A big thanks to **Martino** for the latest BMC gossip, gym encouragement, and for always filling the office with Italian energy.

I am grateful to the NPR unit and **Jia-Yi** for introducing me to A10 back in 2018. Special thanks to **Wen**, **Caroline**, **Alex**, **Edoardo**, **Di**, **Alicja**, and **Laura** for creating a great learning environment and always being willing to help. I would also like to thank all the past and present members of A10: **Elna**, **Andreas**, **Michaela**, **Sara P**, **Xiaoni**, **Marie S**, **Shub**, **Ellen**, **Alina**, **Carolina**, and many more for making it a wonderful place to work.

I would also like to thank numerous people from BMC for making my PhD journey more memorable: **Lluís**, **Rosa**, **Megg**, **Sabine**, **Emma**, **Yiyi**, **Oscar**, **Radhika**, **Tomas R**, **Isak**, **Martina**, **Fredrik**, **Sara C**, **Roberta**, and **Dovile**. Special thanks to **Tomas B**, **Andi**, and **Robert**, for always having your doors open to me, offering help from technical issues to scientific discussions and feedback on my work. Thanks to **Micke** and **Susanne G** for your support in the animal facility and thanks to all of the **CCM** staff. A special thanks to **Anna** for always being available to discuss my flow cytometry experiments.

I would also like to extend my thanks to our collaborators, with a special thanks to **Kathleen** for optimizing my flow cytometry protocols and saving me countless hours in the lab.

To my **family** and **friends**, thank you for your strong support along the way, and for providing much-needed distractions from work. I am especially grateful to my **parents** and **parents-in-law**, the world's greatest grandparents, for always showing up and being there to spend time with Kaj. **Rut**, thanks for forcing me to take all of those walks to clear my head, good girl.

Elina, my beautiful wife and best friend, thank you for your endless support. Without your sacrifices, this thesis would never have been completed. Thank you for being you, and for being the best mother and partner in the world. **Kaj**, more than two years have passed and I still can't grasp the concept of being your father. Watching you grow and develop every day fills me with the purest form of joy. I love both of you more than anything in the world.

References

1. Galea I, Bechmann I, Perry VH. What is immune privilege (not)? Trends Immunol. 2007;28(1):12-8.
2. Louveau A, Harris TH, Kipnis J. Revisiting the Mechanisms of CNS Immune Privilege. Trends Immunol. 2015;36(10):569-77.
3. Carson MJ, Doose JM, Melchior B, Schmid CD, Ploix CC. CNS immune privilege: hiding in plain sight. Immunol Rev. 2006;213:48-65.
4. Dantzer R. Neuroimmune Interactions: From the Brain to the Immune System and Vice Versa. Physiol Rev. 2018;98(1):477-504.
5. Tansey MG, Wallings RL, Houser MC, Herrick MK, Keating CE, Joers V. Inflammation and immune dysfunction in Parkinson disease. Nat Rev Immunol. 2022;22(11):657-73.
6. Rana A, Musto AE. The role of inflammation in the development of epilepsy. J Neuroinflammation. 2018;15(1):144.
7. Li Q, Barres BA. Microglia and macrophages in brain homeostasis and disease. Nat Rev Immunol. 2018;18(4):225-42.
8. Ginhoux F, Greter M, Leboeuf M, Nandi S, See P, Gokhan S, et al. Fate mapping analysis reveals that adult microglia derive from primitive macrophages. Science. 2010;330(6005):841-5.
9. Ransohoff RM. A polarizing question: do M1 and M2 microglia exist? Nat Neurosci. 2016;19(8):987-91.
10. Wes PD, Holtman IR, Boddeke EW, Moller T, Eggen BJ. Next generation transcriptomics and genomics elucidate biological complexity of microglia in health and disease. Glia. 2016;64(2):197-213.
11. Grabert K, Michoel T, Karavolos MH, Clohisey S, Baillie JK, Stevens MP, et al. Microglial brain region-dependent diversity and selective regional sensitivities to aging. Nat Neurosci. 2016;19(3):504-16.
12. Vidal-Itriago A, Radford RAW, Aramideh JA, Maurel C, Scherer NM, Don EK, et al. Microglia morphophysiological diversity and its implications for the CNS. Front Immunol. 2022;13:997786.
13. Ohsawa K, Imai Y, Kanazawa H, Sasaki Y, Kohsaka S. Involvement of Iba1 in membrane ruffling and phagocytosis of macrophages/microglia. J Cell Sci. 2000;113 (Pt 17):3073-84.
14. Jurga AM, Paleczna M, Kuter KZ. Overview of General and Discriminating Markers of Differential Microglia Phenotypes. Front Cell Neurosci. 2020;14:198.

15. Huppa JB, Davis MM. T-cell-antigen recognition and the immunological synapse. Nat Rev Immunol. 2003;3(12):973-83.
16. Clarke LE, Barres BA. Emerging roles of astrocytes in neural circuit development. Nat Rev Neurosci. 2013;14(5):311-21.
17. Pekny M, Wilhelmsson U, Pekna M. The dual role of astrocyte activation and reactive gliosis. Neurosci Lett. 2014;565:30-8.
18. Hol EM, Pekny M. Glial fibrillary acidic protein (GFAP) and the astrocyte intermediate filament system in diseases of the central nervous system. Curr Opin Cell Biol. 2015;32:121-30.
19. Gorina YV, Salmina AB, Erofeev AI, Gerasimov EI, Bolshakova AV, Balaban PM, et al. Astrocyte Activation Markers. Biochemistry (Mosc). 2022;87(9):851-70.
20. Zhao X, Liao Y, Morgan S, Mathur R, Feustel P, Mazurkiewicz J, et al. Noninflammatory Changes of Microglia Are Sufficient to Cause Epilepsy. Cell Rep. 2018;22(8):2080-93.
21. Rostami J, Fotaki G, Sirois J, Mzezewa R, Bergstrom J, Essand M, et al. Astrocytes have the capacity to act as antigen-presenting cells in the Parkinson's disease brain. J Neuroinflammation. 2020;17(1):119.
22. Weiss F, Labrador-Garrido A, Dzamko N, Halliday G. Immune responses in the Parkinson's disease brain. Neurobiol Dis. 2022;168:105700.
23. Dinarello CA. Historical insights into cytokines. Eur J Immunol. 2007;37 Suppl 1(Suppl 1):S34-45.
24. Zhang JM, An J. Cytokines, inflammation, and pain. Int Anesthesiol Clin. 2007;45(2):27-37.
25. Johnson DE, O'Keefe RA, Grandis JR. Targeting the IL-6/JAK/STAT3 signalling axis in cancer. Nat Rev Clin Oncol. 2018;15(4):234-48.
26. Hunter CA, Jones SA. IL-6 as a keystone cytokine in health and disease. Nat Immunol. 2015;16(5):448-57.
27. Rose-John S, Jenkins BJ, Garbers C, Moll JM, Scheller J. Targeting IL-6 trans-signalling: past, present and future prospects. Nat Rev Immunol. 2023;23(10):666-81.
28. Probert L. TNF and its receptors in the CNS: The essential, the desirable and the deleterious effects. Neuroscience. 2015;302:2-22.
29. TNF neutralization in MS: results of a randomized, placebo-controlled multicenter study. The Lenercept Multiple Sclerosis Study Group and The University of British Columbia MS/MRI Analysis Group. Neurology. 1999;53(3):457-65.
30. McCoy MK, Tansey MG. TNF signaling inhibition in the CNS: implications for normal brain function and neurodegenerative disease. J Neuroinflammation. 2008;5:45.
31. Gonzalez Caldito N. Role of tumor necrosis factor-alpha in the central nervous system: a focus on autoimmune disorders. Front Immunol. 2023;14:1213448.

32. Steed PM, Tansey MG, Zalevsky J, Zhukovsky EA, Desjarlais JR, Szymkowski DE, et al. Inactivation of TNF signaling by rationally designed dominant-negative TNF variants. Science. 2003;301(5641):1895-8.
33. Pringsheim T, Jette N, Frolkis A, Steeves TD. The prevalence of Parkinson's disease: a systematic review and meta-analysis. Mov Disord. 2014;29(13):1583-90.
34. Poewe W, Seppi K, Tanner CM, Halliday GM, Brundin P, Volkmann J, et al. Parkinson disease. Nat Rev Dis Primers. 2017;3:17013.
35. Kirkeby A, Nelander J, Hoban DB, Rogelius N, Bjartmarz H, Novo Nordisk Cell Therapy R, et al. Preclinical quality, safety, and efficacy of a human embryonic stem cell-derived product for the treatment of Parkinson's disease, STEM-PD. Cell Stem Cell. 2023;30(10):1299-314 e9.
36. Klein C, Westenberger A. Genetics of Parkinson's disease. Cold Spring Harb Perspect Med. 2012;2(1):a008888.
37. Polymeropoulos MH, Lavedan C, Leroy E, Ide SE, Dehejia A, Dutra A, et al. Mutation in the alpha-synuclein gene identified in families with Parkinson's disease. Science. 1997;276(5321):2045-7.
38. Spillantini MG, Crowther RA, Jakes R, Hasegawa M, Goedert M. alpha-Synuclein in filamentous inclusions of Lewy bodies from Parkinson's disease and dementia with lewy bodies. Proc Natl Acad Sci U S A. 1998;95(11):6469-73.
39. Spillantini MG, Schmidt ML, Lee VM, Trojanowski JQ, Jakes R, Goedert M. Alpha-synuclein in Lewy bodies. Nature. 1997;388(6645):839-40.
40. Kruger R, Kuhn W, Muller T, Woitalla D, Graeber M, Kosel S, et al. Ala30Pro mutation in the gene encoding alpha-synuclein in Parkinson's disease. Nat Genet. 1998;18(2):106-8.
41. Zarranz JJ, Alegre J, Gomez-Esteban JC, Lezcano E, Ros R, Ampuero I, et al. The new mutation, E46K, of alpha-synuclein causes Parkinson and Lewy body dementia. Ann Neurol. 2004;55(2):164-73.
42. Chartier-Harlin MC, Kachergus J, Roumier C, Mouroux V, Douay X, Lincoln S, et al. Alpha-synuclein locus duplication as a cause of familial Parkinson's disease. Lancet. 2004;364(9440):1167-9.
43. Ibanez P, Bonnet AM, Debarges B, Lohmann E, Tison F, Pollak P, et al. Causal relation between alpha-synuclein gene duplication and familial Parkinson's disease. Lancet. 2004;364(9440):1169-71.
44. Singleton AB, Farrer M, Johnson J, Singleton A, Hague S, Kachergus J, et al. alpha-Synuclein locus triplication causes Parkinson's disease. Science. 2003;302(5646):841.
45. Blauwendraat C, Nalls MA, Singleton AB. The genetic architecture of Parkinson's disease. Lancet Neurol. 2020;19(2):170-8.
46. Brolin K, Bandres-Ciga S, Blauwendraat C, Widner H, Odin P, Hansson O, et al. Insights on Genetic and Environmental Factors in Parkinson's Disease from a Regional Swedish Case-Control Cohort. J Parkinsons Dis. 2022;12(1):153-71.

47. Yang F, Pedersen NL, Ye W, Liu Z, Norberg M, Forsgren L, et al. Moist smokeless tobacco (Snus) use and risk of Parkinson's disease. Int J Epidemiol. 2017;46(3):872-80.
48. Hollenbach JA, Norman PJ, Creary LE, Damotte V, Montero-Martin G, Caillier S, et al. A specific amino acid motif of HLA-DRB1 mediates risk and interacts with smoking history in Parkinson's disease. Proc Natl Acad Sci U S A. 2019;116(15):7419-24.
49. Chen Y, Sun X, Lin Y, Zhang Z, Gao Y, Wu IXY. Non-Genetic Risk Factors for Parkinson's Disease: An Overview of 46 Systematic Reviews. J Parkinsons Dis. 2021;11(3):919-35.
50. Freire C, Koifman S. Pesticide exposure and Parkinson's disease: epidemiological evidence of association. Neurotoxicology. 2012;33(5):947-71.
51. Kannarkat GT, Cook DA, Lee JK, Chang J, Chung J, Sandy E, et al. Common Genetic Variant Association with Altered HLA Expression, Synergy with Pyrethroid Exposure, and Risk for Parkinson's Disease: An Observational and Case-Control Study. NPJ Parkinsons Dis. 2015;1.
52. Kim JJ, Vitale D, Otani DV, Lian MM, Heilbron K, andMe Research T, et al. Multi-ancestry genome-wide association meta-analysis of Parkinson's disease. Nat Genet. 2024;56(1):27-36.
53. Hamza TH, Zabetian CP, Tenesa A, Laederach A, Montimurro J, Yearout D, et al. Common genetic variation in the HLA region is associated with late-onset sporadic Parkinson's disease. Nat Genet. 2010;42(9):781-5.
54. Wissemann WT, Hill-Burns EM, Zabetian CP, Factor SA, Patsopoulos N, Hoglund B, et al. Association of Parkinson disease with structural and regulatory variants in the HLA region. Am J Hum Genet. 2013;93(5):984-93.
55. Yu E, Ambati A, Andersen MS, Krohn L, Estiar MA, Saini P, et al. Fine mapping of the HLA locus in Parkinson's disease in Europeans. NPJ Parkinsons Dis. 2021;7(1):84.
56. Sulzer D, Alcalay RN, Garretti F, Cote L, Kanter E, Agin-Liebes J, et al. T cells from patients with Parkinson's disease recognize alpha-synuclein peptides. Nature. 2017;546(7660):656-61.
57. Hasegawa M, Fujiwara H, Nonaka T, Wakabayashi K, Takahashi H, Lee VM, et al. Phosphorylated alpha-synuclein is ubiquitinated in alpha-synucleinopathy lesions. J Biol Chem. 2002;277(50):49071-6.
58. Fujiwara H, Hasegawa M, Dohmae N, Kawashima A, Masliah E, Goldberg MS, et al. alpha-Synuclein is phosphorylated in synucleinopathy lesions. Nat Cell Biol. 2002;4(2):160-4.
59. Samii A, Etminan M, Wiens MO, Jafari S. NSAID use and the risk of Parkinson's disease: systematic review and meta-analysis of observational studies. Drugs Aging. 2009;26(9):769-79.
60. Gao X, Chen H, Schwarzschild MA, Ascherio A. Use of ibuprofen and risk of Parkinson disease. Neurology. 2011;76(10):863-9.

61. Kordower JH, Olanow CW, Dodiya HB, Chu Y, Beach TG, Adler CH, et al. Disease duration and the integrity of the nigrostriatal system in Parkinson's disease. Brain. 2013;136(Pt 8):2419-31.
62. Tagliaferro P, Burke RE. Retrograde Axonal Degeneration in Parkinson Disease. J Parkinsons Dis. 2016;6(1):1-15.
63. Dauer W, Przedborski S. Parkinson's disease: mechanisms and models. Neuron. 2003;39(6):889-909.
64. Burke RE, O'Malley K. Axon degeneration in Parkinson's disease. Exp Neurol. 2013;246:72-83.
65. Cheng HC, Ulane CM, Burke RE. Clinical progression in Parkinson disease and the neurobiology of axons. Ann Neurol. 2010;67(6):715-25.
66. Michel PP, Hirsch EC, Hunot S. Understanding Dopaminergic Cell Death Pathways in Parkinson Disease. Neuron. 2016;90(4):675-91.
67. Rivero-Rios P, Gomez-Suaga P, Fdez E, Hilfiker S. Upstream deregulation of calcium signaling in Parkinson's disease. Front Mol Neurosci. 2014;7:53.
68. Braak H, Del Tredici K, Rub U, de Vos RA, Jansen Steur EN, Braak E. Staging of brain pathology related to sporadic Parkinson's disease. Neurobiol Aging. 2003;24(2):197-211.
69. Halliday GM, McCann H. The progression of pathology in Parkinson's disease. Ann N Y Acad Sci. 2010;1184:188-95.
70. Burke RE, Dauer WT, Vonsattel JP. A critical evaluation of the Braak staging scheme for Parkinson's disease. Ann Neurol. 2008;64(5):485-91.
71. Li JY, Englund E, Holton JL, Soulet D, Hagell P, Lees AJ, et al. Lewy bodies in grafted neurons in subjects with Parkinson's disease suggest host-to-graft disease propagation. Nat Med. 2008;14(5):501-3.
72. Kordower JH, Chu Y, Hauser RA, Olanow CW, Freeman TB. Transplanted dopaminergic neurons develop PD pathologic changes: a second case report. Mov Disord. 2008;23(16):2303-6.
73. McGeer PL, Itagaki S, Boyes BE, McGeer EG. Reactive microglia are positive for HLA-DR in the substantia nigra of Parkinson's and Alzheimer's disease brains. Neurology. 1988;38(8):1285-91.
74. Lehrmann E, Christensen T, Zimmer J, Diemer NH, Finsen B. Microglial and macrophage reactions mark progressive changes and define the penumbra in the rat neocortex and striatum after transient middle cerebral artery occlusion. J Comp Neurol. 1997;386(3):461-76.
75. Imamura K, Hishikawa N, Sawada M, Nagatsu T, Yoshida M, Hashizume Y. Distribution of major histocompatibility complex class II-positive microglia and cytokine profile of Parkinson's disease brains. Acta Neuropathol. 2003;106(6):518-26.
76. Mogi M, Harada M, Riederer P, Narabayashi H, Fujita K, Nagatsu T. Tumor necrosis factor-alpha (TNF-alpha) increases both in the brain and in the cerebrospinal fluid from parkinsonian patients. Neurosci Lett. 1994;165(1-2):208-10.
77. Blum-Degen D, Muller T, Kuhn W, Gerlach M, Przuntek H, Riederer P. Interleukin-1 beta and interleukin-6 are elevated in the cerebrospinal fluid

of Alzheimer's and de novo Parkinson's disease patients. Neurosci Lett. 1995;202(1-2):17-20.
78. Qu Y, Li J, Qin Q, Wang D, Zhao J, An K, et al. A systematic review and meta-analysis of inflammatory biomarkers in Parkinson's disease. NPJ Parkinsons Dis. 2023;9(1):18.
79. Brochard V, Combadiere B, Prigent A, Laouar Y, Perrin A, Beray-Berthat V, et al. Infiltration of CD4+ lymphocytes into the brain contributes to neurodegeneration in a mouse model of Parkinson disease. J Clin Invest. 2009;119(1):182-92.
80. Gate D, Tapp E, Leventhal O, Shahid M, Nonninger TJ, Yang AC, et al. CD4(+) T cells contribute to neurodegeneration in Lewy body dementia. Science. 2021;374(6569):868-74.
81. Lindestam Arlehamn CS, Dhanwani R, Pham J, Kuan R, Frazier A, Rezende Dutra J, et al. alpha-Synuclein-specific T cell reactivity is associated with preclinical and early Parkinson's disease. Nat Commun. 2020;11(1):1875.
82. Schonhoff AM, Figge DA, Williams GP, Jurkuvenaite A, Gallups NJ, Childers GM, et al. Border-associated macrophages mediate the neuroinflammatory response in an alpha-synuclein model of Parkinson disease. Nat Commun. 2023;14(1):3754.
83. Nissen SK, Ferreira SA, Nielsen MC, Schulte C, Shrivastava K, Hennig D, et al. Soluble CD163 Changes Indicate Monocyte Association With Cognitive Deficits in Parkinson's Disease. Mov Disord. 2021;36(4):963-76.
84. Nissen SK, Shrivastava K, Schulte C, Otzen DE, Goldeck D, Berg D, et al. Alterations in Blood Monocyte Functions in Parkinson's Disease. Mov Disord. 2019;34(11):1711-21.
85. Konstantin Nissen S, Farmen K, Carstensen M, Schulte C, Goldeck D, Brockmann K, et al. Changes in CD163+, CD11b+, and CCR2+ peripheral monocytes relate to Parkinson's disease and cognition. Brain Behav Immun. 2022;101:182-93.
86. Carlisle SM, Qin H, Hendrickson RC, Muwanguzi JE, Lefkowitz EJ, Kennedy RE, et al. Sex-based differences in the activation of peripheral blood monocytes in early Parkinson disease. NPJ Parkinsons Dis. 2021;7(1):36.
87. Thome AD, Atassi F, Wang J, Faridar A, Zhao W, Thonhoff JR, et al. Ex vivo expansion of dysfunctional regulatory T lymphocytes restores suppressive function in Parkinson's disease. NPJ Parkinsons Dis. 2021;7(1):41.
88. Bhatia D, Grozdanov V, Ruf WP, Kassubek J, Ludolph AC, Weishaupt JH, et al. T-cell dysregulation is associated with disease severity in Parkinson's Disease. J Neuroinflammation. 2021;18(1):250.
89. Bas J, Calopa M, Mestre M, Mollevi DG, Cutillas B, Ambrosio S, et al. Lymphocyte populations in Parkinson's disease and in rat models of parkinsonism. J Neuroimmunol. 2001;113(1):146-52.

90. Kustrimovic N, Comi C, Magistrelli L, Rasini E, Legnaro M, Bombelli R, et al. Parkinson's disease patients have a complex phenotypic and functional Th1 bias: cross-sectional studies of CD4+ Th1/Th2/T17 and Treg in drug-naive and drug-treated patients. J Neuroinflammation. 2018;15(1):205.
91. Chen Y, Qi B, Xu W, Ma B, Li L, Chen Q, et al. Clinical correlation of peripheral CD4+cell subsets, their imbalance and Parkinson's disease. Mol Med Rep. 2015;12(4):6105-11.
92. Sommer A, Marxreiter F, Krach F, Fadler T, Grosch J, Maroni M, et al. Th17 Lymphocytes Induce Neuronal Cell Death in a Human iPSC-Based Model of Parkinson's Disease. Cell Stem Cell. 2018;23(1):123-31 e6.
93. Mamula D, Khosousi S, He Y, Lazarevic V, Svenningsson P. Impaired migratory phenotype of CD4(+) T cells in Parkinson's disease. NPJ Parkinsons Dis. 2022;8(1):171.
94. Hawkes CH, Del Tredici K, Braak H. Parkinson's disease: a dual-hit hypothesis. Neuropathol Appl Neurobiol. 2007;33(6):599-614.
95. Houser MC, Tansey MG. The gut-brain axis: is intestinal inflammation a silent driver of Parkinson's disease pathogenesis? NPJ Parkinsons Dis. 2017;3:3.
96. Killinger B, Labrie V. The Appendix in Parkinson's Disease: From Vestigial Remnant to Vital Organ? J Parkinsons Dis. 2019;9(s2):S345-S58.
97. Zhu F, Li C, Gong J, Zhu W, Gu L, Li N. The risk of Parkinson's disease in inflammatory bowel disease: A systematic review and meta-analysis. Dig Liver Dis. 2019;51(1):38-42.
98. Peter I, Dubinsky M, Bressman S, Park A, Lu C, Chen N, et al. Anti-Tumor Necrosis Factor Therapy and Incidence of Parkinson Disease Among Patients With Inflammatory Bowel Disease. JAMA Neurol. 2018;75(8):939-46.
99. Cenci MA, Bjorklund A. Animal models for preclinical Parkinson's research: An update and critical appraisal. Prog Brain Res. 2020;252:27-59.
100. Deng I, Corrigan F, Zhai G, Zhou XF, Bobrovskaya L. Lipopolysaccharide animal models of Parkinson's disease: Recent progress and relevance to clinical disease. Brain Behav Immun Health. 2020;4:100060.
101. Jiang P, Dickson DW. Parkinson's disease: experimental models and reality. Acta Neuropathol. 2018;135(1):13-32.
102. Belfiori LF, Duenas Rey A, Ralbovszki DM, Jimenez-Ferrer I, Fredlund F, Balikai SS, et al. Nigral transcriptomic profiles in Engrailed-1 hemizygous mouse models of Parkinson's disease reveal upregulation of oxidative phosphorylation-related genes associated with delayed dopaminergic neurodegeneration. Front Aging Neurosci. 2024;16:1337365.
103. Klein RL, King MA, Hamby ME, Meyer EM. Dopaminergic cell loss induced by human A30P alpha-synuclein gene transfer to the rat substantia nigra. Hum Gene Ther. 2002;13(5):605-12.
104. Kirik D, Rosenblad C, Burger C, Lundberg C, Johansen TE, Muzyczka N, et al. Parkinson-like neurodegeneration induced by targeted overexpression

of alpha-synuclein in the nigrostriatal system. J Neurosci. 2002;22(7):2780-91.
105. Lo Bianco C, Ridet JL, Schneider BL, Deglon N, Aebischer P. alpha -Synucleinopathy and selective dopaminergic neuron loss in a rat lentiviral-based model of Parkinson's disease. Proc Natl Acad Sci U S A. 2002;99(16):10813-8.
106. Ulusoy A, Decressac M, Kirik D, Bjorklund A. Viral vector-mediated overexpression of alpha-synuclein as a progressive model of Parkinson's disease. Prog Brain Res. 2010;184:89-111.
107. Luk KC, Song C, O'Brien P, Stieber A, Branch JR, Brunden KR, et al. Exogenous alpha-synuclein fibrils seed the formation of Lewy body-like intracellular inclusions in cultured cells. Proc Natl Acad Sci U S A. 2009;106(47):20051-6.
108. Volpicelli-Daley LA, Luk KC, Patel TP, Tanik SA, Riddle DM, Stieber A, et al. Exogenous alpha-synuclein fibrils induce Lewy body pathology leading to synaptic dysfunction and neuron death. Neuron. 2011;72(1):57-71.
109. Luk KC, Kehm V, Carroll J, Zhang B, O'Brien P, Trojanowski JQ, et al. Pathological alpha-synuclein transmission initiates Parkinson-like neurodegeneration in nontransgenic mice. Science. 2012;338(6109):949-53.
110. Carta AR, Boi L, Pisanu A, Palmas MF, Carboni E, De Simone A. Advances in modelling alpha-synuclein-induced Parkinson's diseases in rodents: Virus-based models versus inoculation of exogenous preformed toxic species. J Neurosci Methods. 2020;338:108685.
111. Volpicelli-Daley LA, Kirik D, Stoyka LE, Standaert DG, Harms AS. How can rAAV-alpha-synuclein and the fibril alpha-synuclein models advance our understanding of Parkinson's disease? J Neurochem. 2016;139 Suppl 1(Suppl 1):131-55.
112. Chung HK, Ho HA, Perez-Acuna D, Lee SJ. Modeling alpha-Synuclein Propagation with Preformed Fibril Injections. J Mov Disord. 2019;12(3):139-51.
113. Bousset L, Pieri L, Ruiz-Arlandis G, Gath J, Jensen PH, Habenstein B, et al. Structural and functional characterization of two alpha-synuclein strains. Nat Commun. 2013;4:2575.
114. Wakabayashi K, Yoshimoto M, Tsuji S, Takahashi H. Alpha-synuclein immunoreactivity in glial cytoplasmic inclusions in multiple system atrophy. Neurosci Lett. 1998;249(2-3):180-2.
115. Nakamura K, Mori F, Kon T, Tanji K, Miki Y, Tomiyama M, et al. Filamentous aggregations of phosphorylated alpha-synuclein in Schwann cells (Schwann cell cytoplasmic inclusions) in multiple system atrophy. Acta Neuropathol Commun. 2015;3:29.
116. Peng C, Gathagan RJ, Covell DJ, Medellin C, Stieber A, Robinson JL, et al. Cellular milieu imparts distinct pathological alpha-synuclein strains in alpha-synucleinopathies. Nature. 2018;557(7706):558-63.

117. Peelaerts W, Bousset L, Van der Perren A, Moskalyuk A, Pulizzi R, Giugliano M, et al. alpha-Synuclein strains cause distinct synucleinopathies after local and systemic administration. Nature. 2015;522(7556):340-4.
118. Rey NL, Bousset L, George S, Madaj Z, Meyerdirk L, Schulz E, et al. alpha-Synuclein conformational strains spread, seed and target neuronal cells differentially after injection into the olfactory bulb. Acta Neuropathol Commun. 2019;7(1):221.
119. Thakur P, Breger LS, Lundblad M, Wan OW, Mattsson B, Luk KC, et al. Modeling Parkinson's disease pathology by combination of fibril seeds and alpha-synuclein overexpression in the rat brain. Proc Natl Acad Sci U S A. 2017;114(39):E8284-E93.
120. Bjorklund A, Nilsson F, Mattsson B, Hoban DB, Parmar M. A Combined alpha-Synuclein/Fibril (SynFib) Model of Parkinson-Like Synucleinopathy Targeting the Nigrostriatal Dopamine System. J Parkinsons Dis. 2022;12(8):2307-20.
121. Van der Perren A, Toelen J, Casteels C, Macchi F, Van Rompuy AS, Sarre S, et al. Longitudinal follow-up and characterization of a robust rat model for Parkinson's disease based on overexpression of alpha-synuclein with adeno-associated viral vectors. Neurobiol Aging. 2015;36(3):1543-58.
122. Oliveras-Salva M, Van der Perren A, Casadei N, Stroobants S, Nuber S, D'Hooge R, et al. rAAV2/7 vector-mediated overexpression of alpha-synuclein in mouse substantia nigra induces protein aggregation and progressive dose-dependent neurodegeneration. Mol Neurodegener. 2013;8:44.
123. Negrini M, Tomasello G, Davidsson M, Fenyi A, Adant C, Hauser S, et al. Sequential or Simultaneous Injection of Preformed Fibrils and AAV Overexpression of Alpha-Synuclein Are Equipotent in Producing Relevant Pathology and Behavioral Deficits. J Parkinsons Dis. 2022;12(4):1133-53.
124. Decressac M, Mattsson B, Lundblad M, Weikop P, Bjorklund A. Progressive neurodegenerative and behavioural changes induced by AAV-mediated overexpression of alpha-synuclein in midbrain dopamine neurons. Neurobiol Dis. 2012;45(3):939-53.
125. Faustini G, Longhena F, Varanita T, Bubacco L, Pizzi M, Missale C, et al. Synapsin III deficiency hampers alpha-synuclein aggregation, striatal synaptic damage and nigral cell loss in an AAV-based mouse model of Parkinson's disease. Acta Neuropathol. 2018;136(4):621-39.
126. Koliatsos VE, Price WL, Pardo CA, Price DL. Ventral root avulsion: an experimental model of death of adult motor neurons. J Comp Neurol. 1994;342(1):35-44.
127. Lidman O, Swanberg M, Horvath L, Broman KW, Olsson T, Piehl F. Discrete gene loci regulate neurodegeneration, lymphocyte infiltration, and major histocompatibility complex class II expression in the CNS. J Neurosci. 2003;23(30):9817-23.
128. Swanberg M, Lidman O, Padyukov L, Eriksson P, Akesson E, Jagodic M, et al. MHC2TA is associated with differential MHC molecule expression

and susceptibility to rheumatoid arthritis, multiple sclerosis and myocardial infarction. Nat Genet. 2005;37(5):486-94.
129. Harnesk K, Swanberg M, Ockinger J, Diez M, Lidman O, Wallstrom E, et al. Vra4 congenic rats with allelic differences in the class II transactivator gene display altered susceptibility to experimental autoimmune encephalomyelitis. J Immunol. 2008;180(5):3289-96.
130. Jimenez-Ferrer I, Jewett M, Tontanahal A, Romero-Ramos M, Swanberg M. Allelic difference in Mhc2ta confers altered microglial activation and susceptibility to alpha-synuclein-induced dopaminergic neurodegeneration. Neurobiol Dis. 2017;106:279-90.
131. Devinsky O, Vezzani A, O'Brien TJ, Jette N, Scheffer IE, de Curtis M, et al. Epilepsy. Nat Rev Dis Primers. 2018;4:18024.
132. Trinka E, Cock H, Hesdorffer D, Rossetti AO, Scheffer IE, Shinnar S, et al. A definition and classification of status epilepticus--Report of the ILAE Task Force on Classification of Status Epilepticus. Epilepsia. 2015;56(10):1515-23.
133. Fiest KM, Sauro KM, Wiebe S, Patten SB, Kwon CS, Dykeman J, et al. Prevalence and incidence of epilepsy: A systematic review and meta-analysis of international studies. Neurology. 2017;88(3):296-303.
134. Beghi E, Giussani G. Aging and the Epidemiology of Epilepsy. Neuroepidemiology. 2018;51(3-4):216-23.
135. Scheffer IE, Berkovic S, Capovilla G, Connolly MB, French J, Guilhoto L, et al. ILAE classification of the epilepsies: Position paper of the ILAE Commission for Classification and Terminology. Epilepsia. 2017;58(4):512-21.
136. Fisher RS, Cross JH, French JA, Higurashi N, Hirsch E, Jansen FE, et al. Operational classification of seizure types by the International League Against Epilepsy: Position Paper of the ILAE Commission for Classification and Terminology. Epilepsia. 2017;58(4):522-30.
137. Kwan P, Arzimanoglou A, Berg AT, Brodie MJ, Allen Hauser W, Mathern G, et al. Definition of drug resistant epilepsy: consensus proposal by the ad hoc Task Force of the ILAE Commission on Therapeutic Strategies. Epilepsia. 2010;51(6):1069-77.
138. Rogawski MA, Loscher W. The neurobiology of antiepileptic drugs. Nat Rev Neurosci. 2004;5(7):553-64.
139. Josephson CB, Jette N. Psychiatric comorbidities in epilepsy. Int Rev Psychiatry. 2017;29(5):409-24.
140. Lukmanji S, Manji SA, Kadhim S, Sauro KM, Wirrell EC, Kwon CS, et al. The co-occurrence of epilepsy and autism: A systematic review. Epilepsy Behav. 2019;98(Pt A):238-48.
141. Accardo JA, Malow BA. Sleep, epilepsy, and autism. Epilepsy Behav. 2015;47:202-6.
142. Souders MC, Mason TB, Valladares O, Bucan M, Levy SE, Mandell DS, et al. Sleep behaviors and sleep quality in children with autism spectrum disorders. Sleep. 2009;32(12):1566-78.

143. Malow BA, Marzec ML, McGrew SG, Wang L, Henderson LM, Stone WL. Characterizing sleep in children with autism spectrum disorders: a multidimensional approach. Sleep. 2006;29(12):1563-71.
144. Macedo P, Oliveira PS, Foldvary-Schaefer N, Gomes MDM. Insomnia in people with epilepsy: A review of insomnia prevalence, risk factors and associations with epilepsy-related factors. Epilepsy Res. 2017;135:158-67.
145. Goldman SE, Alder ML, Burgess HJ, Corbett BA, Hundley R, Wofford D, et al. Characterizing Sleep in Adolescents and Adults with Autism Spectrum Disorders. J Autism Dev Disord. 2017;47(6):1682-95.
146. Allik H, Larsson JO, Smedje H. Sleep patterns of school-age children with Asperger syndrome or high-functioning autism. J Autism Dev Disord. 2006;36(5):585-95.
147. Hodge D, Carollo TM, Lewin M, Hoffman CD, Sweeney DP. Sleep patterns in children with and without autism spectrum disorders: developmental comparisons. Res Dev Disabil. 2014;35(7):1631-8.
148. de Weerd A, de Haas S, Otte A, Trenite DK, van Erp G, Cohen A, et al. Subjective sleep disturbance in patients with partial epilepsy: a questionnaire-based study on prevalence and impact on quality of life. Epilepsia. 2004;45(11):1397-404.
149. Kaleyias J, Cruz M, Goraya JS, Valencia I, Khurana DS, Legido A, et al. Spectrum of polysomnographic abnormalities in children with epilepsy. Pediatr Neurol. 2008;39(3):170-6.
150. Diaz-Roman A, Zhang J, Delorme R, Beggiato A, Cortese S. Sleep in youth with autism spectrum disorders: systematic review and meta-analysis of subjective and objective studies. Evid Based Ment Health. 2018;21(4):146-54.
151. Lin Z, Si Q, Xiaoyi Z. Association between epilepsy and systemic autoimmune diseases: A meta-analysis. Seizure. 2016;41:160-6.
152. Devinsky O, Vezzani A, Najjar S, De Lanerolle NC, Rogawski MA. Glia and epilepsy: excitability and inflammation. Trends Neurosci. 2013;36(3):174-84.
153. Ortinski PI, Dong J, Mungenast A, Yue C, Takano H, Watson DJ, et al. Selective induction of astrocytic gliosis generates deficits in neuronal inhibition. Nat Neurosci. 2010;13(5):584-91.
154. Vezzani A, Maroso M, Balosso S, Sanchez MA, Bartfai T. IL-1 receptor/Toll-like receptor signaling in infection, inflammation, stress and neurodegeneration couples hyperexcitability and seizures. Brain Behav Immun. 2011;25(7):1281-9.
155. Rodgers KM, Hutchinson MR, Northcutt A, Maier SF, Watkins LR, Barth DS. The cortical innate immune response increases local neuronal excitability leading to seizures. Brain. 2009;132(Pt 9):2478-86.
156. Marchi N, Fan Q, Ghosh C, Fazio V, Bertolini F, Betto G, et al. Antagonism of peripheral inflammation reduces the severity of status epilepticus. Neurobiol Dis. 2009;33(2):171-81.

157. Grabenstatter HL, Del Angel YC, Carlsen J, Wempe MF, White AM, Cogswell M, et al. The effect of STAT3 inhibition on status epilepticus and subsequent spontaneous seizures in the pilocarpine model of acquired epilepsy. Neurobiol Dis. 2014;62:73-85.
158. Zattoni M, Mura ML, Deprez F, Schwendener RA, Engelhardt B, Frei K, et al. Brain infiltration of leukocytes contributes to the pathophysiology of temporal lobe epilepsy. J Neurosci. 2011;31(11):4037-50.
159. Fabene PF, Navarro Mora G, Martinello M, Rossi B, Merigo F, Ottoboni L, et al. A role for leukocyte-endothelial adhesion mechanisms in epilepsy. Nat Med. 2008;14(12):1377-83.
160. Yamanaka G, Morichi S, Takamatsu T, Watanabe Y, Suzuki S, Ishida Y, et al. Links between Immune Cells from the Periphery and the Brain in the Pathogenesis of Epilepsy: A Narrative Review. Int J Mol Sci. 2021;22(9).
161. Liimatainen S, Fallah M, Kharazmi E, Peltola M, Peltola J. Interleukin-6 levels are increased in temporal lobe epilepsy but not in extra-temporal lobe epilepsy. J Neurol. 2009;256(5):796-802.
162. Alapirtti T, Rinta S, Hulkkonen J, Makinen R, Keranen T, Peltola J. Interleukin-6, interleukin-1 receptor antagonist and interleukin-1beta production in patients with focal epilepsy: A video-EEG study. J Neurol Sci. 2009;280(1-2):94-7.
163. Ahl M, Taylor MK, Avdic U, Lundin A, Andersson M, Amandusson A, et al. Immune response in blood before and after epileptic and psychogenic non-epileptic seizures. Heliyon. 2023;9(3):e13938.
164. Rusina E, Bernard C, Williamson A. The Kainic Acid Models of Temporal Lobe Epilepsy. eNeuro. 2021;8(2).
165. Curia G, Longo D, Biagini G, Jones RS, Avoli M. The pilocarpine model of temporal lobe epilepsy. J Neurosci Methods. 2008;172(2):143-57.
166. Feng J, Chi P, Blanpied TA, Xu Y, Magarinos AM, Ferreira A, et al. Regulation of neurotransmitter release by synapsin III. J Neurosci. 2002;22(11):4372-80.
167. Greco B, Manago F, Tucci V, Kao HT, Valtorta F, Benfenati F. Autism-related behavioral abnormalities in synapsin knockout mice. Behav Brain Res. 2013;251:65-74.
168. Michetti C, Caruso A, Pagani M, Sabbioni M, Medrihan L, David G, et al. The Knockout of Synapsin II in Mice Impairs Social Behavior and Functional Connectivity Generating an ASD-like Phenotype. Cereb Cortex. 2017;27(10):5014-23.
169. Chen J, Yu S, Fu Y, Li X. Synaptic proteins and receptors defects in autism spectrum disorders. Front Cell Neurosci. 2014;8:276.
170. Garcia CC, Blair HJ, Seager M, Coulthard A, Tennant S, Buddles M, et al. Identification of a mutation in synapsin I, a synaptic vesicle protein, in a family with epilepsy. J Med Genet. 2004;41(3):183-6.
171. Fassio A, Patry L, Congia S, Onofri F, Piton A, Gauthier J, et al. SYN1 loss-of-function mutations in autism and partial epilepsy cause impaired synaptic function. Hum Mol Genet. 2011;20(12):2297-307.

172. Cavalleri GL, Weale ME, Shianna KV, Singh R, Lynch JM, Grinton B, et al. Multicentre search for genetic susceptibility loci in sporadic epilepsy syndrome and seizure types: a case-control study. Lancet Neurol. 2007;6(11):970-80.
173. Corradi A, Fadda M, Piton A, Patry L, Marte A, Rossi P, et al. SYN2 is an autism predisposing gene: loss-of-function mutations alter synaptic vesicle cycling and axon outgrowth. Hum Mol Genet. 2014;23(1):90-103.
174. Etholm L, Bahonjic E, Walaas SI, Kao HT, Heggelund P. Neuroethologically delineated differences in the seizure behavior of synapsin 1 and synapsin 2 knock-out mice. Epilepsy Res. 2012;99(3):252-9.
175. Chugh D, Ali I, Bakochi A, Bahonjic E, Etholm L, Ekdahl CT. Alterations in Brain Inflammation, Synaptic Proteins, and Adult Hippocampal Neurogenesis during Epileptogenesis in Mice Lacking Synapsin2. PLoS One. 2015;10(7):e0132366.
176. Medrihan L, Ferrea E, Greco B, Baldelli P, Benfenati F. Asynchronous GABA Release Is a Key Determinant of Tonic Inhibition and Controls Neuronal Excitability: A Study in the Synapsin II-/- Mouse. Cereb Cortex. 2015;25(10):3356-68.
177. Mendez M, Lim G. Seizures in elderly patients with dementia: epidemiology and management. Drugs Aging. 2003;20(11):791-803.
178. Gruntz K, Bloechliger M, Becker C, Jick SS, Fuhr P, Meier CR, et al. Parkinson disease and the risk of epileptic seizures. Ann Neurol. 2018;83(2):363-74.
179. Simonet C, Bestwick J, Jitlal M, Waters S, Ben-Joseph A, Marshall CR, et al. Assessment of Risk Factors and Early Presentations of Parkinson Disease in Primary Care in a Diverse UK Population. JAMA Neurol. 2022;79(4):359-69.
180. Belete D, Jacobs BM, Simonet C, Bestwick JP, Waters S, Marshall CR, et al. Association Between Antiepileptic Drugs and Incident Parkinson Disease. JAMA Neurol. 2023;80(2):183-7.
181. Basselin M, Chang L, Chen M, Bell JM, Rapoport SI. Chronic carbamazepine administration attenuates dopamine D2-like receptor-initiated signaling via arachidonic acid in rat brain. Neurochem Res. 2008;33(7):1373-83.
182. Ramadan E, Basselin M, Taha AY, Cheon Y, Chang L, Chen M, et al. Chronic valproate treatment blocks D2-like receptor-mediated brain signaling via arachidonic acid in rats. Neuropharmacology. 2011;61(8):1256-64.
183. Dal S, Whyte S. 035 Valproate-induced parkinsonism ‘an early warning’: case reports and review of literature. Journal of Neurology, Neurosurgery & Psychiatry. 2019;90(e7):A12-A.
184. Willis AW, Roberts E, Beck JC, Fiske B, Ross W, Savica R, et al. Incidence of Parkinson disease in North America. NPJ Parkinsons Dis. 2022;8(1):170.

185. Calabrese V, Santoro A, Monti D, Crupi R, Di Paola R, Latteri S, et al. Aging and Parkinson's Disease: Inflammaging, neuroinflammation and biological remodeling as key factors in pathogenesis. Free Radic Biol Med. 2018;115:80-91.
186. Harms AS, Cao S, Rowse AL, Thome AD, Li X, Mangieri LR, et al. MHCII is required for alpha-synuclein-induced activation of microglia, CD4 T cell proliferation, and dopaminergic neurodegeneration. J Neurosci. 2013;33(23):9592-600.
187. Williams GP, Schonhoff AM, Jurkuvenaite A, Thome AD, Standaert DG, Harms AS. Targeting of the class II transactivator attenuates inflammation and neurodegeneration in an alpha-synuclein model of Parkinson's disease. J Neuroinflammation. 2018;15(1):244.
188. Gonzalez De La Cruz E, Vo Q, Moon K, McFarland KN, Weinrich M, Williams T, et al. MhcII Regulates Transmission of alpha-Synuclein-Seeded Pathology in Mice. Int J Mol Sci. 2022;23(15).
189. DeSandro A, Nagarajan UM, Boss JM. The bare lymphocyte syndrome: molecular clues to the transcriptional regulation of major histocompatibility complex class II genes. Am J Hum Genet. 1999;65(2):279-86.
190. Penagarikano O, Abrahams BS, Herman EI, Winden KD, Gdalyahu A, Dong H, et al. Absence of CNTNAP2 leads to epilepsy, neuronal migration abnormalities, and core autism-related deficits. Cell. 2011;147(1):235-46.
191. Strauss KA, Puffenberger EG, Huentelman MJ, Gottlieb S, Dobrin SE, Parod JM, et al. Recessive symptomatic focal epilepsy and mutant contactin-associated protein-like 2. N Engl J Med. 2006;354(13):1370-7.
192. Lai MC, Baron-Cohen S. Identifying the lost generation of adults with autism spectrum conditions. Lancet Psychiatry. 2015;2(11):1013-27.
193. Bargiela S, Steward R, Mandy W. The Experiences of Late-diagnosed Women with Autism Spectrum Conditions: An Investigation of the Female Autism Phenotype. J Autism Dev Disord. 2016;46(10):3281-94.
194. Lundstrom S, Marland C, Kuja-Halkola R, Anckarsater H, Lichtenstein P, Gillberg C, et al. Assessing autism in females: The importance of a sex-specific comparison. Psychiatry Res. 2019;282:112566.
195. Huntington TE, Srinivasan R. Adeno-Associated Virus Expression of alpha-Synuclein as a Tool to Model Parkinson's Disease: Current Understanding and Knowledge Gaps. Aging Dis. 2021;12(4):1120-37.
196. Low K, Aebischer P. Use of viral vectors to create animal models for Parkinson's disease. Neurobiol Dis. 2012;48(2):189-201.
197. Albert K, Voutilainen MH, Domanskyi A, Piepponen TP, Ahola S, Tuominen RK, et al. Downregulation of tyrosine hydroxylase phenotype after AAV injection above substantia nigra: Caution in experimental models of Parkinson's disease. J Neurosci Res. 2019;97(3):346-61.
198. Ulusoy A, Sahin G, Bjorklund T, Aebischer P, Kirik D. Dose optimization for long-term rAAV-mediated RNA interference in the nigrostriatal projection neurons. Mol Ther. 2009;17(9):1574-84.

199. Sanchez-Guajardo V, Febbraro F, Kirik D, Romero-Ramos M. Microglia acquire distinct activation profiles depending on the degree of alpha-synuclein neuropathology in a rAAV based model of Parkinson's disease. PLoS One. 2010;5(1):e8784.
200. Harms AS, Thome AD, Yan Z, Schonhoff AM, Williams GP, Li X, et al. Peripheral monocyte entry is required for alpha-Synuclein induced inflammation and Neurodegeneration in a model of Parkinson disease. Exp Neurol. 2018;300:179-87.
201. Albert K, Voutilainen MH, Domanskyi A, Airavaara M. AAV Vector-Mediated Gene Delivery to Substantia Nigra Dopamine Neurons: Implications for Gene Therapy and Disease Models. Genes (Basel). 2017;8(2).
202. Brand DD, Latham KA, Rosloniec EF. Collagen-induced arthritis. Nat Protoc. 2007;2(5):1269-75.
203. Peng C, Gathagan RJ, Lee VM. Distinct alpha-Synuclein strains and implications for heterogeneity among alpha-Synucleinopathies. Neurobiol Dis. 2018;109(Pt B):209-18.
204. Harms AS, Delic V, Thome AD, Bryant N, Liu Z, Chandra S, et al. alpha-Synuclein fibrils recruit peripheral immune cells in the rat brain prior to neurodegeneration. Acta Neuropathol Commun. 2017;5(1):85.
205. Sacino AN, Brooks M, Thomas MA, McKinney AB, Lee S, Regenhardt RW, et al. Intramuscular injection of alpha-synuclein induces CNS alpha-synuclein pathology and a rapid-onset motor phenotype in transgenic mice. Proc Natl Acad Sci U S A. 2014;111(29):10732-7.
206. Holmqvist S, Chutna O, Bousset L, Aldrin-Kirk P, Li W, Bjorklund T, et al. Direct evidence of Parkinson pathology spread from the gastrointestinal tract to the brain in rats. Acta Neuropathol. 2014;128(6):805-20.
207. Matsuda W, Furuta T, Nakamura KC, Hioki H, Fujiyama F, Arai R, et al. Single nigrostriatal dopaminergic neurons form widely spread and highly dense axonal arborizations in the neostriatum. J Neurosci. 2009;29(2):444-53.
208. Luk KC, Covell DJ, Kehm VM, Zhang B, Song IY, Byrne MD, et al. Molecular and Biological Compatibility with Host Alpha-Synuclein Influences Fibril Pathogenicity. Cell Rep. 2016;16(12):3373-87.
209. Rey NL, Steiner JA, Maroof N, Luk KC, Madaj Z, Trojanowski JQ, et al. Widespread transneuronal propagation of alpha-synucleinopathy triggered in olfactory bulb mimics prodromal Parkinson's disease. J Exp Med. 2016;213(9):1759-78.
210. Howe JW, Sortwell CE, Duffy MF, Kemp CJ, Russell CP, Kubik M, et al. Preformed fibrils generated from mouse alpha-synuclein produce more inclusion pathology in rats than fibrils generated from rat alpha-synuclein. Parkinsonism Relat Disord. 2021;89:41-7.
211. Mattsson B, Parmar M, Bjorklund A. Athymic Nude Rat Brain Atlas. 1st ed. San Diego: Elsevier Academic Press; 2023.

212. Hanell A, Marklund N. Structured evaluation of rodent behavioral tests used in drug discovery research. Front Behav Neurosci. 2014;8:252.
213. Young D, Lawlor PA, Leone P, Dragunow M, During MJ. Environmental enrichment inhibits spontaneous apoptosis, prevents seizures and is neuroprotective. Nat Med. 1999;5(4):448-53.
214. Korbey SM, Heinrichs SC, Leussis MP. Seizure susceptibility and locus ceruleus activation are reduced following environmental enrichment in an animal model of epilepsy. Epilepsy Behav. 2008;12(1):30-8.
215. Ahl M, Avdic U, Strandberg MC, Chugh D, Andersson E, Hallmarker U, et al. Physical Activity Reduces Epilepsy Incidence: a Retrospective Cohort Study in Swedish Cross-Country Skiers and an Experimental Study in Seizure-Prone Synapsin II Knockout Mice. Sports Med Open. 2019;5(1):52.
216. Manno I, Macchi F, Caleo M, Bozzi Y. Environmental enrichment reduces spontaneous seizures in the Q54 transgenic mouse model of temporal lobe epilepsy. Epilepsia. 2011;52(9):e113-7.
217. Vrinda M, Sasidharan A, Aparna S, Srikumar BN, Kutty BM, Shankaranarayana Rao BS. Enriched environment attenuates behavioral seizures and depression in chronic temporal lobe epilepsy. Epilepsia. 2017;58(7):1148-58.
218. Dezsi G, Ozturk E, Salzberg MR, Morris M, O'Brien TJ, Jones NC. Environmental enrichment imparts disease-modifying and transgenerational effects on genetically-determined epilepsy and anxiety. Neurobiol Dis. 2016;93:129-36.
219. Hingray C, McGonigal A, Kotwas I, Micoulaud-Franchi JA. The Relationship Between Epilepsy and Anxiety Disorders. Curr Psychiatry Rep. 2019;21(6):40.
220. Zaboski BA, Storch EA. Comorbid autism spectrum disorder and anxiety disorders: a brief review. Future Neurol. 2018;13(1):31-7.
221. Olsson M, Nikkhah G, Bentlage C, Bjorklund A. Forelimb akinesia in the rat Parkinson model: differential effects of dopamine agonists and nigral transplants as assessed by a new stepping test. J Neurosci. 1995;15(5 Pt 2):3863-75.
222. Schallert T, Fleming SM, Leasure JL, Tillerson JL, Bland ST. CNS plasticity and assessment of forelimb sensorimotor outcome in unilateral rat models of stroke, cortical ablation, parkinsonism and spinal cord injury. Neuropharmacology. 2000;39(5):777-87.
223. Michetti C, Romano E, Altabella L, Caruso A, Castelluccio P, Bedse G, et al. Mapping pathological phenotypes in reelin mutant mice. Front Pediatr. 2014;2:95.
224. Podhorna J, Didriksen M. The heterozygous reeler mouse: behavioural phenotype. Behav Brain Res. 2004;153(1):43-54.
225. Kim H, Son J, Yoo H, Kim H, Oh J, Han D, et al. Effects of the Female Estrous Cycle on the Sexual Behaviors and Ultrasonic Vocalizations of

Male C57BL/6 and Autistic BTBR T+ tf/J Mice. Exp Neurobiol. 2016;25(4):156-62.
226. Nadler JJ, Moy SS, Dold G, Trang D, Simmons N, Perez A, et al. Automated apparatus for quantitation of social approach behaviors in mice. Genes Brain Behav. 2004;3(5):303-14.
227. Paylor R, Zhao Y, Libbey M, Westphal H, Crawley JN. Learning impairments and motor dysfunctions in adult Lhx5-deficient mice displaying hippocampal disorganization. Physiol Behav. 2001;73(5):781-92.
228. Raber J, Rola R, LeFevour A, Morhardt D, Curley J, Mizumatsu S, et al. Radiation-induced cognitive impairments are associated with changes in indicators of hippocampal neurogenesis. Radiat Res. 2004;162(1):39-47.
229. Seeger T, Fedorova I, Zheng F, Miyakawa T, Koustova E, Gomeza J, et al. M2 muscarinic acetylcholine receptor knock-out mice show deficits in behavioral flexibility, working memory, and hippocampal plasticity. J Neurosci. 2004;24(45):10117-27.
230. Patil SS, Sunyer B, Hoger H, Lubec G. Evaluation of spatial memory of C57BL/6J and CD1 mice in the Barnes maze, the Multiple T-maze and in the Morris water maze. Behav Brain Res. 2009;198(1):58-68.
231. Gawel K, Gibula E, Marszalek-Grabska M, Filarowska J, Kotlinska JH. Assessment of spatial learning and memory in the Barnes maze task in rodents-methodological consideration. Naunyn Schmiedebergs Arch Pharmacol. 2019;392(1):1-18.
232. Kraeuter AK, Guest PC, Sarnyai Z. The Y-Maze for Assessment of Spatial Working and Reference Memory in Mice. Methods Mol Biol. 2019;1916:105-11.
233. Miedel CJ, Patton JM, Miedel AN, Miedel ES, Levenson JM. Assessment of Spontaneous Alternation, Novel Object Recognition and Limb Clasping in Transgenic Mouse Models of Amyloid-beta and Tau Neuropathology. J Vis Exp. 2017(123).
234. Tucker LB, McCabe JT. Measuring Anxiety-Like Behaviors in Rodent Models of Traumatic Brain Injury. Front Behav Neurosci. 2021;15:682935.
235. Porsolt RD, Bertin A, Jalfre M. Behavioral despair in mice: a primary screening test for antidepressants. Arch Int Pharmacodyn Ther. 1977;229(2):327-36.
236. Porsolt RD, Le Pichon M, Jalfre M. Depression: a new animal model sensitive to antidepressant treatments. Nature. 1977;266(5604):730-2.
237. Thomas AM, Schwartz MD, Saxe MD, Kilduff TS. Cntnap2 Knockout Rats and Mice Exhibit Epileptiform Activity and Abnormal Sleep-Wake Physiology. Sleep. 2017;40(1).
238. Grabert K, McColl BW. Isolation and Phenotyping of Adult Mouse Microglial Cells. Methods Mol Biol. 2018;1784:77-86.
239. Kadic E, Moniz RJ, Huo Y, Chi A, Kariv I. Effect of cryopreservation on delineation of immune cell subpopulations in tumor specimens as

determinated by multiparametric single cell mass cytometry analysis. BMC Immunol. 2017;18(1):6.
240. West MJ, Slomianka L, Gundersen HJ. Unbiased stereological estimation of the total number of neurons in thesubdivisions of the rat hippocampus using the optical fractionator. Anat Rec. 1991;231(4):482-97.
241. Penttinen AM, Parkkinen I, Blom S, Kopra J, Andressoo JO, Pitkanen K, et al. Implementation of deep neural networks to count dopamine neurons in substantia nigra. Eur J Neurosci. 2018;48(6):2354-61.
242. Bennett ML, Bennett FC, Liddelow SA, Ajami B, Zamanian JL, Fernhoff NB, et al. New tools for studying microglia in the mouse and human CNS. Proc Natl Acad Sci U S A. 2016;113(12):E1738-46.
243. Barnum CJ, Chen X, Chung J, Chang J, Williams M, Grigoryan N, et al. Peripheral administration of the selective inhibitor of soluble tumor necrosis factor (TNF) XPro(R)1595 attenuates nigral cell loss and glial activation in 6-OHDA hemiparkinsonian rats. J Parkinsons Dis. 2014;4(3):349-60.
244. Henderson MX, Cornblath EJ, Darwich A, Zhang B, Brown H, Gathagan RJ, et al. Spread of alpha-synuclein pathology through the brain connectome is modulated by selective vulnerability and predicted by network analysis. Nat Neurosci. 2019;22(8):1248-57.
245. Wilhelmsson U, Bushong EA, Price DL, Smarr BL, Phung V, Terada M, et al. Redefining the concept of reactive astrocytes as cells that remain within their unique domains upon reaction to injury. Proc Natl Acad Sci U S A. 2006;103(46):17513-8.
246. Liddelow SA, Guttenplan KA, Clarke LE, Bennett FC, Bohlen CJ, Schirmer L, et al. Neurotoxic reactive astrocytes are induced by activated microglia. Nature. 2017;541(7638):481-7.
247. Duffy MF, Collier TJ, Patterson JR, Kemp CJ, Luk KC, Tansey MG, et al. Lewy body-like alpha-synuclein inclusions trigger reactive microgliosis prior to nigral degeneration. J Neuroinflammation. 2018;15(1):129.
248. Gordon S. Alternative activation of macrophages. Nat Rev Immunol. 2003;3(1):23-35.
249. Ponomarev ED, Maresz K, Tan Y, Dittel BN. CNS-derived interleukin-4 is essential for the regulation of autoimmune inflammation and induces a state of alternative activation in microglial cells. J Neurosci. 2007;27(40):10714-21.
250. George S, Rey NL, Tyson T, Esquibel C, Meyerdirk L, Schulz E, et al. Microglia affect alpha-synuclein cell-to-cell transfer in a mouse model of Parkinson's disease. Mol Neurodegener. 2019;14(1):34.
251. Yang Y, Garcia-Cruzado M, Zeng H, Camprubi-Ferrer L, Bahatyrevich-Kharitonik B, Bachiller S, et al. LPS priming before plaque deposition impedes microglial activation and restrains Abeta pathology in the 5xFAD mouse model of Alzheimer's disease. Brain Behav Immun. 2023;113:228-47.

252. Williams GP, Schonhoff AM, Jurkuvenaite A, Gallups NJ, Standaert DG, Harms AS. CD4 T cells mediate brain inflammation and neurodegeneration in a mouse model of Parkinson disease. Brain. 2021.
253. George S, Tyson T, Rey NL, Sheridan R, Peelaerts W, Becker K, et al. T Cells Limit Accumulation of Aggregate Pathology Following Intrastriatal Injection of alpha-Synuclein Fibrils. J Parkinsons Dis. 2021;11(2):585-603.
254. Constantinescu CS, Farooqi N, O'Brien K, Gran B. Experimental autoimmune encephalomyelitis (EAE) as a model for multiple sclerosis (MS). Br J Pharmacol. 2011;164(4):1079-106.
255. Watson MB, Richter F, Lee SK, Gabby L, Wu J, Masliah E, et al. Regionally-specific microglial activation in young mice over-expressing human wildtype alpha-synuclein. Exp Neurol. 2012;237(2):318-34.
256. Hirsch EC, Standaert DG. Ten Unsolved Questions About Neuroinflammation in Parkinson's Disease. Mov Disord. 2021;36(1):16-24.
257. Gerhard A. TSPO imaging in parkinsonian disorders. Clin Transl Imaging. 2016;4:183-90.
258. Gerhard A, Pavese N, Hotton G, Turkheimer F, Es M, Hammers A, et al. In vivo imaging of microglial activation with [11C](R)-PK11195 PET in idiopathic Parkinson's disease. Neurobiol Dis. 2006;21(2):404-12.
259. Ouchi Y, Yoshikawa E, Sekine Y, Futatsubashi M, Kanno T, Ogusu T, et al. Microglial activation and dopamine terminal loss in early Parkinson's disease. Ann Neurol. 2005;57(2):168-75.
260. Bartels AL, Willemsen AT, Doorduin J, de Vries EF, Dierckx RA, Leenders KL. [11C]-PK11195 PET: quantification of neuroinflammation and a monitor of anti-inflammatory treatment in Parkinson's disease? Parkinsonism Relat Disord. 2010;16(1):57-9.
261. Galiano-Landeira J, Torra A, Vila M, Bove J. CD8 T cell nigral infiltration precedes synucleinopathy in early stages of Parkinson's disease. Brain. 2020;143(12):3717-33.
262. Munoz-Delgado L, Macias-Garcia D, Perinan MT, Jesus S, Adarmes-Gomez AD, Bonilla Toribio M, et al. Peripheral inflammatory immune response differs among sporadic and familial Parkinson's disease. NPJ Parkinsons Dis. 2023;9(1):12.
263. Russell CD, Parajuli A, Gale HJ, Bulteel NS, Schuetz P, de Jager CPC, et al. The utility of peripheral blood leucocyte ratios as biomarkers in infectious diseases: A systematic review and meta-analysis. J Infect. 2019;78(5):339-48.
264. Munoz-Delgado L, Macias-Garcia D, Jesus S, Martin-Rodriguez JF, Labrador-Espinosa MA, Jimenez-Jaraba MV, et al. Peripheral Immune Profile and Neutrophil-to-Lymphocyte Ratio in Parkinson's Disease. Mov Disord. 2021;36(10):2426-30.
265. Qin XY, Zhang SP, Cao C, Loh YP, Cheng Y. Aberrations in Peripheral Inflammatory Cytokine Levels in Parkinson Disease: A Systematic Review and Meta-analysis. JAMA Neurol. 2016;73(11):1316-24.

266. Williams-Gray CH, Wijeyekoon R, Yarnall AJ, Lawson RA, Breen DP, Evans JR, et al. Serum immune markers and disease progression in an incident Parkinson's disease cohort (ICICLE-PD). Mov Disord. 2016;31(7):995-1003.
267. Chen X, Hu Y, Cao Z, Liu Q, Cheng Y. Cerebrospinal Fluid Inflammatory Cytokine Aberrations in Alzheimer's Disease, Parkinson's Disease and Amyotrophic Lateral Sclerosis: A Systematic Review and Meta-Analysis. Front Immunol. 2018;9:2122.
268. Earls RH, Menees KB, Chung J, Barber J, Gutekunst CA, Hazim MG, et al. Intrastriatal injection of preformed alpha-synuclein fibrils alters central and peripheral immune cell profiles in non-transgenic mice. J Neuroinflammation. 2019;16(1):250.
269. Karampetsou M, Ardah MT, Semitekolou M, Polissidis A, Samiotaki M, Kalomoiri M, et al. Phosphorylated exogenous alpha-synuclein fibrils exacerbate pathology and induce neuronal dysfunction in mice. Sci Rep. 2017;7(1):16533.
270. Theodore S, Cao S, McLean PJ, Standaert DG. Targeted overexpression of human alpha-synuclein triggers microglial activation and an adaptive immune response in a mouse model of Parkinson disease. J Neuropathol Exp Neurol. 2008;67(12):1149-58.
271. Chung CY, Koprich JB, Siddiqi H, Isacson O. Dynamic changes in presynaptic and axonal transport proteins combined with striatal neuroinflammation precede dopaminergic neuronal loss in a rat model of AAV alpha-synucleinopathy. J Neurosci. 2009;29(11):3365-73.
272. McCoy MK, Martinez TN, Ruhn KA, Szymkowski DE, Smith CG, Botterman BR, et al. Blocking soluble tumor necrosis factor signaling with dominant-negative tumor necrosis factor inhibitor attenuates loss of dopaminergic neurons in models of Parkinson's disease. J Neurosci. 2006;26(37):9365-75.
273. McCoy MK, Ruhn KA, Martinez TN, McAlpine FE, Blesch A, Tansey MG. Intranigral lentiviral delivery of dominant-negative TNF attenuates neurodegeneration and behavioral deficits in hemiparkinsonian rats. Mol Ther. 2008;16(9):1572-9.
274. Harms AS, Barnum CJ, Ruhn KA, Varghese S, Trevino I, Blesch A, et al. Delayed dominant-negative TNF gene therapy halts progressive loss of nigral dopaminergic neurons in a rat model of Parkinson's disease. Mol Ther. 2011;19(1):46-52.
275. MacPherson KP, Sompol P, Kannarkat GT, Chang J, Sniffen L, Wildner ME, et al. Peripheral administration of the soluble TNF inhibitor XPro1595 modifies brain immune cell profiles, decreases beta-amyloid plaque load, and rescues impaired long-term potentiation in 5xFAD mice. Neurobiol Dis. 2017;102:81-95.
276. Ishida Y, Nagai A, Kobayashi S, Kim SU. Upregulation of protease-activated receptor-1 in astrocytes in Parkinson disease: astrocyte-mediated

neuroprotection through increased levels of glutathione peroxidase. J Neuropathol Exp Neurol. 2006;65(1):66-77.
277. Recasens A, Dehay B, Bove J, Carballo-Carbajal I, Dovero S, Perez-Villalba A, et al. Lewy body extracts from Parkinson disease brains trigger alpha-synuclein pathology and neurodegeneration in mice and monkeys. Ann Neurol. 2014;75(3):351-62.
278. Soos JM, Morrow J, Ashley TA, Szente BE, Bikoff EK, Zamvil SS. Astrocytes express elements of the class II endocytic pathway and process central nervous system autoantigen for presentation to encephalitogenic T cells. J Immunol. 1998;161(11):5959-66.
279. Nikcevich KM, Piskurich JF, Hellendall RP, Wang Y, Ting JP. Differential selectivity of CIITA promoter activation by IFN-gamma and IRF-1 in astrocytes and macrophages: CIITA promoter activation is not affected by TNF-alpha. J Neuroimmunol. 1999;99(2):195-204.
280. Stuve O, Youssef S, Slavin AJ, King CL, Patarroyo JC, Hirschberg DL, et al. The role of the MHC class II transactivator in class II expression and antigen presentation by astrocytes and in susceptibility to central nervous system autoimmune disease. J Immunol. 2002;169(12):6720-32.
281. Booth HDE, Hirst WD, Wade-Martins R. The Role of Astrocyte Dysfunction in Parkinson's Disease Pathogenesis. Trends Neurosci. 2017;40(6):358-70.
282. Masi A, Glozier N, Dale R, Guastella AJ. The Immune System, Cytokines, and Biomarkers in Autism Spectrum Disorder. Neurosci Bull. 2017;33(2):194-204.
283. Filiano AJ, Gadani SP, Kipnis J. Interactions of innate and adaptive immunity in brain development and function. Brain Res. 2015;1617:18-27.
284. Bozzi Y, Provenzano G, Casarosa S. Neurobiological bases of autism-epilepsy comorbidity: a focus on excitation/inhibition imbalance. Eur J Neurosci. 2018;47(6):534-48.
285. Chugh D, Nilsson P, Afjei SA, Bakochi A, Ekdahl CT. Brain inflammation induces post-synaptic changes during early synapse formation in adult-born hippocampal neurons. Exp Neurol. 2013;250:176-88.
286. Avdic U, Chugh D, Osman H, Chapman K, Jackson J, Ekdahl CT. Absence of interleukin-1 receptor 1 increases excitatory and inhibitory scaffolding protein expression and microglial activation in the adult mouse hippocampus. Cell Mol Immunol. 2015;12(5):645-7.
287. van Vliet EA, Aronica E, Gorter JA. Blood-brain barrier dysfunction, seizures and epilepsy. Semin Cell Dev Biol. 2015;38:26-34.
288. Saghazadeh A, Ataeinia B, Keynejad K, Abdolalizadeh A, Hirbod-Mobarakeh A, Rezaei N. A meta-analysis of pro-inflammatory cytokines in autism spectrum disorders: Effects of age, gender, and latitude. J Psychiatr Res. 2019;115:90-102.
289. Bauer S, Cepok S, Todorova-Rudolph A, Nowak M, Koller M, Lorenz R, et al. Etiology and site of temporal lobe epilepsy influence postictal cytokine release. Epilepsy Res. 2009;86(1):82-8.

290. Ashwood P, Krakowiak P, Hertz-Picciotto I, Hansen R, Pessah IN, Van de Water J. Altered T cell responses in children with autism. Brain Behav Immun. 2011;25(5):840-9.
291. Ashwood P, Krakowiak P, Hertz-Picciotto I, Hansen R, Pessah I, Van de Water J. Elevated plasma cytokines in autism spectrum disorders provide evidence of immune dysfunction and are associated with impaired behavioral outcome. Brain Behav Immun. 2011;25(1):40-5.
292. Gupta S, Aggarwal S, Rashanravan B, Lee T. Th1- and Th2-like cytokines in CD4+ and CD8+ T cells in autism. J Neuroimmunol. 1998;85(1):106-9.
293. Li X, Chauhan A, Sheikh AM, Patil S, Chauhan V, Li XM, et al. Elevated immune response in the brain of autistic patients. J Neuroimmunol. 2009;207(1-2):111-6.
294. Enstrom AM, Lit L, Onore CE, Gregg JP, Hansen RL, Pessah IN, et al. Altered gene expression and function of peripheral blood natural killer cells in children with autism. Brain Behav Immun. 2009;23(1):124-33.
295. Enstrom AM, Onore CE, Van de Water JA, Ashwood P. Differential monocyte responses to TLR ligands in children with autism spectrum disorders. Brain Behav Immun. 2010;24(1):64-71.
296. Sarkis RA, Jehi L, Silveira D, Janigro D, Najm I. Patients with generalised epilepsy have a higher white blood cell count than patients with focal epilepsy. Epileptic Disord. 2012;14(1):57-63.
297. Bauer S, Koller M, Cepok S, Todorova-Rudolph A, Nowak M, Nockher WA, et al. NK and CD4+ T cell changes in blood after seizures in temporal lobe epilepsy. Exp Neurol. 2008;211(2):370-7.
298. Fields CR, Bengoa-Vergniory N, Wade-Martins R. Targeting Alpha-Synuclein as a Therapy for Parkinson's Disease. Front Mol Neurosci. 2019;12:299.
299. Espay AJ, Lees AJ. Loss of monomeric alpha-synuclein (synucleinopenia) and the origin of Parkinson's disease. Parkinsonism Relat Disord. 2024;122:106077.
300. Update on STEM-PD clinical trial – stem cell-based transplant for Parkinson's disease: Lund University; 2024 [Available from: https://www.lunduniversity.lu.se/article/update-stem-pd-clinical-trial-stem-cell-based-transplant-parkinsons-disease.
301. Kim TW, Koo SY, Riessland M, Chaudhry F, Kolisnyk B, Cho HS, et al. TNF-NF-kappaB-p53 axis restricts in vivo survival of hPSC-derived dopamine neurons. Cell. 2024.
302. Pitkanen A, Loscher W, Vezzani A, Becker AJ, Simonato M, Lukasiuk K, et al. Advances in the development of biomarkers for epilepsy. Lancet Neurol. 2016;15(8):843-56.